UNIVERSITEIT VAN PRETORIA
UNIVERSITY OF PRETORIA
YUNIBESITHI YA PRETORIA

IMPROVED SYNTHESIS TECHNIQUES FOR UNIFORMLY-SPACED PLANAR ARRAYS

by

EUGENE BOTHA

Presented in partial fulfilment of the requirements for the degree M.Ing in the

Faculty of Engineering
University of Pretoria

March 1991

© University of Pretoria Digitised by the Department of Library Services in support of open access to information, University of Pretoria, 2019

UNIVERSITEIT VAN PRETORIA
UNIVERSITY OF PRETORIA
YUNIBESITHI YA PRETORIA

VERBETERDE SINTESE TEGNIEKE VIR UNIFORM-GESPASIEëRDE VLAKSAMESTELLINGS

deur

EUGENE BOTHA

Voorgelê vir die gedeeltelike vervulling van die vereistes vir die graad M.Ing in die

Fakulteit Ingenieurswese
Universiteit van Pretoria

Maart 1991

© University of Pretoria Digitised by the Department of Library Services in support of open access to information, University of Pretoria, 2019

UNIVERSITEIT VAN PRETORIA
UNIVERSITY OF PRETORIA
YUNIBESITHI YA PRETORIA

Bedankings

Ek wil graag my dank betuig aan die volgende persone, wie se hulp die tesis moontlik gemaak het:

- my studieleier, Prof. D.A. M^{c}Namara, wat my belangstelling in die veld geprikkel het, vir sy leiding en entoesiasme,
- my vrou, Jo-Anne, vir al haar opoffering, bystand en bemoediging.

© University of Pretoria Digitised by the Department of Library Services in support of open access to information, University of Pretoria, 2019

UNIVERSITEIT VAN PRETORIA
UNIVERSITY OF PRETORIA
YUNIBESITHI YA PRETORIA

SYNOPSIS

TITLE: Improved Synthesis Techniques for Uniformly-Spaced Planar Arrays

AUTHOR: Eugene Botha

PROMOTER: Prof. D.A. McNamara

DEPARTMENT: Electronics and Computer Engineering

DEGREE: M.Ing

A direct synthesis technique for high directivity discrete planar arrays has been proposed. The generalised Villeneuve linear distribution array synthesis method has been extended to the planar array case by means of the Baklanov transformation. Parametric studies of the performance of the distribution have been conducted.

A direct synthesis technique to produce discrete planar arrays with contoured beams has been developed. The technique utilises a transformation that divides the problem into two decoupled sub-problems. The one sub-problem consists of a linear array synthesis and the other involves the determination of certain transformation coefficients in order to achieve the required footprint contours.

© University of Pretoria Digitised by the Department of Library Services in support of open access to information, University of Pretoria, 2019

UNIVERSITEIT VAN PRETORIA
UNIVERSITY OF PRETORIA
YUNIBESITHI YA PRETORIA

ABSTRACT

There has until the present time been no planar array equivalent of the generalized Villeneuve (linear) distribution. The generalised Villeneuve linear distribution array synthesis method has been extended to the planar array case by means the Baklanov transformation. The Baklanov transformation ensures that the resulting planar array factor is ψ-symmetric. Aside from the sidelobe level, two additional parameters have been introduced; they are the transition index $\bar{n}$ that determines the position at which the sidelobe must decay and the taper rate υ that determines the decay rate of the far-out sidelobes. The generalised Villeneuve distribution for planar arrays enables the direct synthesis of discrete array distributions for high efficiency patterns of arbitrary sidelobe levels and envelope taper. The synthesis method is extremely rapid; consequently, design trade-off studies are feasible. For a set number of elements and sidelobe ratio, the values of the transition index and the taper rate for a specific application will depend on the relative importance of farther-out sidelobe levels and the excitation efficiency (or directivity) desired. Parametric studies of the distribution's performance have been conducted; curves of directivity versus element number as well as curves of the influence of the additional parameters ($\bar{n}$ and υ) on the array factor are provided. It has also been shown how the generalised planar Villeneuve distribution method can be used for the synthesis of planar arrays with a circular boundaries, without the directivity performance being disadvantaged.

A direct method to synthesise an array factor with an arbitrarily contoured main beam has been developed. The technique utilises a transformation that divides the problem into two decoupled sub-problems. In the antenna array context, one sub-problem consists of a linear array synthesis, for which there exist various powerful methods for determining appropriate element excitations. The other involves the determination of certain coefficients of the transform in order to achieve the required footprint contours. The number of coefficients which are needed depends on the complexity of the desired contour, but is very small in comparison to the number of planar array elements. The size required for this prototype linear array depends on the

© University of Pretoria Digitised by the Department of Library Services in support of open access to information, University of Pretoria, 2019

UNIVERSITEIT VAN PRETORIA
UNIVERSITY OF PRETORIA
YUNIBESITHI YA PRETORIA

sidelobe level, the allowable ripple in the coverage region, number of transformation coefficients used and the planar array size. Alternatively, it could be stated that the final planar array size depends on the number of transformation coefficients and the prototype linear array size. Simple formulas then determine the final planar array excitations from the information forthcoming from the above two sub-problem solutions. Thus the method is computational efficient and the time required to perform such a synthesis is relatively short; thus trade-of studies are feasible even for very large arrays. Simple formulas for the calculation of the transform coefficients for circular and elliptical contours have been derived, but the more general contour problem has also been discussed. Application of the newly developed transformation technique has been examined through number of specific examples.

© University of Pretoria Digitised by the Department of Library Services in support of open access to information, University of Pretoria, 2019

UNIVERSITEIT VAN PRETORIA
UNIVERSITY OF PRETORIA
YUNIBESITHI YA PRETORIA

SAMEVATTING

Tot op hede is daar geen sintese-metode vir vlaksamestellings ekwivalent aan die veralgemeende Villeneuve-verspreiding metode nie. Die veralgemeende Villeneuve liniêre samestelling sintese-metode is uitgebrei na vlaksamestellings met behulp van die Baklanov-transformasie. Die Baklanov-transfomasie verseker 'n ϕ-simmetriese vlak-samestelling stralingspatroon. Naas die sylobvlak is nog twee ekstra parameters bygevoeg; dit is die oorgangsindeks $\bar{n}$ wat bepaal waar die sylobbe moet begin afplat en die afplattempo υ wat die afneemtempo van die sylobbe bepaal. Die direkte sintese van vlaksamestellings met arbitrêre sylobvlakke en afplattempo's word moontlik gemaak deur die veralgemeende Villeneuve-verspreiding vir vlaksamestellings. Die sinteseproses kan vinnig uitgevoer word; dus kan ontwerpstudies geredelik gedoen word. Vir 'n vasgestelde aantal elemente en sylobvlak hang die waardes van die oorgangsindeks en die afplattempo af van die relatiewe belangrikheid van die sylobvlakke op die kante en die aandrywings-effektiwiteit (of die direktiwiteit) wat verlang word. 'n Parameteriese studie van die samestellingskenmerke is gedoen; grafieke van die direktiwiteit teenoor die aantal elemente sowel as die invloed van die addisionele parameters word vertoon. Die veralgemeende Villeneuve vlaksamestelling kan ook gebruik word om vlaksamestellings met sirkulêre rande te sintetiseer sonder dat die direktiwiteit benadeel word.

'n Direkte sintese-metode vir 'n samestellingsfaktor waarvan die hooflob 'n arbitrêre vorm kan hê, is ontwikkel. Die metode maak gebruik van 'n transformasie om die probleem te verdeel in twee afsonderlike sub-probleme. Die een sub-probleem behels die ontwerp van 'n liniêre samestelling waarvoor daar verskeie metodes bestaan. Die ander sub-probleem behels die berekening van die transformasie-koëffisiënte om die verlangde vorm van die hooflob te verkry. Die aantal koëffisiënte wat benodig word hang af van die kompleksiteit van die verlangde vorm, maar is klein in verhouding met aantal elemente in die vlaksamestelling. Die grootte van die liniêre samestelling word bepaal deur die sylobvlakke, die hoeveelheid riffel toelaatbaar in die hooflob, die aantal transfomasie-koëffisiënte en die grootte van die vlaksamestelling. Die element-aandrywings word dan met eenvoudige formules bereken. Omdat die metode vinnig

© University of Pretoria Digitised by the Department of Library Services in support of open access to information, University of Pretoria, 2019

UNIVERSITEIT VAN PRETORIA
UNIVERSITY OF PRETORIA
YUNIBESITHI YA PRETORIA

uitgevoer kan word, kan baie groot samestelling geredelik gesintetiseer word. Eenvoudige formules vir die tranformasie-koëffisiënte ten einde sirkulêre en elliptiese kontoere te bepaal, word afgelei. Die algemene kontoerbenaderingsprobleem word ook aangespreek. Toepassing van die nuwe metode word ondersoek aan die hand van spesifieke voorbeelde.

© University of Pretoria Digitised by the Department of Library Services in support of open access to information, University of Pretoria, 2019

UNIVERSITEIT VAN PRETORIA
UNIVERSITY OF PRETORIA
YUNIBESITHI YA PRETORIA

TABLE OF CONTENTS

© University of Pretoria Digitised by the Department of Library Services in support of open access to information, University of Pretoria, 2019

UNIVERSITEIT VAN PRETORIA
UNIVERSITY OF PRETORIA
YUNIBESITHI YA PRETORIA

© University of Pretoria Digitised by the Department of Library Services in support of open access to information, University of Pretoria, 2019

UNIVERSITEIT VAN PRETORIA
UNIVERSITY OF PRETORIA
YUNIBESITHI YA PRETORIA

© University of Pretoria Digitised by the Department of Library Services in support of open access to information, University of Pretoria, 2019

UNIVERSITEIT VAN PRETORIA
UNIVERSITY OF PRETORIA
YUNIBESITHI YA PRETORIA

CHAPTER 1

INTRODUCTION

1.1 ANTENNA REQUIREMENTS

Communication or the transfer of information is of primary importance to civilized human beings. At first, communication was achieved by sound through the human voice, drums, etc. For longer distances visual methods such as smoke signals, signal flags and so forth, were employed. Today, long distance communication systems make use of the electromagnetic spectrum because electrical signals are easy to control and travel at, or near, the speed of light. Everyday examples of communication systems are telephone, radio and television. Global communication is often conducted via satellite.

Modern communication systems depend on transmission (by some type of guided structure) or propagation (in free space) of electromagnetic waves. The antenna is instrumental in many of these systems in that it provides a transition of a guided wave to a free space wave (and vice versa in the receiving case). By reciprocity [1] the antenna patterns are the same whether obtained in transmission or reception, thus it is common practice to consider all cases in transmission for ease of analysis.

Antennas can be divided into many classes, each with different requirements. The function of a satellite antenna can be divided into two classes. An essential requirement of the first class is the ability to receive signal using a directive antenna beam which is pointed towards the source. The characteristics of the antenna must be such that it has a single main lobe with as high as possible a directivity subject to a given set of sidelobe constraints. The second class of satellite antenna must have a radiation pattern shaped

© University of Pretoria Digitised by the Department of Library Services in support of open access to information, University of Pretoria, 2019

UNIVERSITEIT VAN PRETORIA
UNIVERSITY OF PRETORIA
YUNIBESITHI YA PRETORIA

in such a way that some irregularly shaped angular region on the earth is illuminated with a specified minimum level of electromagnetic energy in order to achieve an adequate signal-to-noise ratio over the said area.

1.2 ARRAY ANTENNAS

A source of electromagnetic radiation may take many different forms. It could be a conducting wire, horn radiator, waveguide slot, or one of many other possibilities. The radiation pattern of a single element is fixed for a given frequency of excitation and consists, in general, of a main beam and a number of smaller sidelobes. In many applications there is a need for improving the performance above that obtainable with a single radiating element. There are, broadly speaking, two methods available for this purpose. One technique uses a properly shaped reflector or lens fed by a radiating element, and the other employs a number of radiating elements correctly arranged in space to form an antenna array. Whether the reflector or array option is to be used depends on a multitude of factors related to particular applications and environments in which the antenna is to operate. Up to the present time reflector antennas have dominated the satellite antenna domain. More recently, the potential advantages of using arrays for such applications have been pointed out [3, 5]. The planar array represents a more compact configuration since it could be so fabricated that it does not protrude as much from the satellite body.

Array antenna development can be divided into three stages: *specification*, *synthesis* and *realisation*. These should not be taken as clear-cut divisions, however, as there is a considerable amount of overlap between the last two stages. Means of unambiguously *specifying* the required performance of an antenna are discussed in the following chapter. The *synthesis* problem involves the determination of the excitations and spacings of the array elements required to obtain desired radiation characteristics. Synthesis is usually performed subject to a set of constraints. The latter may set bounds on certain radiation pattern characteristics (e.g. sidelobe levels in the case of Class #1 satellite antennas, and specified contours in the case of Class #2 satellite antennas), but may also include constraints on other quantities in an attempt to allow easier practical

© University of Pretoria Digitised by the Department of Library Services in support of open access to information, University of Pretoria, 2019

UNIVERSITEIT VAN PRETORIA
UNIVERSITY OF PRETORIA
YUNIBESITHI YA PRETORIA

realizability. This second kind of constraint may include factors such as the sensitivity of the array performance to imperfections, or constraints on the complexity of the feed network. It is in the setting down of constraints that engineering judgement must be exercised in the midst of the mathematical techniques. The final step in the design of an antenna array is the actual establishment of the determined excitations in the form of hardware. The *realisation* of the array includes the selection of the radiating elements to be used, though this would no doubt have been kept in mind during the synthesis stage. The realisation phase would further involve the determination (theoretically or experimentally) of the element radiation characteristics and the coupling between elements, both externally and internally via the feed network. This information is then used to establish the correct excitation determined from the synthesis procedure.

1.3 OVERVIEW OF THE THESIS

This thesis deals exclusively with array synthesis. In order to be clear on exactly which aspects of antenna array synthesis are pertinent to the matters at hand here, it is perhaps best to state clearly which categories are not of concern. Firstly, arrays with non-uniform inter-element spacing, and those which can be classified as thinned arrays (certain elements having been removed for various reasons), will not form part of the discussion in this thesis. Secondly, conformal arrays will also be set aside, with only linear and planar arrays entering into the discussion. Although this may seem overly restrictive, such is not really the case, since this type of array is still that most widely used in practical systems.

Chapter 2 first gives essential information on array analysis relevant to this work. Thereafter the definitions of numerous factors used in the literature that would be required to specify the performance of antennas, irrespective of the particular type used, are summarised. Secondly, the development of the array synthesis techniques relevant to the present problem is reviewed. The chapter concludes (Section 2.10) with a summary of synthesis problems which have not been adequately dealt with in the literature, and which form the subject of this thesis.

© University of Pretoria Digitised by the Department of Library Services in support of open access to information, University of Pretoria, 2019

UNIVERSITEIT VAN PRETORIA
UNIVERSITY OF PRETORIA
YUNIBESITHI YA PRETORIA

Chapters 3 and 4 contain the principal contributions of the present work to the theory of array synthesis. A more detailed indication of the contents of these chapters is more appropriate after the limitations of existing synthesis techniques has been gauged; this is therefore postponed until the end of the second chapter (Section 2.10).

Finally, some general conclusions are reached in Chapter 5, and the research reported herein put into perspective.

Appendices A and B contain details of certain mathematical derivations related to Chapters 3 and 4, respectively.

1.4 REFERENCES

[1] R.S.Elliott, *Antenna Theory and Design*, Englewood Cliffs: Prentice-Hall, 1981.

[2] M.T.Ma, *Theory and Application of Antenna Arrays*, New York: John Wiley & Sons, 1974.

[3] R.S.Elliott and G.J.Stern, "Footprint patterns obtained by planar arrays", *IEE Proc.*, Pt.H, Vol.137, No.2, pp.108-112, April 1990.

[4] R.F.E.Guy, "General radiation-pattern synthesis technique for array antennas of arbitrary configuration and element type", *IEE Proc.*, Pt.H., Vol.135, No.4, pp.241-248, Aug.1988.

[5] P.B.Bornemann, and P.Balling and W.J.English, "Synthesis of spacecraft array antennas for Intelsat frequency reuse multiple contoured beams", *IEEE Trans. Antennas Propagat.*, Vol.AP-33, No.11, pp.1186-1193, Nov.1985.

© University of Pretoria Digitised by the Department of Library Services in support of open access to information, University of Pretoria, 2019

UNIVERSITEIT VAN PRETORIA
UNIVERSITY OF PRETORIA
YUNIBESITHI YA PRETORIA

CHAPTER 2

REVIEW OF RELEVANT ARRAY SYNTHESIS TECHNIQUES

2.1 INTRODUCTORY REMARKS

Several radiating elements can be arranged in space and interconnected to produce a directional radiation pattern. Such a group of antenna elements is referred to as an array antenna, or simply, an array. The radiation pattern of the array is dependant on the individual antenna elements' radiation pattern, the relative excitation of each element and the geometry of the array. The primary goal of antenna synthesis is to obtain a radiation pattern with specified characteristics.

The best way to learn synthesis is to learn all you can about analysis. This chapter therefore begins with a discussion of the relevant array analysis techniques, followed by a discussion of various array performance indices. The development of array synthesis techniques relevant to the thesis is also reviewed. The chapter concludes with a summary of two synthesis problems which have not been adequately dealt with in the literature and which form the subject of this thesis.

© University of Pretoria Digitised by the Department of Library Services in support of open access to information, University of Pretoria, 2019

2.2 ARRAY ANALYSIS

2.2.1 Isotropic Radiators and Array Space Factor

If the radiation pattern of the individual elements of an array is broad the significant features of the array pattern are controlled by what is known as the array factor (also called the space factor) [1: p.117]. This is most often the case since the array elements usually have low directivity, otherwise the elements themselves will be large, requiring wide spacings and hence grating lobes. The array factor represents the pattern of an array of isotropic radiators, with spacings identical to those between the phase centres of the actual elements, and with relative complex (amplitude and phase) weighting or excitations equal to those of the actual array elements. The synthesis problem deals with the array factor. Henceforth, if the "radiation pattern" of an array is mentioned, it is the array factor that is being referred to.

2.2.2 Linear Arrays

If all the elements of an array lie along a straight line, they form a linear array. This geometry is not only important in its own right, but is also an essential building block of the majority of planar arrays. The synthesis of such linear arrays is therefore fundamental to all array design. Before a synthesis problem can be attempted, means of analyzing a linear array must be available. Such analyses are treated in some detail in reference [1] to [5] and a complete treatment is not intended here. Instead, only the most relevant material will be considered, certain new expressions presented, and some concepts written in a more concise form. In what follows, the background to any statements made without proof can be found in the above references.

Consider the linear array geometry shown in Figure 2.1, consisting of $2N$ elements with uniform element spacing d. The normalised complex excitation of the nth element (numbered as in Figure 2.1), is a_n. The discrete distribution of excitations is called the aperture distribution of the array. The array factor is a superposition of contributions from each element, and is given by [1: p.142],

$$F(\theta) = \sum_{n=1}^{N} \left[a_n e^{j\frac{1}{2}(2n-1)kd\sin\theta} + a_{-n} e^{-j\frac{1}{2}(2n-1)kd\sin\theta} \right] \qquad (2.1)$$

© University of Pretoria Digitised by the Department of Library Services in support of open access to information, University of Pretoria, 2019

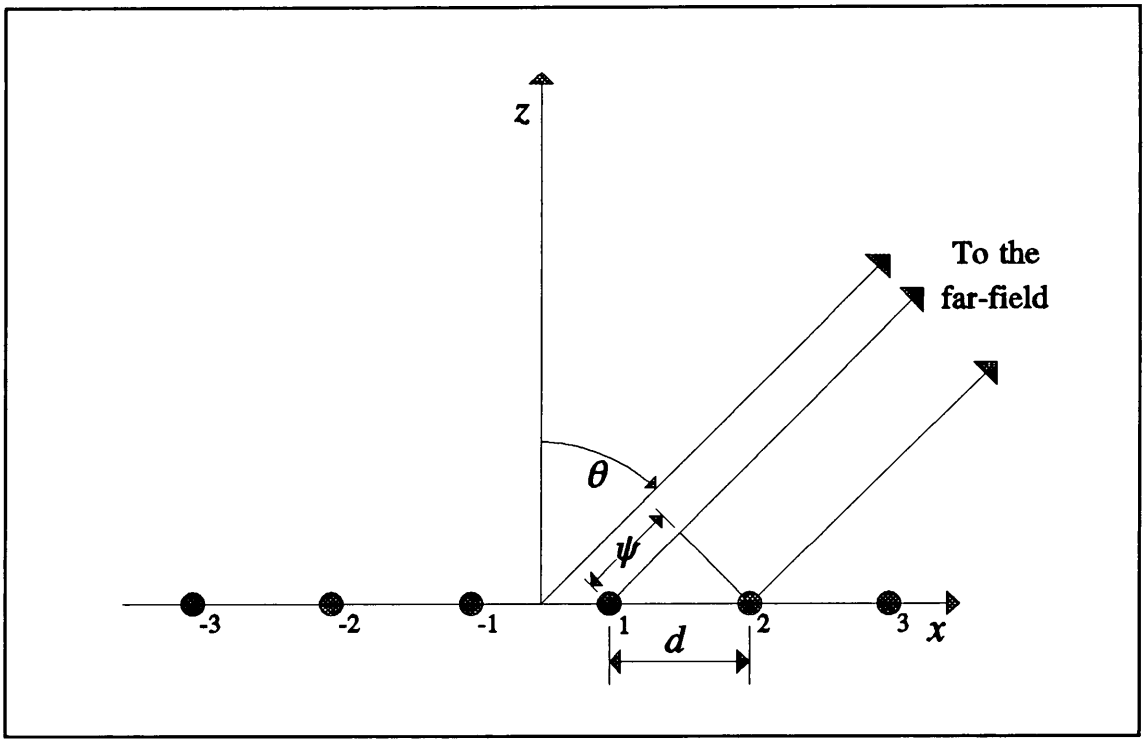

Figure 2.1 Linear array geometry

where k is the free-space wavenumber. It is convenient to define an additional variable, namely the path length difference, $\psi = kd\sin\theta$. This variable will be used interchangeably with θ to denote the pattern angle. If this new variable is used, an alternative expression for the array factor is

$$F(\psi) = \sum_{n=1}^{N} \left[a_n e^{j\frac{1}{2}(2n-1)\psi} + a_{-n} e^{-j\frac{1}{2}(2n-1)\psi} \right] \tag{2.2}$$

Distributions for which $|a_{-n}| = |a_n|$ are of particular importance; with symmetrical excitation $a_{-n} = a_n$ (sum pattern) the array factor becomes [1: p.142],

$$F(\psi) = 2\sum_{n=1}^{N} a_n \cos\left[\frac{1}{2}(2n-1)\psi\right] \tag{2.3}$$

Recall that the array factor expressions given apply to an array of $2N$ elements (an even number). An array of $2N+1$ elements (an odd number), symmetrically excited has an array factor expression given by

© University of Pretoria Digitised by the Department of Library Services in support of open access to information, University of Pretoria, 2019

UNIVERSITEIT VAN PRETORIA
UNIVERSITY OF PRETORIA
YUNIBESITHI YA PRETORIA

$$F(\psi) = a_0 + 2\sum_{n=1}^{N} a_n \cos(n\psi) \tag{2.4}$$

Expressions for array performance measures, to be discussed in Section 2.3, can be concisely written through use of matrix notation [6, 10, 11]. The vectors and matrices needed for the performance indices of a linear array will be defined here. For a linear array of N elements, the excitation vector is defined as,

$$\bar{J} = [a_1;\ a_2;\ .....;\ a_N]^T \tag{2.5}$$

The radiation vector is defined as,

$$\bar{F} = [e^{j\psi};\ e^{j2\psi};\ .....;\ e^{jN\psi}]^T \tag{2.6}$$

The corresponding array factor is,

$$F(\psi) = \bar{F}^T \bar{J} \tag{2.7}$$

where $[\ ]^T$ denotes the Hermitian transpose or adjoint operation (transpose of the conjugate). Two matrices are needed. They are $\tilde{A}$,

$$\tilde{A} = \bar{F}\bar{F}^T \tag{2.8}$$

and $\tilde{B}$ with b_{mn}, its components as,

$$b_{mn} = sinc(n-m)kd \qquad m,n = 1,2,....,N \tag{2.9}$$

2.2.3 Planar Arrays

In order to describe a planar array geometry it is necessary to specify both its element lattice and the boundary shape. Three basic lattices have been dealt with in the literature: the rectangular lattice the triangular lattice, and the circular lattice[1] (for which the elements lie on concentric circles). For a complete analyses of planar arrays see references [1], [7] and [8]. Only those synthesis techniques applicable to the

[1]Note that *circular lattice* and *circular boundary shape* do not mean the same thing. An array with a rectangular lattice may have a circular boundary.

© University of Pretoria Digitised by the Department of Library Services in support of open access to information, University of Pretoria, 2019

UNIVERSITEIT VAN PRETORIA
UNIVERSITY OF PRETORIA
YUNIBESITHI YA PRETORIA

rectangular lattice case are of interest here.

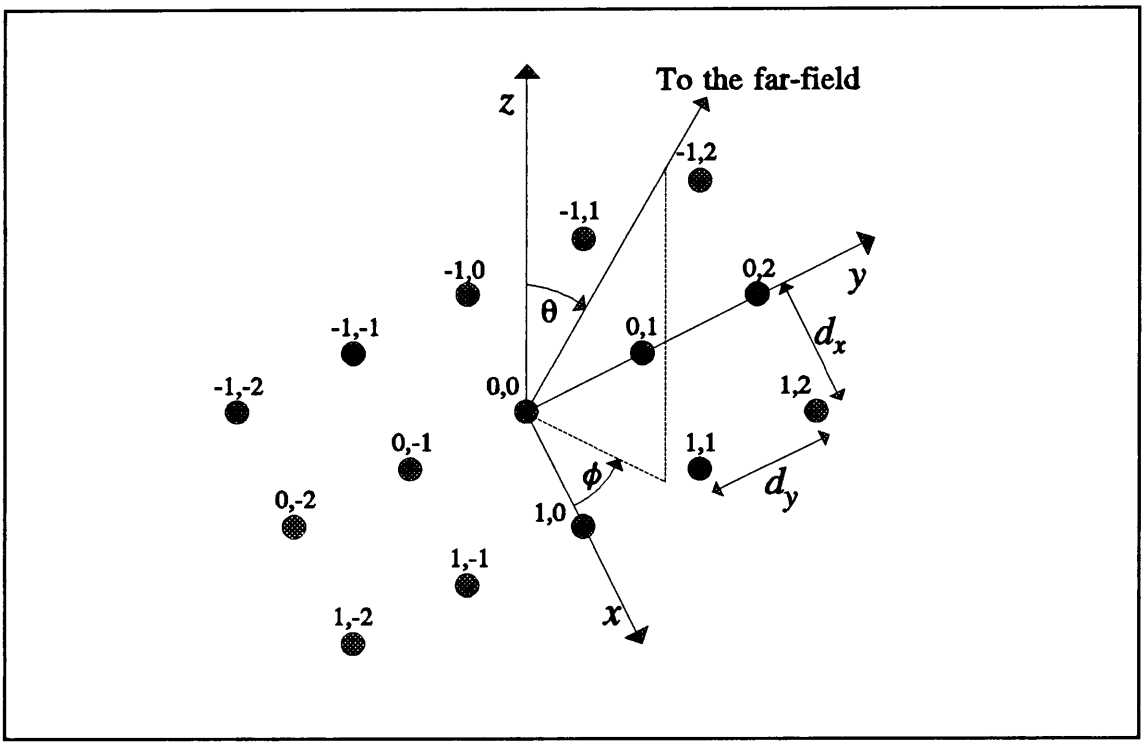

Figure 2.2 *2M+1* by *2N+1* Planar array geometry

Consider the planar array, with a rectangular lattice and rectangular boundary, shown in Figure 2.2, consisting of *2M+1* by *2N+1* elements with uniform element spacing d_x and d_y in the *x*- and *y*-directions respectively. The normalised complex excitation of the *mn*th element is a_{mn}, with the numbering scheme as shown in Figure 2.2. The direction of the observation point in the far-field is given by θ and ϕ, with θ measured from the positive *z*-axis and ϕ measured in the *xy*-plane from the *x*-axis towards the positive *y*-axis, as in the usual spherical coordinate system. The array factor can be expressed as [1: p.197]

$$F(\theta,\phi) = \sum_{m=-M}^{M} \sum_{n=-N}^{N} a_{mn} e^{jk(md_x \sin\theta\cos\phi + nd_y \sin\theta\cos\phi)} \qquad (2.10)$$

The following new variables are defined for convenience, $u = kd_x \sin\theta\cos\phi$ and $v = kd_y \sin\theta\sin\phi$ (note that the polar angle of any point (u,v) in the *uv*-plane is simply ϕ). If these new variables is used the array factor can be rewritten as

© University of Pretoria Digitised by the Department of Library Services in support of open access to information, University of Pretoria, 2019

$$F(u,v) = \sum_{m=-M}^{M} \sum_{n=-N}^{N} a_{mn} e^{j(mu+nv)} \tag{2.11}$$

If the elements are excited with quadrantal symmetry, $a_{m,n} = a_{-m,n} = a_{-m,-n} = a_{m,-n}$, the array factor becomes

$$F(u,v) = 4\sum_{m=0}^{M} \sum_{n=0}^{N} \zeta_m \zeta_n a_{mn} \cos(mu)\cos(nv)$$

$$\text{where } \zeta_i = \begin{cases} \frac{1}{2} & \text{if } i = 0 \\ 1 & \text{if } i \geq 1 \end{cases} \tag{2.12}$$

The array factor expression of an array consisting of *2M* by *2N*, depicted in Figure 2.3, with quadrantal symmetrical excited elements, is

$$F(u,v) = \sum_{m=1}^{M} \sum_{n=1}^{N} a_{mn} \cos\left(\frac{2m-1}{2}u\right)\cos\left(\frac{2n-1}{2}v\right) \tag{2.13}$$

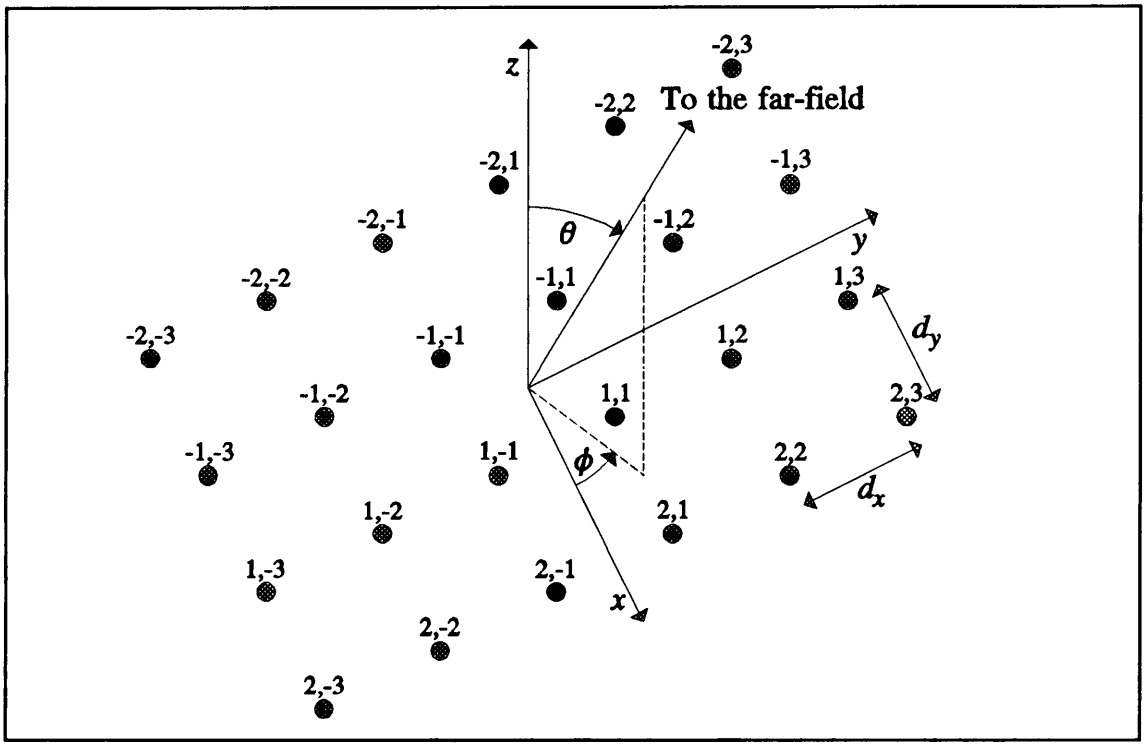

Figure 2.3 *2M* by *2N* Planar array geometry

© University of Pretoria Digitised by the Department of Library Services in support of open access to information, University of Pretoria, 2019

The vectors and matrices, necessary to write the performance indices (Section 2.3) in concise form, for general M by N rectangular planar array are [10] the excitation vector,

$$\bar{J} = [a_{11};\ a_{12};\ \ldots;\ a_{mn};\ \ldots;\ a_{MN}]^T \tag{2.14}$$

radiation vector,

$$\bar{F} = \begin{bmatrix} e^{jk(u+v)} \\ e^{jk(u+2v)} \\ \vdots \\ e^{jk(mu+nv)} \\ \vdots \\ e^{jk(Mu+Nv)} \end{bmatrix} \tag{2.15}$$

and b_{mn} (the components of $\bar{B}$)

$$b_{Nm+n-1;\,N\dot{m}+\dot{n}-1} = \operatorname{sinc}\left[k\sqrt{(n-\dot{n})^2 d_x^2 + (m-\dot{m})^2 d_y^2}\right] \tag{2.16}$$

in which

$$m,\dot{m} = 1,2,\ldots,M \quad and \quad n,\dot{n} = 1,2,\ldots,N \tag{2.17}$$

2.3 ARRAY PERFORMANCE INDICES

2.3.1 Introduction

The primary goal of antenna design is the establishment of a radiation pattern with specified characteristics. Such specifications must of course all be measurable in practice. Except for its terminal (network) properties, the parameters used to characterise the performance of an antenna are all dependant on the shape of the radiation pattern. Performance optimisation is therefore the process of maximisation or minimisation of certain pattern performance indices subject to constraints on others. Before such a process can be effected, it is of course necessary that these measures of

© University of Pretoria Digitised by the Department of Library Services in support of open access to information, University of Pretoria, 2019

performance be precisely and unambiguously defined. This will be done here. Though all of the performance specifications considered are applicable to antennas in general, the terminology here is specifically directed toward arrays.

2.3.2 Directivity and Excitation Efficiency

The directivity $D(\theta,\phi)$ in a direction (θ,ϕ) is defined as the ratio of the radiation intensity (radiated power per unit solid angle) in the direction (θ,ϕ) to the average radiation intensity [4: p.744, 10, 11].

$$D(\theta,\phi) = \frac{\bar{J}^T \tilde{A} \bar{J}}{\bar{J}^T \tilde{B} \bar{J}} \tag{2.18}$$

Let the maximum directivity of the pattern (in the direction of the pattern peak) of the given array be denoted by D_m. Furthermore, let D_{max} be the maximum possible directivity obtainable with the given array; this will be that obtained when the elements have identical excitations (in both amplitude and phase). The excitation efficiency is then defined as

$$\eta = \frac{D_m}{D_{\max}} \tag{2.19}$$

Here the conversion efficiency is assumed to be unity, so that gain and directivity $D(\theta,\phi)$ are identical.

2.3.3 Other Indices and Specifications

In an engineering problem an important question is that concerning the sensitivity of a particular synthesised array excitation. Since the practical realisation of the aperture distribution is never exact, it is important to ascertain how such imperfections will affect array factor. Tolerance sensitivity is a measure of the effect a imperfections in the aperture distribution $\bar{J}$ will have on the array factor [4, p.744]. A small tolerance sensitivity, that is, he array factor is not very sensitive to imperfections in $\bar{J}$ is always desirable.

Further specifications relating to the pattern are illustrated in Figure 2.4. All pattern sidelobe levels are measured relative to the pattern maximum, thus the array

© University of Pretoria Digitised by the Department of Library Services in support of open access to information, University of Pretoria, 2019

factor or pattern is normalised to its maximum value. The sidelobe level (*SLL*) is the level of the highest sidelobe with respect to the pattern maximum. The sidelobe ratio (*SLR*) is the reciprocal of the sidelobe level. Therefore the sidelobe level, in decibels, will be a negative number and the sidelobe ratio positive. In the shaped beam case, the ripple is defined as the maximum peak-to-peak deviation of the radiation pattern from the ideal behaviour in the shaped beam region. The beamwidth of the main beam can be specified in two ways, namely the -3dB (or half power) beamwidth and the beamwidth between first nulls.

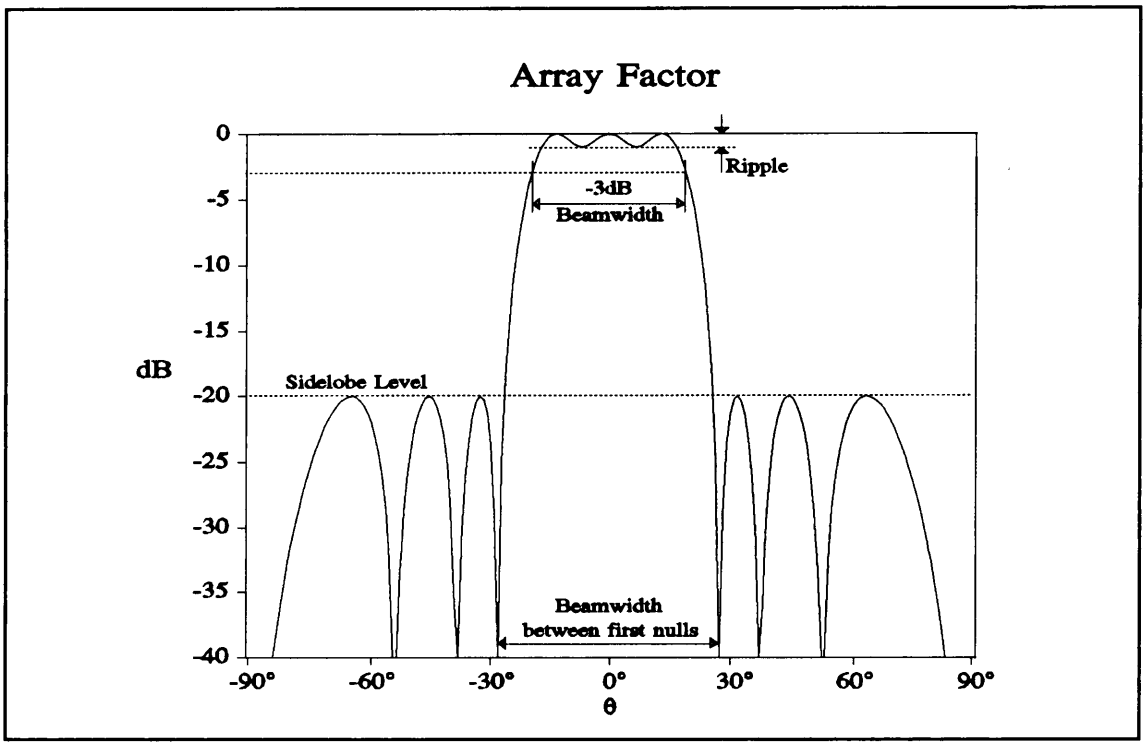

Figure 2.4 Array factor specifications

2.3.4 Shaped Beam Arrays

There can be no general method of specifying shaped beam patterns since each is shaped in its own general way! It is perhaps best to name some typical shaped beam patterns that might be desired by systems designers and to suggest the reasons why this might be so.

The most common shaped beam pattern is probably the *cosecant* elevation beam. This beam shape used in airport beacons. At a certain ground distance away from the beacon, the actual distance to the aircraft varies with the aircraft's altitude. This beam

© University of Pretoria Digitised by the Department of Library Services in support of open access to information, University of Pretoria, 2019

UNIVERSITEIT VAN PRETORIA
UNIVERSITY OF PRETORIA
YUNIBESITHI YA PRETORIA

shape radiates more electromagnetic energy at a higher elevation angle to compensate for the difference in actual distance to the aircraft.

A $cosec^2\theta \cdot cos\theta$ beam shape in the vertical plane and a pencil beam horizontal pattern is used for ground mapping radars. The vertical beam shape compensate for the difference in distance to and form a point on the ground with respect to the elevation angle θ

Flat-top patterns are widely in used in satellite applications, where a certain area must be illuminated by an electromagnetic field of uniform strength.

2.4 CLASSIFICATION OF ARRAY SYNTHESIS TECHNIQUES

Antenna array synthesis problems can be succinctly stated as that of finding the excitation $\bar{J}$, that will produce a radiation pattern $F(\theta,\phi)$ with certain performance indices maximised or constrained, and subject to specified constraints on the pattern and even the excitations themselves. Such constraints cannot be completely arbitrary and must be consistent with the basic physical properties of the array.

Array synthesis is, from a mathematical point of view, a problem of optimisation theory, and many engineers apply this approach. It can on the other hand in certain cases also be approached from the point of view of approximation theory. Early work was based almost entirely on the latter type of considerations, and research in this area continues. Optimisation and approximation theory are disciplines which are of course inextricably linked, though this connection is not always recognised in the array antenna area.

Work on the synthesis of antenna arrays may be divided up in a number of ways. For instance, one could classify synthesis techniques according to whether linear or planar arrays are being considered. Alternatively, synthesis methods could be separated into those which deal with continuous sources (from which array excitations are obtained by some form of sampling) or discrete elements directly (for which the array element excitations can be obtained in a direct manner without the need for any further approximation, sampling or perturbation procedures). On the other hand, synthesis techniques could be grouped in terms of whether they are applicable to single lobe high-

© University of Pretoria Digitised by the Department of Library Services in support of open access to information, University of Pretoria, 2019

UNIVERSITEIT VAN PRETORIA
UNIVERSITY OF PRETORIA
YUNIBESITHI YA PRETORIA

directivity or shaped beam patterns. Lastly, we could classify methods according to whether they are analytical in character or rely on some numerical optimisation procedure.

Most of the work on array synthesis methods described in the literature deals with the linear array problem. These methods are often incorporated in some way to synthesise planar arrays. However, this does not always provide the best results, and attempts have been made to devise approaches which tackle the planar array problem more effectively. Their use usually assumes a knowledge of the standard linear array methods.

2.5 DIRECT SYNTHESIS OF LINEAR ARRAYS OF DISCRETE ELEMENTS

2.5.1 Maximum Directivity for Fixed Spacing and Element Number

Consider an array with a given number of elements and a fixed spacing between elements, and assume that the element excitations necessary for maximisation of the directivity in the broadside direction are desired. The directivity can be written as the ratio of two quadratic forms (2.17), both of whose operator matrices are Hermitian, with that in the denominator being positive-definite. These properties enable the desired excitations to be obtained directly as the solution of a set of linear simultaneous equations. Results of such computations have been considered by Ma [2], Hansen [9], Cheng [10], Pritchard [25] and Lo et al. [66]. Hansen [9: Fig.2] has shown that for spacings above a half-wavelength, the maximum directivity is almost identical to that obtained when the elements are excited with uniform amplitude and phase. For smaller spacings the maximum directivity obtainable is greater than that of a uniform array; this phenomenon is called superdirectivity. However, the excitations required for superdirectivity have large oscillatory variations in amplitude and phase from one element to another [4: p.761], and are always associated with an enormously large tolerance sensitivity. For this reason fabrication difficulties are usually prohibitive and superdirectivity is avoided in most instances. Experimentally it is difficult to produce an array with a directivity much in excess of that produced by a uniformly excited array. In

© University of Pretoria Digitised by the Department of Library Services in support of open access to information, University of Pretoria, 2019

UNIVERSITEIT VAN PRETORIA
UNIVERSITY OF PRETORIA
YUNIBESITHI YA PRETORIA

general the sidelobes of a uniformly excited array will be too high for practical use; hence the synthesis techniques to be described immediately below.

2.5.2 Dolph-Chebyshev Synthesis

Rather than maximise the directivity of the array, consider the problem of minimisation of beamwidth; the two approaches are not necessarily equivalent. Beamwidth minimisation subject to a constraint on the sidelobe ratio is the classical array synthesis problem solved by C.L.Dolph in his monumental 1946 paper [12]. The underlying argument behind Dolph's approach has been put concisely by Hansen [9]: "A symmetrically tapered (amplitude) distribution over the array ..... is associated with a pattern having lower sidelobes than those of the uniform (amplitude) array. Lowering the sidelobes broadens the beamwidth ..... Some improvement in both beamwidth and efficiency is obtained by raising the farther out sidelobes. Intuitively one might expect equal level sidelobes to be optimum for a given sidelobe level". In order to synthesize such a pattern for broadside arrays with inter-element spacing greater than or equal to a half-wavelength, Dolph made use of the Chebyshev polynomials. Expressions for computing the required excitations can be derived from these polynomials. Such formulas have been derived by Barbiere [14], Stegen [15, 18], van der Maas [16] and Bresler [23]. With current computational capabilities those derived by Stegen [15] can be used directly.

Dolph [12] was able to prove that the array so synthesised is optimum in the sense that for the specified sidelobe ratio and element number, the beamwidth (between first nulls) is the narrowest possible. Alternatively, for a specified first-null beamwidth, the sidelobe level is the lowest obtainable from the given array geometry. This means that it is impossible to find another set of excitation coefficients yielding better performance, in both beamwidth and sidelobe ratio, for the given element number and uniform spacing d. It represents a closed form solution to the optimisation problem of beamwidth minimisation subject to sidelobe constraints.

The Dolph-Chebyshev theory is indispensable and serves as a firm foundation for sum pattern synthesis. It provides a means of understanding array principles and indicates upper bounds on the performance that can be achieved. However, it does have a number of drawbacks with regard to its use as a practical distribution. There is a

© University of Pretoria Digitised by the Department of Library Services in support of open access to information, University of Pretoria, 2019

UNIVERSITEIT VAN PRETORIA
UNIVERSITY OF PRETORIA
YUNIBESITHI YA PRETORIA

tendency of equal sidelobe level distributions such as the Dolph-Chebyshev to have large excitation peaks at the array ends (a non-monotonic distribution) for certain element number/sidelobe ratio combinations. For a given number of elements there will be a certain sidelobe ratio for which the distribution of excitations is "just" monotonic. If the number of elements is increased but this same sidelobe ratio is desired, the required distribution will be non-monotonic. Increasing the sidelobe ratio (lower sidelobes) will allow a monotonic distribution once more.

The peaks in the distribution at the array ends (called edge brightening) are not only disadvantageous in that they are difficult to implement and make an array which is realised more susceptible to edge effects, but they are also indicative of an increase in the tolerance sensitivity [4].

Optimum beamwidth arrays do not necessarily provide optimum directivity, especially if the array is large [3: p.91]. To see this, one can consider a Dolph-Chebyshev array with a fixed sidelobe ratio. Let the array size increase (increase the element number with the spacing held fixed), at each stage keeping the sidelobe ratio constant and normalising the radiation pattern. This is permissible because the directivity to be found at each stage is only dependent on the angular distribution of the radiation and not on any absolute levels. It is then observed that the denominator of the directivity expression is dominated by the power in the sidelobes after a certain array size is reached, and remains roughly constant thereafter. This is called directivity compression [3: p.91]. Thus it is found that the Dolph-Chebyshev distribution has a directivity limit [18] because of its constant sidelobe level property, and for a given array size and maximum sidelobe level, may not be optimum from a directivity point of view. To remove this limitation a taper must be incorporated into the far-out sidelobes.

2.5.3 Villeneuve Distributions

As recently as 1982 Hansen [4: p.698] could correctly state that there were "no discrete distributions that yield a highly efficient tapered sidelobe pattern" directly and that in designing most arrays a continuous distribution had to be sampled in some manner. For the narrow beam, low sidelobe pattern, this is no longer the case as a result of an ingenious approach devised by Villeneuve [26]. The method utilises the important principle of synthesising aperture distributions by correct positioning of the space factor

© University of Pretoria Digitised by the Department of Library Services in support of open access to information, University of Pretoria, 2019

zeros. The Villeneuve distribution is the discrete equivalent of the highly desirable Taylor $\bar{n}$ distribution of continuous line sources (to be discussed in Section 2.6.3). The array element excitations can be obtained in a direct manner with the Villeneuve approach.

The application of the Villeneuve procedure consists of the following: Take an array of elements with the maximum sidelobe level specified. The first step consists of determining the space factor zeros for a Dolph-Chebyshev distribution with the same sidelobe level. Next determine the zeroes of a uniformly excited array of the same number of elements (who's array factor will have a tapered sidelobe envelope). Next alter the zeroes of the Chebyshev array so that all except the first $\bar{n}$-1 zeroes now coincide with those of the uniform array. In addition, multiply each of the first $\bar{n}$-1 Chebyshev zeros by a dilation factor σ [4: p.722]. Use these final zeroes of the perturbed Chebyshev array to determine the final element excitations. Villeneuve [26] has devised efficient ways of doing this. These excitations are those of a discrete "Taylor-like" distribution (Section 2.6.3), with the close-in sidelobes close to the design maximum specified, and the further out ones decreasing at the rate $1/u$ $(u=Nd/\lambda \sin\theta)$ in amplitude as their position becomes more remote from the main beam. As with the continuous Taylor distribution, $\bar{n}$ is a design variable. A comparison of the excitation efficiencies of the Villeneuve (discrete) and Taylor (continuous) distributions has been published by Hansen [27]. The above technique is now generally referred to as the Villeneuve $\bar{n}$ distribution [27].

Finally, a generalised Villeneuve $\bar{n}$ distribution has been developed by McNamara [28] which can be used to directly synthesize discrete array distributions for high efficiency sum patterns of arbitrary sidelobe level and envelope taper. The Dolph-Chebyshev distribution serves as a "parent" space factor. The correct perturbation of the zeros of this "parent" space factor serves to incorporate the sidelobe behaviour desired, while at the same time keeping the excitation efficiency and beamwidths as close to their optimum values as is possible under the required sidelobe ratio and envelope taper conditions. The level of the first sidelobe is set by the parent Dolph-Chebyshev distribution, the envelope taper rate controlled by a parameter υ, and the point at which the required taper proper begins determined by the transition index $\bar{n}$. The excitations are obtained from the perturbed space factor zeros through solution of a set of linear

© University of Pretoria Digitised by the Department of Library Services in support of open access to information, University of Pretoria, 2019

simultaneous equations. The synthesis procedure is rapid and consequently design trade-off studies are feasible. The proper choice of the values of $\bar{n}$ and υ for a particular application will depend on the relative importance of the peak sidelobe level compared to that of the farther-out sidelobes, the root-mean-square sidelobe ratio desired, and their effect on the excitation efficiency.

2.5.4 Synthesis of Linear Arrays with Shaped Beams

The array factor can be divided into two regions, the shaped region consisting of the shaped main beam, and the sidelobe region. The shaping function, $S(\psi)$, represents the ideal behaviour of the array factor in the shaped region. Ideally the array factor must be zero in the sidelobe region, although this is physically impossible.

The array factor resulting from an array of identical discrete radiators (elements) is the sum of the excitation of each element weighted by the path length difference (or spatial phase delay) from each element to the far-field point. The array factor summation is very similar to a Fourier series of the same order as the number of elements in the array. The Fourier series synthesis method [5: p.531] is, then, to use element excitations equal to the Fourier series coefficients calculated from the desired pattern. Due to the limited extent (harmonics) of the Fourier series, the resulting array factor exhibit very large ripple in the shaped region with high sidelobes in the sidelobe region.

A particularly convenient way to synthesize a radiation pattern is to sample the ideal pattern at various points. The WoodWard-Lawson [30, 5: p.526], technique is the most popular of these methods. The technique relies on the fact that any realisable pattern, of a N-element array, can be analyzed as the weighted summation of a set of N orthogonal beams, each having a basic $sin(Nx)/sin(x)$ shape. The maximum of each of the $sin(Nx)/sin(x)$-shaped beams coincides with a zero in all the other beams. Woodward's synthesis technique samples the ideal pattern at increments of $2\pi/N$. The synthesized array is thus the superposition of array factors from N uniform amplitude, linear phase (or uniform progressive phase) arrays with the phase increment of each array such that the array factor peak is placed at the sampling point. Although the array factor is equal to the ideal pattern at the sample points, it exhibits large ripples in the shaped region and high uncontrollable sidelobes in the sidelobe region.

© University of Pretoria Digitised by the Department of Library Services in support of open access to information, University of Pretoria, 2019

An objection to the Woodward method is that in only uses data form N points, whereas there are $2N-1$ degrees of freedom (N amplitudes and $N-1$ relative phases) available. Milne published a method [36] that effectively takes $2N-1$ sample points to determine a realisable array factor

Consider an array of $N+1$ elements. By the introduction of the following substitution $w=e^{j\psi}$, the array factor (2.2) can be written as a polynomial of degree N, with N distinct roots.

$$F(w) = \sum_{n=0}^{N} a_n w^n = \prod_{n=1}^{N} (w - w_n) \tag{2.20}$$

Schelkunoff [31] introduced the extremely useful concept of constructing a unit circle in the complex w plane. The array factor is thus controlled by the placement of the roots w_n. The synthesis of any desired pattern can be viewed as a problem of finding the proper positions of the roots. Multiplying out the factors will yield the relative excitations. Three obvious features can be noted viz.

(a) If the roots are placed on the unit circle, a pattern with deep nulls will result.

(b) If successive roots are moved closer together (further apart) the intervening lobe will be lower (higher).

(c) If some of the roots are moved off the unit circle, null-filling will result and a shaped beam pattern can be achieved.

Orchard et al. [33] presented an iterative method by which the angular and radial positions of all the roots are simultaneously adjusted so that the amplitude of each ripple in the shaped region and the height of each sidelobe in the in the nonshaped region are individually controlled. The method was extended by Kim and Elliott [35] to produce pure real distributions for symmetric patterns, eg flat-top patterns.

© University of Pretoria Digitised by the Department of Library Services in support of open access to information, University of Pretoria, 2019

UNIVERSITEIT VAN PRETORIA
UNIVERSITY OF PRETORIA
YUNIBESITHI YA PRETORIA

2.6 ANALYTICAL SYNTHESIS OF CONTINUOUS LINE SOURCE DISTRIBUTIONS

2.6.1 Introduction

Although arrays of discrete radiating elements are being dealt with in this work, no review of synthesis techniques would be complete without reference to similar work on the synthesis of continuous line-source distributions. Line-source synthesis is important in the array context for several reasons. Firstly, some general principles are equally applicable to arrays. Secondly, continuous distributions can be sampled for use with discrete arrays. Furthermore, the direct discrete array synthesis methods have generally developed "under the guidance" of the theory on continuous distributions.

Perhaps the most startling result on continuous distributions is that obtained by Bouwkamp and de Bruyn [38], who showed that with a continuous line-source of fixed length it is possible (in theory) to achieve any desired directivity. Although this implies that there is no limit to the directivity, any directivity increase above that obtained from the aperture when it is uniformly excited is accompanied by a sharp increase in the net reactive power required at the source to produce it [7: p.3], and thus a large tolerance sensitivity. Practical considerations therefore make it unacceptable, as in the case of the unconstrained maximisation of the directivity of the discrete array (Section 2.5.1). To be realisable physically, some constraint has to be placed on the proportion of reactive to radiative power, or equivalently on the quality factor [3: pp.3-4].

It is customary, when dealing with continuous line-source distributions, to use the variable $u=(L/\lambda)\sin\theta$, where L is the length of the source and λ is free-space wavelength. This practice will be followed here.

2.6.2 Maximisation of Directivity Subject to a Sidelobe Level Constraint

The next question regarding continuous distributions is that of the determining of a distribution which provides the narrowest beamwidth for a given sidelobe level, and vice versa. This was answered by Taylor [39], who used the Dolph-Chebyshev theory as starting point. Using an asymptotic relationship for the Chebyshev polynomials given by van der Maas [16], Taylor derived the continuous equivalent of the Dolph-Chebyshev distribution. This distribution has a pattern with all sidelobes of equal level, and is

© University of Pretoria Digitised by the Department of Library Services in support of open access to information, University of Pretoria, 2019

UNIVERSITEIT VAN PRETORIA
UNIVERSITY OF PRETORIA
YUNIBESITHI YA PRETORIA

optimum in the sense that it provides the narrowest beamwidth for a given sidelobe ratio of any non-superdirective distribution. Taylor called this the "ideal" line-source distribution. "Ideal" because of the fact that it is not realizable, having a singularity at each end.

2.6.3 Maximisation of Directivity Subject to a Tapered Sidelobe Level Constraint

A solution to the problem of singularities at the ends of the distribution was also devised by Taylor [38]. He recognised that the synthesis problem is one of correctly positioning the zeros of the space factor. Taylor observed that close-in zeros should maintain their spacings to keep the close-in sidelobes suitably low and the beamwidth narrow. But at the same time further out sidelobes should decay as $1/u$ [3: p.55, 4: p.720]. Such sidelobe decay is found in the space factor of a uniform line-source distribution. Taylor stretched the u scale slightly by a dilation factor σ slightly greater than unity (so that the close-in zero locations are not shifted much) and chosen such that at some point a shifted zero is made to coincide with an integer $\bar{n}$. From this transition point, the zeros of the ideal line-source are replaced by those of the uniform line-source. This pattern has its first few sidelobes (which number is determined by the position of the transition point selected) roughly equal, with a $1/u$-sidelobe decay thereafter. The corresponding aperture distribution is then found as a Fourier series obtained from the above information on the zeros [3: p.58]. The final result is a distribution (the Taylor $\bar{n}$ distribution) which, for a given sidelobe ratio, gives both a narrower beamwidth and higher directivity than any comparable continuous line-source distribution. Information relating the sidelobe ratio, dilation factor and $\bar{n}$ values has been given by Hansen [3: p.57]. Also given are expressions for the aperture distribution itself [3: p.58]. Too large a value for $\bar{n}$ (exactly how large depends on the specified sidelobe ratio) implies that the ideal line-source distribution is "being approached too closely". The aperture distribution then becomes non-monotonic with peaks at the aperture ends (though the singularities of the ideal source do not occur), with an accompanying increase in excitation tolerances. The Taylor $\bar{n}$ distribution was generalised by Rhodes [7: pp.129-137] to a distribution dependent on the transition variable $\bar{n}$, and an additional variable, which controls the taper rate of the sidelobe envelope for a selected transition zero. The "ideal" line-source and Taylor $\bar{n}$ approaches just described are special cases

© University of Pretoria Digitised by the Department of Library Services in support of open access to information, University of Pretoria, 2019

UNIVERSITEIT VAN PRETORIA
UNIVERSITY OF PRETORIA
YUNIBESITHI YA PRETORIA

of this generalised distribution.

A third continuous distribution due to Taylor is his one-parameter line-source distribution [3: p.58]. The Taylor $\bar{n}$ distribution essentially selects a design between the "ideal" and one-parameter cases. However, for the same first sidelobe ratio, the Taylor $\bar{n}$ distribution has a higher excitation efficiency (and hence directivity), and is therefore used more often. The reason for this is that the $\bar{n}$ distribution tends to flatten out at the ends of the line source while the one-parameter case does not.

The Taylor one-parameter distribution was generalised by Bickmore and Spellmire, whose work has been reported in [40] and [4: pp.731-733], into a two-parameter continuous line-source distribution. One of the parameters selects the starting sidelobe ratio, while the other selects the rate of decay of the sidelobes. These two parameters are completely independent and the space factor is the Lambda function. As expected, the Taylor one-parameter distribution can be shown to be a special case of the Bickmore-Spellmire distribution.

2.6.4 Discrete Versus Continuous Line Source Synthesis

It is clear from the previous section that the theory of continuous aperture line-source distributions for sum patterns is extensive and well-developed. If these are to be used with arrays of discrete elements, some form of discretization process must be performed. The earliest discretization methods simply sampled the continuous distributions at the element locations. Unless the arrays are extremely large (that is, larger than most practical arrays) a badly degraded pattern may be obtained [41, 58]. An alternative technique was proposed by Winter [42]. The initial array element excitations are determined by sampling the continuous distribution and then iteratively adjusting these using Newton-Raphson minimisation of an error expression comprised of the sum of the squares of the differences between calculated (discrete) and specified (continuous) levels for a selected number of sidelobes. A more sophisticated yet direct alternative method was devised by Elliott [1: pp.172-180, 41]. This method matches zeros. Instead of sampling the continuous aperture distribution, one requires that the pattern zeros of the continuous case also occur in the starting pattern of the discrete case. If the resulting pattern does not meet the design goal, a linear perturbation of the positions is iteratively applied to the discrete distribution in order to bring the final

© University of Pretoria Digitised by the Department of Library Services in support of open access to information, University of Pretoria, 2019

UNIVERSITEIT VAN PRETORIA
UNIVERSITY OF PRETORIA
YUNIBESITHI YA PRETORIA

pattern within specification.

2.7 TECHNIQUES FOR PLANAR ARRAY SYNTHESIS

2.7.1 Introduction

The previous sections form a relatively complete summary of analytical methods that can be used to synthesise linear arrays providing high directivity, low sidelobe patterns. Regarding their relation to planar array synthesis, Elliott [1: p.196] notes that: "Under certain circumstances, much of what was developed there (for linear arrays) can be carried over to apply to planar arrays. However, practical considerations will at times require the use of design techniques that are peculiar to planar arrays." The linear array synthesis methods relying on root-placement can't be extended to planar synthesis due to the lack of a general two-dimensional factorization theorem.

In order to describe a planar array geometry it is necessary to specify both its element lattice and the boundary shape, as mentioned earlier. Again, only those synthesis techniques applicable to the rectangular lattice case are of interest here. In what follows we will briefly list those methods for planar arrays that can be classed as "analytical", in that no form of iteration, perturbation or numerical optimisation is needed (although a considerable amount of computation may still be required) once the set of specifications for the final pattern has been set.

2.7.2 Collapsed Distributions

Consider a planar array with a rectangular lattice. If the excitations of the elements of each row are added a linear array along the y-axis is obtained. We refer to this as the *collapsed distribution* along the y-axis. Similarly, if the excitations of the elements of each column are added a linear array (collapsed distribution) along the x-axis is obtained [43]. The above comments apply to the rectangular lattice case irrespective of the boundary shape.

© University of Pretoria Digitised by the Department of Library Services in support of open access to information, University of Pretoria, 2019

UNIVERSITEIT VAN PRETORIA
UNIVERSITY OF PRETORIA
YUNIBESITHI YA PRETORIA

2.7.3 Separable Distributions

For rectangular arrays, if the boundary shape is square or rectangular, and if the aperture distribution is separable, the pattern is the product of the patterns of two spatially orthogonal linear arrays (collapsed distributions), and all the methods mentioned for linear arrays in earlier sections can be extended readily. However, separable distributions suffer from some directivity limitations [1: p.211] which are highly undesirable in practice. The separable distribution *overachieves* in most of the sidelobe region (i.e. gives sidelobe levels far lower than necessary). This reduction is bought at the price of beam broadening with its concomitant lowering in directivity. These limitations can only be overcome through use of ϕ-symmetric patterns.

2.7.4 Direct Synthesis of Discrete Arrays

The Dolph-Chebyshev technique has not been extended to general planar arrays. However, Tseng and Cheng [46] have shown how it can be done for a planar array with a rectangular lattice and a rectangular boundary shape, if the number of elements in each direction (that is, the x- and y-directions) is the same[2] using the Baklanov transformation [45]. This so-called Tseng-Cheng distribution is non-separable, and gives a Dolph-Chebyshev pattern in every ϕ-cut. More recently, Kim and Elliott [48] have shown that the restriction of equal numbers of elements in each direction can be lifted, but only for certain fixed relationships between the element number in each direction.

2.7.5 Direct Synthesis of Continuous Planar Source Distributions

Taylor [49] extended his continuous line-source analysis to the case of a planar aperture with circular boundary shape with a ϕ-symmetric aperture distribution. A one-parameter circular distribution has been described by Hansen [50] following the procedure Taylor used for his one-parameter line source (see Section 2.6.3). Although similar to the Taylor distribution, the Hansen one-parameter distribution is "slightly less efficient, but the required distribution is smoother and more robust" [4: p.855]. Various extensions to Taylor's method have been proposed [52, 53, 54]. The most significant

[2]But the inter-element spacing in the x- and y-direction need not be equal, and thus the array need not be square.

© University of Pretoria Digitised by the Department of Library Services in support of open access to information, University of Pretoria, 2019

UNIVERSITEIT VAN PRETORIA
UNIVERSITY OF PRETORIA
YUNIBESITHI YA PRETORIA

contribution was made by Elliott and Stern [55, 56], who succeeded in combining Taylor's method with the linear array synthesis method proposed by Orchard, Elliott and Stern [33].

2.7.6 The Sampling of Continuous Planar Distributions For Use as Excitations in Planar Arrays

If the continuous distributions described in Section 2.7.5 are to be used with arrays of discrete elements, some form of discretization must be performed. As indicated for the linear array situation (in Section 2.6.4), the naive direct sampling of the continuous distribution may lead to noticeable pattern degradation unless the array is very large[3]. Unfortunately, the rather convenient improved sampling ideas for linear arrays, discussed in Section 2.6.4, do not carry over to planar arrays, reasons for which are given by Elliott [1: pp.243-249]. Less direct approaches (albeit using the continuous distributions as starting points) are required to iteratively alter the sampled distribution in order to improve the array pattern performance, and these are better classified as numerical synthesis procedures to be discussed in Section 2.8.

2.8 NUMERICAL SYNTHESIS OF ARRAYS

2.8.1 Introduction

Numerical techniques which do not either take advantage of the peculiar properties of the array factor or of information available from the analytical solution to related synthesis problems, or both, are usually slowly converging and inefficient. Therefore, although it is always possible to formulate the array synthesis problem very precisely as a nonlinear optimisation problem with nonlinear constraints, such general optimisation approaches are in practice undesirable. More direct methods are preferred which exploit known characteristics and insight into the array synthesis problem.

In order to summarise these array synthesis methods it will be convenient to

---

[3]Exactly what can be considered a "very large" array depends also on the sidelobe levels involved.

© University of Pretoria Digitised by the Department of Library Services in support of open access to information, University of Pretoria, 2019

divide the numerical synthesis approaches into two groups:

(a) Those that can be considered perturbation methods which begin with results obtained from one of the synthesis procedures discussed in earlier sections.

(b) Those that make use of minimisation/maximisation (i.e.optimisation algorithms) of some array performance index subject to a set of constraints.

2.8.2 Iterative Perturbation Methods

In Section 2.7.5 the direct synthesis of continuous planar source distributions was mentioned. It was indicated there that the relatively straightforward altered sampling approaches applicable to linear arrays do not carry over to the planar array case. Elliott [1: pp.243-249] has described an iterative procedure which tries to improve on the starting conventionally-sampled continuous planar distribution, the final set of non-separable excitations being distinctly different from the starting ones. Application of this iterative technique to the sampling of continuous planar distributions [1: pp.256-261] is also described.

2.8.3 Use of Collapsed Distributions

The concept of a collapsed distribution was described in Section 2.7.2. A planar array synthesis method which uses linear array synthesis on the two orthogonal collapsed distributions of a given planar array, and then spreads out the collapsed distributions using the conjugate gradient technique or the iterative method of Section 2.8.2, has been described by Elliott [43]. The method is applicable to both sum and difference patterns and can yield non-separable final distributions. It has the advantage of beginning with the use of established linear array techniques. In spite of the claims that such a method is a sort of panacea to all planar array synthesis problems, this is not always the case, as evidenced by attempts at further improvements by Autrey [57] and Elliott and Stern [55].

© University of Pretoria Digitised by the Department of Library Services in support of open access to information, University of Pretoria, 2019

2.8.4 The Method of Generalised Projections

The use of the so-called method of projections for the synthesis of antenna arrays has grown out of the development of techniques in the field of image processing, in particular image restoration. Details of the method will not be given here, since these are clearly described in Levi and Stark [58]. Suffice it to say that an early version of the method (called the method of alternating projections) was applied by Prasad [60] to the planar array synthesis problem. Limitations on the type of constraints that could be used led to improvements resulting in the method of successive (or generalised) projections. This has been applied to arrays by Poulton [61]. More recently the generalised projection technique has been used as the basis for a synthesis method [62, 63, 64, 65] which allows constraints not only on the sidelobe levels but also on the excitations (eg. dynamic range, smoothness of the distribution), something that is most advantageous when having to deal with mutual coupling effects.

2.8.5 Constrained Minimisation/Maximisation (Optimisation) of Some Array Performance Index Subject to a Set of Constraints

These methods differ in :

(a) The way in which the array problem is formulated as an optimisation problem (e.g. the choice of performance indices to be minimised or maximised).

(b) The type of constraints which are applied (e.g. limited Q, maximum sidelobe levels allowed).

(c) The particular optimisation algorithm used (e.g. linear programming, quadratic programming, use of ratios of Hermitian quadratic forms, general nonlinear function maximisation/minimisation).

A summary of general methods of this nature has been given by Hansen [4: pp.743-748]; as indicated earlier the use of such general methods are not always practical. Detailed overviews have also been given by Cheng [10] and Lo et al. [66], as well as Sanzgiri and Butler [67]. If the directivity must be maximised subject to a set of sidelobe constraints, the papers by Einarsson [68] and DeFord & Gandhi [71] largely contain all the information one might need for this type of synthesis. Einarsson [68] introduced a technique which maximises directivity by minimising an associated quadratic

© University of Pretoria Digitised by the Department of Library Services in support of open access to information, University of Pretoria, 2019

UNIVERSITEIT VAN PRETORIA
UNIVERSITY OF PRETORIA
YUNIBESITHI YA PRETORIA

form. By writing the sidelobe constraints as a linear set, he was able to formulate the optimisation problem as a quadratic programming one.

2.9 SYNTHESIS OF PLANAR ARRAYS WITH CONTOURED BEAM PATTERNS

Contoured beam antennas are primarily used on spacecraft or satellite. The satellite antennas are required to have radiation patterns shaped in such a way that some given irregularly shaped angular region on the earth is illuminated with a specified minimum gain in order to achieve an adequate signal-to-noise ratio over the said service area. Such shaped beams are also said to have a *contoured footprint* on the earth [56]. The ideal antenna would have uniform gain over the coverage region and no radiation elsewhere, in order to best utilise the limited spacecraft transmitter power and reduce possible interference problems with other coverage areas. The fact that a real antenna is of finite size, along with several other practical limitations, means that there will be some sidelobe radiation outside the defined irregularly shaped coverage region. Presently, this is accomplished using a parabolic reflector and a horn cluster feed. Each feed horn results in a pencil beam being directed to a sub-portion of the reflector to be illuminated. The mosaic overlapping pencil beams gives a quasi-uniform coverage of the designated area. Several methods, all employing optimization techniques, have been proposed to synthesize this antenna configuration. Galindo-Israel et al. [78] and Klein [79] adopted a minimax optimisation procedure, while Wood and Boswell [80] used spherical wave expansion to obtain global coverage. This antenna configuration suffers from fairly high ripple in the shaped region and provides poor control of the sidelobe levels, unless an excessive number of beams are used.

Jorgensen [81] used the method of aperture field synthesis to provide contoured beams with an antenna consisting of a shaped reflector with a single feed.

Observing that the size, mass and complexity (especially of the feed arrays) of satellite antennas has grown significantly with each new system, Bornemann, Balling and English [82] have remarked that:

"If the trend toward increased multibeam frequency reuse and larger radiating

© University of Pretoria Digitised by the Department of Library Services in support of open access to information, University of Pretoria, 2019

UNIVERSITEIT VAN PRETORIA
UNIVERSITY OF PRETORIA
YUNIBESITHI YA PRETORIA

apertures continues, the feed array size will ultimately exceed the reflector size and the antenna mass and volume requirements will have an even more significant impact on spacecraft design and launch costs. Thus, it may become advantageous to eliminate the reflector and excite the feed array as a multiple beam array in which the amplitude and phase of each radiating element is a design variable. This approach is a potential key antenna technology to meet prospective future satellite traffic requirements which clearly point to the direction of electronically reconfigurable and steerable antennas."

All the planar synthesis techniques mentioned in Section 2.7 can be used synthesize the *direct radiating array*. Bornemann [82] uses a method similar to Woodward's, applied to a planar array, to achieve various complex beamshapes and contours. Guy [75] has reported that successful design of contoured beam antennas has been achieved by specifying the far-zone pattern requirement in two dimensions. Elliott [56] proposed an extension of Taylor's circular aperture pattern synthesis technique, to synthesize a continuous distribution. The continuous circular distribution is then discretisized to obtain the element excitations.

2.10 PLANAR ARRAY SYNTHESIS TECHNIQUES DEVELOPED IN THIS THESIS

The conventional synthesis methods have been treated in the previous sections. Two inadequacies have been identified: firstly, there is currently no direct synthesis technique for high directivity discrete planar arrays that have been studied in any detail and secondly, no direct method exists to synthesise a array factor with an arbitrary contoured main beam. Methods to address these inadequacies have been developed in this thesis and are summarised here.

There has until the present time been no planar array equivalent of the Villeneuve linear array $\bar{n}$-distribution. Chapter 3 of this thesis extends existing techniques to such an exact procedure for planar arrays. A parametric study of the performance of the resulting array is also conducted.

© University of Pretoria Digitised by the Department of Library Services in support of open access to information, University of Pretoria, 2019

UNIVERSITEIT VAN PRETORIA
UNIVERSITY OF PRETORIA
YUNIBESITHI YA PRETORIA

Currently no direct synthesis technique exists to produces discrete planar arrays with contoured beams. Chapter 4 considers the development of a such a new planar array synthesis technique. The synthesis technique developed utilises a transformation that divides the problem into two decoupled sub-problems. In the antenna array context, one sub-problem consists of a linear array synthesis, for which there exist powerful methods for determining appropriate element excitations. The other involves the determination of certain coefficients of the transform in order to achieve the required footprint contours. The number of coefficients which need to be used depends on the complexity of the desired contour, but is very small in comparison to the number of planar array elements. The size required for this prototype linear array depends on the number of transformation coefficients used and the planar array size. Simple formulas then determine the final planar array excitations from the information forthcoming from the above two sub-problem solutions. Thus the method is computational efficient. Simple formulas for the calculation of the transformation coefficients for circular and elliptical contours will be derived, but the more general contour problem is also discussed. Application of the newly developed transformation technique is examined by a number of specific examples.

Finally, Chapter 5 completes the thesis by drawing a number of general conclusions.

© University of Pretoria Digitised by the Department of Library Services in support of open access to information, University of Pretoria, 2019

UNIVERSITEIT VAN PRETORIA
UNIVERSITY OF PRETORIA
YUNIBESITHI YA PRETORIA

2.11 REFERENCES

[1] R.S.Elliott, *Antenna Theory and Design*, Englewood Cliffs: Prentice-Hall, 1981.

[2] M.T.Ma, *Theory and Application of Antenna Arrays*, New York: John Wiley & Sons, 1974.

[3] R.C.Hansen, *Microwave Scanning Antennas, Volume 1*, New York: Academic Press, 1964.

[4] R.C.Hansen, "Linear arrays", Chapter 9 of *The Handbook of Antenna Design: Volume 1 and 2*, A.W.Rudge, K.Milne, A.D.Olver and P.Knight (Edits.), London: Peter Peregrinus, 1982.

[5] W.L.Stutzman and G.A.Thiele, *Antenna Theory and Design*, New York: John Wiley and Sons, 1981.

[6] R.E.Collin and F.J.Zugker, Chapter 5 of *Antenna Theory: Part 1*, New York: McGraw-Hill, 1969

[7] D.R.Rhodes, *Synthesis of Planar Antenna Sources*, London: Clarendon Press, 1974.

[8] R.C.Hansen, "Planar arrays", Chapter 10 of *The Handbook of Antenna Design: Volume 1 and 2*, A.W.Rudge, K.Milne, A.D.Olver and P.Knight (Edits.), London: Peter Peregrinus, 1982.

[9] R.C.Hansen, "Fundamental limitations in antennas", *Proc. IEEE*, Vol.69, No.2, pp.170-182, Feb.1981.

[10] D.K.Cheng, "Optimisation techniques for antenna arrays", *Proc. IEEE*, Vol.59, No.12, pp.1664-1674, Dec.1971.

[11] D.A.McNamara, "Quadratic forms for the performance indices of symmetrical and anti-symmetrical linear arrays", *Electron. Lett.*, pp.148-149, Vol.23, No.4, Feb.1987.

[12] C.L.Dolph, "A current distribution for broadside arrays which optimises the relationship between beam width and side-lobe level", *Proc. IRE*, Vol.34, pp.335-348, June 1946.

[13] H.J.Riblet, "Discussion on 'A current distribution for broadside arrays which optimises the relationship between beam width and sidelobe level'.", *Proc. IRE*, Vol.35, pp.489-492, May 1947.

[14] D.Barbiere, "A method of calculating the current distribution of Tschebyscheff arrays", *Proc. IRE*, Vol.40, pp.78-82, Jan.1952.

© University of Pretoria Digitised by the Department of Library Services in support of open access to information, University of Pretoria, 2019

UNIVERSITEIT VAN PRETORIA
UNIVERSITY OF PRETORIA
YUNIBESITHI YA PRETORIA

[15] R.J.Stegen, "Excitation coefficients and beamwidths of Tschebyscheff arrays", *Proc. IRE*, Vol.41, pp.1671-1674, Nov.1953.

[16] G.J.van der Maas, "A simplified calculation for Dolph-Tchebycheff arrays", *J. Appl. Phys.*, Vol.25, No.1, pp.121-124, Jan.1954.

[17] J.L.Brown, "A simplified derivation of the Fourier coefficients for Chebyshev patterns", *Proc. IEE*, Vol.105C, pp.167-168, Nov.1957.

[18] R.J.Stegen, "Gain of Tchebycheff arrays", *IRE Trans. Antennas Propagat.*, Vol.AP-8, pp.629-631, Nov.1960.

[19] J.L.Brown, "On the determination of excitation coefficients for a Tchebycheff pattern", *IRE Trans. Antennas Propagat.*, Vol.AP-10, pp.215-216, March 1962.

[20] C.J.Drane, "Derivation of excitation coefficients for Chebyshev arrays", *IEE Proc.*, Pt.H, Vol.110, pp.1755-1758, Oct.1963.

[21] C.J.Drane, "Dolph-Chebyshev excitation coefficient approximation", *IEEE Trans. Antennas Propagat.*, Vol.AP-12, pp.781-782, Nov.1964.

[22] H.E.Salzer, "Calculating Fourier coefficients for Chebyshev patterns", *Proc. IEEE*, Vol.63, pp.195-197, Jan.1975.

[23] A.D.Bresler, "A new algorithm for calculating the current distributions of Dolph-Chebyshev arrays", *IEEE Trans. Antennas Propagat.*, Vol.AP-28, No.6, pp.951-952, Nov.1980.

[24] F.Ares and E.Moreno, "New method for computing Dolph-Chebyshev array, and its comparison with other methods", *IEE Proc.* Pt.H, Vol.135, No.2, pp.129-131, April 1988.

[25] R.L.Pritchard, "Optimum directivity patterns for linear point arrays", *J. Acoust. Soc. Amer.*, Vol.25, No.5, pp.879-891, Sept.1953.

[26] A.T.Villeneuve, "Taylor patterns for discrete arrays", *IEEE Trans. Antennas Propagat.*, Vol.AP-32, No.10, pp.1089-1093, Oct.1984.

[27] R.C.Hansen, "Aperture efficiency of Villeneuve-n̄ arrays", *IEEE Trans. Antennas Propagat.*, Vol.AP-33, No.6, pp.668-669, June 1985.

[28] D.A.McNamara, "Generalised Villeneuve n̄-distribution", *IEE Proc.*, Pt.H, Vol.136, No.3, pp.245-249, June 1989.

[29] W.L.Stutzman, "Sidelobe controle of antenna pattern", *IEEE Trans. Antennas Propagat.*, Vol.AP-20, No.1, pp.102-104, Jan.1972.

© University of Pretoria Digitised by the Department of Library Services in support of open access to information, University of Pretoria, 2019

UNIVERSITEIT VAN PRETORIA
UNIVERSITY OF PRETORIA
YUNIBESITHI YA PRETORIA

[30] P.M.Woodward, "Method of calculating the field over a plane aperture required to produce a given polar diagram", *J. IEE*, Pt.IIIA, Vol.93, pp.1554-1558, 1947.

[31] S.A.Shelkunoff, "A Mathematical theory of linear arrays", *Bell Syst. Tech. J.*, Vol.22, pp80-107, 1943.

[32] R.S.Elliott, "Improved pattern synthesis for equispaced linear arrays", *Alta Frequenza*, Vol.52, pp.12-17, 1983.

[33] H.J.Orchard, R.S.Elliott and G.J.Stern, "Optimising the synthesis of shaped beam antenna patterns", *IEE Proc.*, Pt.H, Vol.132, No.1, pp.63-68, Feb.1985.

[34] R.S.Elliott, "Array pattern synthesis", *IEEE Antenna Propagat. Soc. Newsletter*, pp.5-9, Oct.1985.

[35] Y.U.Kim and R.S.Elliott, "Shaped-pattern synthesis using pure real distributions", *IEEE Trans. Antennas and Propagat.*, Vol.36, No.11, pp.1645-1649, Nov.1988.

[36] K.Mline, "Synthesis of power radiation pattern for linear array antennas", *IEE Proc.*, Pt.H, Vol.134, No.3, pp.285-296, June 1987.

[37] W.-X.Zhang and Y.-M.Bo, "Pattern synthesis for linear equal-spaced antenna array using iterative eigenmodes method", *IEE Proc.* Pt.H, Vol.135 No.3, pp.167-170, June 1988.

[38] C.J.Bouwkamp and N.G.de Bruyn, "The problem of optimum current distribution", *Philips Res. Rep.*, Vol.1, pp.135-158, 1945-1946.

[39] T.T.Taylor, "Design of line-source antennas for narrow beamwidth and low sidelobes", *IRE Trans. Antennas Propagat.*, Vol.AP-3, pp.16-28, Jan.1955.

[40] R.W.Bickmore and R.J.Spellmire, "A two-parameter family of line sources", *Rept. TM595*, Hughes Aircraft Co., Culver City, 1956.

[41] R.S.Elliott, "On discretizing continuous aperture distributions", *IEEE Trans. Antennas Propagat.*, Vol.AP-25, No.5, pp.617-621, Sept.1977.

[42] C.F.Winter, "Using continuous aperture illuminations discretely", *IEEE Trans. Antennas Propagat.*, Vol.AP-25, No.5, pp.695-700, Sept.1977.

[43] R.S.Elliott, "Array pattern synthesis - Part II: Planar arrays", *IEEE Antennas Propagat. Soc. Newsletter*, pp.5-10, April 1986.

[44] N.Goto, "Non-separable pattern of planar arrays", *IEEE Trans. Antennas Propagat.*, Vol.AP-20, No.1, pp.104-106, Jan.1972.

[45] Y.V.Baklanov, "Chebyshev distribution of current for a planar array of radiators",

© University of Pretoria Digitised by the Department of Library Services in support of open access to information, University of Pretoria, 2019

UNIVERSITEIT VAN PRETORIA
UNIVERSITY OF PRETORIA
YUNIBESITHI YA PRETORIA

Radio Eng. Electron. Phys. (USSR), Vol.11, pp.640-642, 1966.

[46] F.I.Tseng and D.K.Cheng, "Optimum scannable planar arrays with an invariant side lobe level", *Proc.IEEE*, Vol.56, No.11, pp.1771-1778, Nov.1968.

[47] R.S.Elliott, "Synthesis of rectangular planar arrays for sum patterns with ring side lobes of arbitrary topography", *Radio Sci.*, Vol.12, pp.653-657, 1977.

[48] Y.U.Kim and R.S.Elliott, "Extensions of the Tseng-Cheng pattern synthesis technique", *J. Electromagn. Waves Applic.*, Vol.2, No.3/4, pp.255-268, 1988.

[49] T.T.Taylor, "Design of circular apertures for narrow beamwidth and low side lobes", *IRE Trans. Antennas Propagat.*, Vol.AP-8, pp.17-22, Jan.1960.

[50] R.C.Hansen, "Circular aperture distribution with one parameter", *Electron. Lett.*, Vol.11, p.184, April 1975.

[51] R.S.Elliott, "Design of circular apertures for narrow beamwidth and asymmetric side lobes", *IEEE Trans. Antennas Propagat.*, Vol.AP-23, pp.523-527, July 1975.

[52] R.C.Hansen, "A one-parameter circular aperture distribution with narrow beamwidth and low sidelobes", *IEEE Trans. Antennas Propagat.*, Vol.AP-24, pp.477-480, July 1976.

[53] W.D.White, "Circular aperture distribution functions", *IEEE Trans. Antennas Propagat.*, Vol.AP-25, No.5, pp.714-716, Sept.1977.

[54] O.Graham, R.M.Johnson and R.S.Elliott, "Design of circular apertures for sum patterns with ring side lobes of individually arbitrary heights", *Alta Frequenza*, Vol.47, pp.21-25, 1978.

[55] R.S.Elliott and G.J.Stern, "Shaped patterns from a continuous planar aperture distribution", *IEE Proc.*, Pt.H, Vol.135, No.6, pp.366-370, Dec.1988.

[56] R.S.Elliott and G.J.Stern, "Footprint patterns obtained by planar arrays", *IEE Proc.*, Pt.H, Vol.137, No.2, pp.108-112, April 1990.

[57] S.W.Autrey, "Approximate synthesis of nonseparable design responses for rectangular arrays", *IEEE Trans. Antennas Propagat.*, Vol.AP-35, No.8, pp.907-912, Aug.1987.

[58] A.Levi and H.Stark, "Image restoration by the method of generalised projections with application to restoration from magnitude", *J. Opt. Soc. Am.*, Pt.A., Vol.1, No.9, pp.932-943, Sept.1984.

[59] R.Barakat and G.Newsam, "Algorithms for reconstruction of partially known, bandlimited Fourier transform pairs from noisy data : II. The nonlinear problem

© University of Pretoria Digitised by the Department of Library Services in support of open access to information, University of Pretoria, 2019

UNIVERSITEIT VAN PRETORIA
UNIVERSITY OF PRETORIA
YUNIBESITHI YA PRETORIA

of phase retrieval", *J. Integral. Eq.*, Vol.9, pp.77-125, 1985.

[60] S.Prasad, "Generalised array pattern synthesis by the method of alternating orthogonal projections", *IEEE Trans. Antennas Propagat.*, Vol.AP-28, No.3, pp.328-332, May 1980.

[61] G.T.Poulton, "Antenna power pattern synthesis using the method of successive projections", *Electron. Lett.*, Vol.22, No.20, pp.1042-1043, Sept.1986.

[62] G.Franceschetti, G.Mazzarella and G.Panariello, "Array synthesis with excitation constraints", *IEE Proc.*, Pt.H, Vol.135, No.6, pp.400-407, Dec.1988.

[63] O.M.Bucci, G.Franceschetti, G.Mazzarella and G.Panariello, "A general projection approach to array synthesis", *IEEE AP-S Int. Antennas Propagat. Symp. Digest*, pp.146-149, June 1989.

[64] O.M.Bucci, G.Mazzarella and G.Panariello, "Reconfigurable array by phase-only control", *IEEE AP-S INT. Antenna Propagat. Symp. Digest*, pp.142-145, June 1989.

[65] O.M.Bucci, G.Mazzarella and G.Panariello, "Array synthesis with smooth excitation", *IEEE AP-S Int. Antennas Propagat. Symp. Digest*, Vol.II, pp.856-859, May 1990.

[66] Y.T.Lo, S.W.Lee and Q.H.Lee, "Optimisation of directivity and signal-to-noise ratio of an arbitrary antenna array", *Proc. IEEE*, Vol.54, No.8, pp.1033-1045, Aug.1966.

[67] S.M.Sanzgiri and J.K.Butler, "Constrained optimization of the performance indices of arbitrary array antennas", *IEEE Trans. Antenna Propagat.*, Vol.AP-19, pp.493-498, July 1971.

[68] O.Einarsson, "Optimisation of planar arrays", *IEEE Trans. Antennas Propagat.*, Vol.AP-27, No.1, pp.86-92, Jan.1979.

[69] P.Owen and J.C.Mason, "The use of linear programming in the design of antenna patterns with prescribed nulls and other constraints", *COMPEL*, Vol.3, No.4, pp.201-215, Dec.1984.

[70] T.S.Ng and M.A.Magdy, "Fast algorithms for optimal weight computation in linear array pattern synthesis having null constraints", *IEE Proc.*, Pt.H, Vol.131, No.6, pp.395-396, Dec.1984.

[71] J.F.DeFord and O.P.Gandhi, "Phase-only synthesis of minimum peak sidelobe patterns for linear and planar arrays", *IEEE Trans. Antennas Propagat.*, Vol.AP-36, No.2, pp.191-201, Feb.1988.

[72] Y.U.Kim, "Peak directivity optimisation under sidelobe level constraints in

© University of Pretoria Digitised by the Department of Library Services in support of open access to information, University of Pretoria, 2019

UNIVERSITEIT VAN PRETORIA
UNIVERSITY OF PRETORIA
YUNIBESITHI YA PRETORIA

antenna arrays", *Electromagnetics*, Vol.8, No.1, pp.51-70, 1988.

[73] F.R. Gantmacher, *Theory of Matrices*, Vol. I, Chelsea Publ. Co., 1960.

[74] P.E. Gill, W. Murray and M. Wright, *Practical Optimisation*, New York: Academic Press, 1981.

[75] R.F.E.Guy, "General radiation-pattern synthesis technique for array antennas of arbitrary configuration and element type", *IEE Proc.*, Pt.H., Vol.135, No.4, pp.241-248, Aug.1988.

[76] K.Hirasawa, "The application of a biquadratic programming method to phase-only optimization of antenna arrays", *IEEE Trans. Antennas and Propagat.*, Vol.AP-36, No.11, pp1545-1550, Nov.1988.

[77] G.L.Wilson, "Computer optimization of transducer array patterns", *J. Acoust. Soc. Am.*, Vol.59, No.1, pp.195-203, Jan.1976.

[78] V.Galindo-Israel, L.Shung-Wu and R.Mittra, "Synthesis of a laterally displaced cluster feed for a reflector antenna with applications to multiple beam contoured patterns", *IEEE Trans. Antennas Propagat.*, Vol.AP-26, No.2, pp.220-228, March 1978.

[79] C.A.Klein, "Design of shaped beam antennas through minimas gain optimisation", *IEEE Trans. Antennas Propagat.*, Vol.AP-32, No.9, pp.963-968, Sept.1984.

[80] P.J.Wood and A.G.P.Boswell, "Optimisation of antenna gain for earth coverage from geostationary satellite", *Electron. Lett.*, Vol.10, No.11, pp.227-228, May 1974.

[81] R.Jorgensen, "Coverage shaping of contoured beam antennas by aperture field synthesis", *IEE Proc.*, Pt.H, Vol.127, No.4, pp.201-208, Aug.1980.

[82] P.B.Bornemann, and P.Balling and W.J.English, "Synthesis of spacecraft array antennas for Intelsat frequency reuse multiple contoured beams", *IEEE Trans. Antennas Propagat.*, Vol.AP-33, No.11, pp.1186-1193, Nov.1985.

[83] C.B.Wylie and A.D.Monk, "Tele-Communication antennas for the UNISAT I satellite", *Proc. ICAP'85*, Warwick, England, 1985.

[84] R.A.Perrot, R.F.E.Guy, A.D.Monk and P.W.Crampton, "A high efficiency global coverage array", *Proc. ICAP'85*, Warwick, England, 1985.

© University of Pretoria Digitised by the Department of Library Services in support of open access to information, University of Pretoria, 2019

UNIVERSITEIT VAN PRETORIA
UNIVERSITY OF PRETORIA
YUNIBESITHI YA PRETORIA

CHAPTER 3

THE DIRECT SYNTHESIS OF NEAR-OPTIMUM TAPERED SIDELOBE PATTERNS FOR PLANAR ARRAYS

3.1 INTRODUCTORY REMARKS

For a given number of elements and interelement spacing of a linear array, the Dolph-Chebyshev distribution [1] is optimum in the sense that the first null beamwidth is the narrowest possible for the specified sidelobe ratio. Minimum beamwidth arrays do not necessarily provide maximum directivity, especially for large arrays. Directivity compression and "edge brightening" are due to the equal level sidelobes of the Dolph-Chebyshev array. To remove these undesirable phenomena a tapered sidelobe envelope must be incorporated.

Using the work by Dolph, Taylor devised the Taylor $\bar{n}$-distribution [2], for continuous line sources, which produces a radiation pattern with a tapered sidelobe envelope. Rhodes [3, 4] generalised Taylor's method by introducing an additional variable v to control the taper rate.

Villeneuve [5] conceived a technique for linear arrays, equivalent to the Taylor $\bar{n}$-distribution for line sources, which yields the discrete excitations directly. The Villeneuve $\bar{n}$-distribution was generalised by McNamara [6] as the discrete equivalent of the generalised Taylor $\bar{n}$-distribution of Rhodes [3, 4]. Although the first null

© University of Pretoria Digitised by the Department of Library Services in support of open access to information, University of Pretoria, 2019

beamwidth is increased slightly, a significant increase in excitation efficiency and directivity is possible.

Perhaps the first direct synthesis procedure for planar arrays was that by Tseng and Cheng [8] for planar Dolph-Chebyshev arrays with equal numbers of elements along the two principal axes, but did not require that d_x and d_y be equal, and a rectangular lattice and boundary shape. Use of the Baklanov [7] transformation allowed them to convert [8] the quadrantal symmetric planar array space factor (in two variables, u and v) to a polynomial in one variable. If this is equated to some polynomial (which we will call the *prototype polynomial*) with certain desirable characteristics, it is possible through algebraic manipulation to relate the coefficients of the polynomial to the array excitations in such a way that the space factor (pattern) will be symmetric, with its characteristics determined by the polynomial behaviour. Tseng and Cheng [8] used the Chebyshev polynomials for this purpose.

Elliott [9] used the above concepts to synthesise arrays of arbitrary sidelobe topography by a perturbation of a suitable polynomial, which was then used as a prototype polynomial. More recently, Kim and Elliott [10] have further extended the technique to allow synthesis of arrays with not only unequal spacings d_x and d_y, but also certain combinations of unequal numbers of elements along the two directions, through use of a generalisation of the original Baklanov transformation.

In this chapter the performance of planar arrays synthesised via the method of Tseng and Cheng [8], but using as prototype polynomials those associated with the generalised Villeneuve $\bar{n}$-distribution, is investigated. Section 3.2 provides an detailed synthesis procedure of the even case; that is, an even number of elements in both main directions. Computational and other difficulties encountered will be discussed in Section 3.2.2. A parametric study of the planar generalised Villeneuve distribution is presented in Section 3.2.3. The number of array elements, sidelobe ratio, transition index and taper rate are used as the parameters. The formulation for $2N+1$ by $2N+1$ elements (the odd case) will be treated in Section 3.4

© University of Pretoria Digitised by the Department of Library Services in support of open access to information, University of Pretoria, 2019

3.2 SYNTHESIS OF NEAR-OPTIMUM PLANAR ARRAYS: THE EVEN CASE

3.2.1 Formulation

The formulation consists of two parts, firstly a mapping of variables by means of a modified Baklanov [7] transformation, and secondly the determination of a one-dimensional polynomial.

Consider a rectangular grid planar array with a rectangular boundary and uniformly spaced elements in the *xy*-plane. The planar array space factor of a *2N* by *2N* array with symmetry about both the *x*- and *y*-axes is, from expression (2.13)

$$F(\dot{u},\dot{v}) = 4\sum_{m=1}^{N}\sum_{n=1}^{N} a_{mn}\cos[(2m-1)\dot{u}]\cos[(2n-1)\dot{v}] \tag{3.1}$$

in which

$$\begin{aligned}\dot{u} &= \tfrac{1}{2}kd_x(\sin\theta\cos\phi - \sin\theta_0\cos\phi_0)\\ \dot{v} &= \tfrac{1}{2}kd_y(\sin\theta\sin\phi - \sin\theta_0\sin\phi_0)\end{aligned} \tag{3.2}$$

with d_x, d_y the interelement spacings (d_x and d_y need not be equal) and θ_0, ϕ_0 the pointing direction of the main beam.

Tseng and Cheng [8] used the Baklanov transformation [7] to relate the above array factor to a polynomial of one variable. They chose the prototype polynomial to be a Chebyshev polynomial, thus succeeding in synthesising a nonseperable Dolph-Chebyshev planar array distribution. If the desired array factor is more complex (eg. different sidelobe heights and/or a shaped main beam) a more general polynomial must be selected. Kim and Elliott [9] extended the method using a slightly modified Baklanov transformation, namely

$$w = \cos\dot{u}\cos\dot{v} \tag{3.3}$$

Now a general polynomial of degree *2N-1* can be written in the form

© University of Pretoria Digitised by the Department of Library Services in support of open access to information, University of Pretoria, 2019

UNIVERSITEIT VAN PRETORIA
UNIVERSITY OF PRETORIA
YUNIBESITHI YA PRETORIA

$$P_{2N-1}(w) = \sum_{i=1}^{N} b_{2i-1} w^{2i-1} \tag{3.4}$$

But since

$$\cos^{2i-1}x = \frac{1}{2^{2i-2}} \sum_{p=1}^{i} \binom{2i-1}{i-p} \cos(2p-1)x \tag{3.5}$$

use of (3.3) in (3.4) reduces the latter to

$$\begin{aligned} P_{2N-1}(\dot{u},\dot{v}) &= \sum_{i=1}^{N} b_{2i-1} \cos^{2i-1}\dot{u} \cos^{2i-1}\dot{v} \\ &\quad - \sum_{i=1}^{N} \sum_{k=1}^{i} \sum_{l=1}^{i} \frac{b_{2i-1}}{4^{2i-2}} \binom{2i-1}{i-k} \binom{2i-1}{i-l} \cos[(2k-1)\dot{u}] \cos[(2l-1)\dot{v}] \end{aligned} \tag{3.6}$$

The array factor $F(\dot{u},\dot{v})$ and the polynomial $P_{2N-1}(\dot{u},\dot{v})$ must have the same characteristics, consequently, a comparison between the array factor (3.1) and the polynomial (3.6) gives the element excitation as

$$a_{mn} = \sum_{i=(m,n)}^{N} \frac{b_{2i-1}}{4^{2i-1}} \binom{2i-1}{i-m} \binom{2i-1}{i-n} \tag{3.7}$$

where

$$(m,n) = \begin{cases} m, & \text{if } m \geq n \\ n, & \text{if } m < n \end{cases} \tag{3.8}$$

The polar angle of any point in the normilized $\dot{u}\dot{v}$-plane ($\dot{u}/\frac{1}{2}kd_x, \dot{v}/\frac{1}{2}kd_y$) is merely ϕ. The constant w contours obtained from the mapping is depicted in Figure 3.1. Although the mapping is not perfectly ϕ-symmetric (circular contours), the inner contours are almost circular. Visible space is the region where $0 \leq \theta \leq \pi$ and $0 \leq \phi \leq 2\pi$. From the definition of $\dot{u}$ and $\dot{v}$ (3.2) a elliptical disc, with semi-major axis $\frac{1}{2}kd_x$ and semi-minor axis $\frac{1}{2}kd_y$, constitutes visible space in the $\dot{u}\dot{v}$-plane [12].

For near-optimum arrays the characteristic polynomial $P_{2N-1}(w)$ is obtained by using a method developed by McNamara [6] for the synthesis of generalised Villeneuve $\bar{n}$-distributions. Consider a linear array with $2N$ elements. For a given sidelobe ratio,

© University of Pretoria Digitised by the Department of Library Services in support of open access to information, University of Pretoria, 2019

UNIVERSITEIT VAN PRETORIA
UNIVERSITY OF PRETORIA
YUNIBESITHI YA PRETORIA

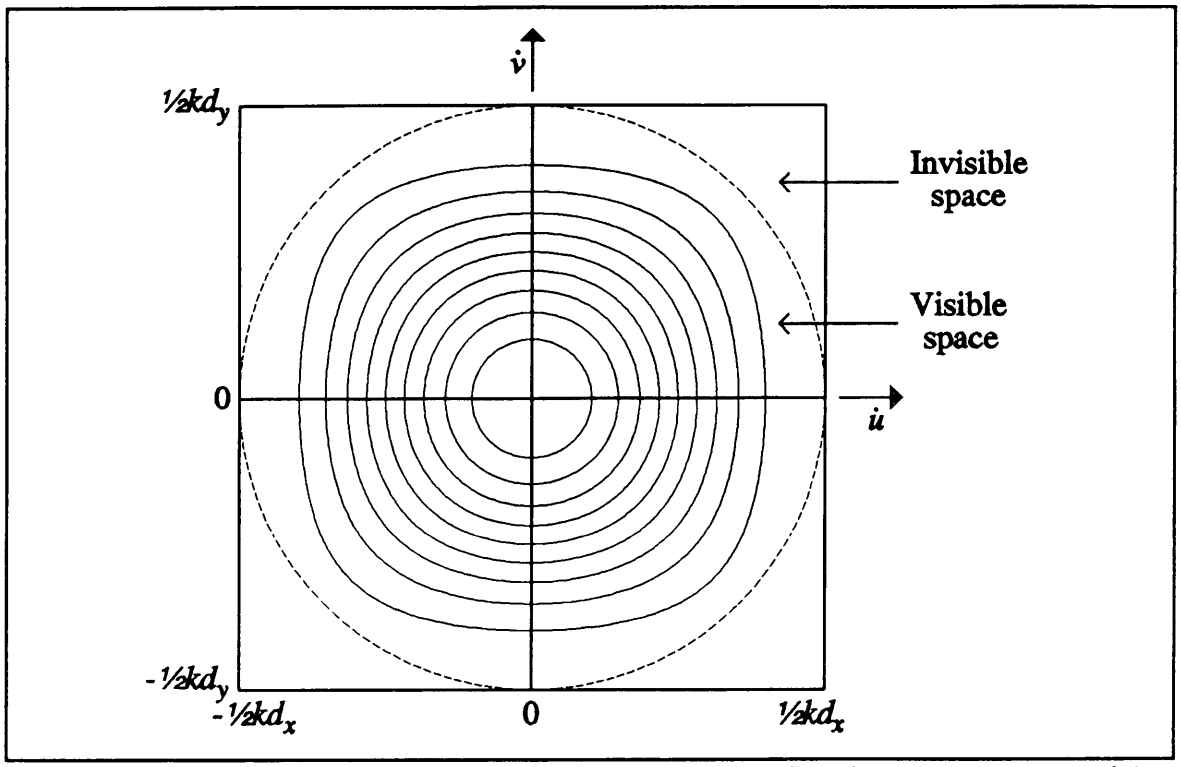

Figure 3.1 Constant *w* contour plot of the transformation, in constant steps of *0.2*.

SLR, the *2N-1* zeros of a Dolph-Chebyshev array factor ("parent" array factor) are

$$\psi_{\pm n} = \pm 2\cos^{-1}\left\{\frac{1}{u_0}\cos\left[\frac{(2n-1)\pi}{2(2N-1)}\right]\right\} \qquad n = 1,2,.....,N \tag{3.9}$$

in which

$$u_0 = \cosh\left[\frac{1}{2N-1}\ln\left(SLR + \sqrt{SLR^2-1}\right)\right] \tag{3.10}$$

The zeros of an uniform array of *2N* radiators are at

$$\psi^0_{\pm n} = \frac{\pm n\pi}{N} \qquad n = 1,2,.....,N \tag{3.11}$$

Let the array factor zeros now be adjusted to the set ψ'_n, with

$$\psi'_{\pm n} = \begin{cases} \sigma\,\psi_{\pm n} & |n| \le \bar{n} \\ \psi_{\pm n} + (\upsilon + 1)\left(\psi^0_{\pm n} - \psi_{\pm n}\right) & |n| \ge \bar{n} \end{cases} \tag{3.12}$$

wherein $\bar{n}$ is the transition index, υ is the taper rate and the dilation factor σ is

© University of Pretoria Digitised by the Department of Library Services in support of open access to information, University of Pretoria, 2019

$$\sigma = \frac{1}{\psi_{\bar{n}}}\left[\psi_{\bar{n}} + (\upsilon + 1)\left(\psi_{\bar{n}}^{0} - \psi_{\bar{n}}\right)\right] \tag{3.13}$$

Instead of determining the linear array distribution, the zeros are transformed the ψ-plane to the w-plane by

$$w = \cos\left(\frac{\psi}{2}\right) \tag{3.14}$$

The zeros of the characteristic polynomial $P_{2N-1}(w)$ is now known, and hence the coefficients b_i can be obtained by multiplication of the zeros. A recursive algorithm for the calculation of the coefficients of a polynomial from the roots of a product series is given in Appendix A. Because of symmetry, all the zeros, except the zero at $\psi=\pi$ or $w=0$, are in pairs; the same magnitude but alternating signs. This will cause the characteristic polynomial to have only odd non-zero coefficients, eg. b_{2i-1}.

A quantitative summary of the above synthesis procedure is in order. The synthesis procedure for the direct synthesis of planar arrays with generalised Villeneuve distributions is an adaptation of the procedure originally developed by Tseng and Cheng [8], and its subsequent extensions [9, 10]. The procedure used consists of the following: The space factor zeros of the generalised Villeneuve linear array we wish to have in every ϕ-pattern cut of the final planar array are determined according to [5, 6]. Thereafter a relatively straightforward recursive relation is used to find from these zeros the coefficients of the associated array prototype polynomial. These polynomial coefficients are then used with an algebraic expression linking the coefficients of the polynomial in the single variable w to the array excitations [8, 9, 10] to complete the planar array synthesis. Note that a value of $\upsilon=-1$ corresponds to the case studied by Tseng and Cheng [8]; that is, a planar array which is optimum in the Chebyshev sense. The value $\upsilon=0$ results in a discrete equivalent of the Taylor $\bar{n}$-distribution for circular apertures. As an example Figure 3.2 depicts the array factor of a *16* by *16* ($N=8$) element Villeneuve ($\upsilon=0.0$) planar array with all sidelobes under *-25dB* and $\bar{n}=3$.

© University of Pretoria Digitised by the Department of Library Services in support of open access to information, University of Pretoria, 2019

UNIVERSITEIT VAN PRETORIA
UNIVERSITY OF PRETORIA
YUNIBESITHI YA PRETORIA

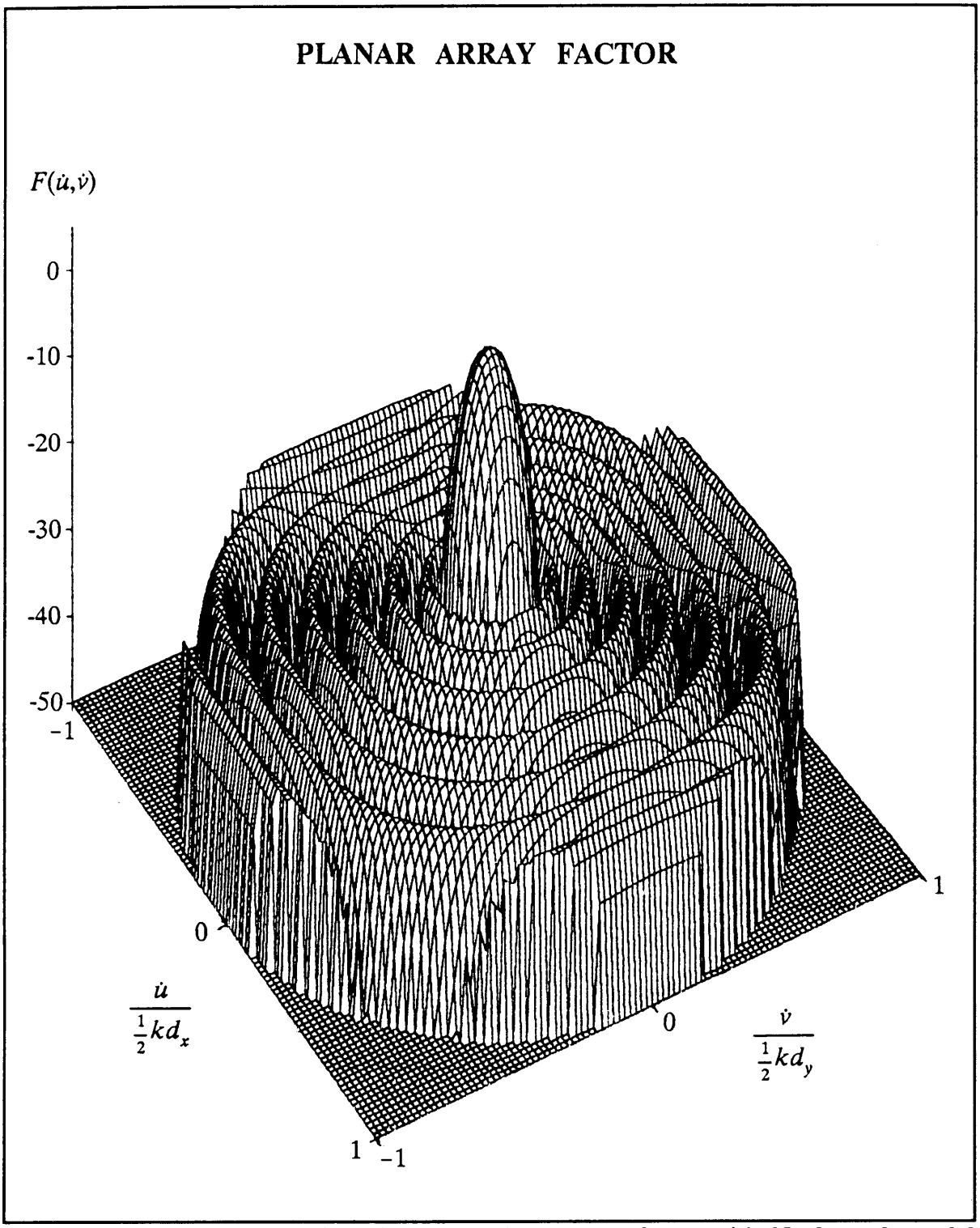

Figure 3.2 An example of a Villeneuve planar array factor with $N=8$, $\bar{n}=3$, $\upsilon=0.0$ and $SLR=25dB$.

© University of Pretoria Digitised by the Department of Library Services in support of open access to information, University of Pretoria, 2019

3.2.2 Some Computational Details and Difficulties

The characteristic polynomial $P_{2N-1}(w)$ is relatively ill-conditioned; that is, the coefficients b_{2i-1} are very large numbers of alternating sign. As the polynomial is bounded, for most part, between $+1$ and -1, a very high accuracy for these coefficients are required if the order of the polynomial is high. This is indeed possible if extended precision is used on modern computers. The magnitude of the coefficients that should be zero can serve as an indication of the accuracy of the non-zero coefficients.

As stated previously, the Dolph-Chebyshev distribution gives an optimum beamwidth for a specified maximum sidelobe ratio and number of elements. Thus the following condition must be imposed on the dilation factor,

$$\sigma \geq 1 \tag{3.15}$$

This condition results in a minimum allowable $\bar{n}$ of

$$\bar{n} \geq \frac{N \psi_{\bar{n}}}{\pi} \tag{3.16}$$

The condition (3.16) is a necessary but not a sufficient condition, but serves as a good indicator especially for arrays with directivity compression. Besides enforcing condition (3.16) it is also necessary to ensure that the maxima and minima of the characteristic polynomial are within the bounds set by the *SLR*. These maxima and minima can be found using the Newton-Raphson method to find the roots of the first derivative of the polynomial.

3.2.3 Parametric Study

The expression for directivity is (2.18)

$$D = \frac{\bar{J}^T \tilde{A} \bar{J}}{\bar{J}^T \tilde{B} \bar{J}} \tag{3.17}$$

For planar arrays this expression results into a double summation in the numerator and a four-fold summation in the denominator. Assume the pointing direction of the main beam is in the direction $(\theta_0, \phi_0) = (0,0)$. By making use of symmetry the peak directivity of a $2M$ by $2N$ element array can be expressed, through simplification of (3.17), as

© University of Pretoria Digitised by the Department of Library Services in support of open access to information, University of Pretoria, 2019

$$D = \frac{8\left|\sum_{m=1}^{M}\sum_{n=1}^{N} a_{mn}\right|^2}{\sum_{m=1}^{M}\sum_{n=1}^{N}\sum_{k=1}^{M}\sum_{l=1}^{N} a_{mn}a_{kl}\Gamma(m,n,k,l)} \tag{3.18}$$

with

$$\Gamma(m,n,k,l) = \gamma(m-k,n-l) + \gamma(m-k,n+l) + \gamma(m+k,n-l) + \gamma(m+k,n+l) \tag{3.19}$$

where

$$\gamma(p,q) = sinc\left[k\sqrt{(pd_x)^2 + (qd_y)^2}\right] \tag{3.20}$$

The directivity and the excitation efficiency are invariably linked, as can be seen from equation (2.19); a 3dB increase (or doubling) in directivity will cause a doubling in excitation efficiency. For this reason only the directivity will be plotted in what follows.

Directivity versus number of elements N, with the transition index $\bar{n}$ and the taper factor υ as parameters, are plotted in Figure 3.3 to Figure 3.6, for various sidelobe ratios. The value $\upsilon=-1$, corresponding to the planar Dolph-Chebyshev distribution, indicates the relation between the onset of directivity compression, the number of elements and the *SLR*. For a higher *SLR (lower sidelobe level)*, directivity compression occurs at a larger number of elements. As expected, when using the planar Villeneuve synthesis method, a drastic increase in the directivity (and excitation efficiency) results in those cases where the "parent" distribution suffers from directivity compression.

© University of Pretoria Digitised by the Department of Library Services in support of open access to information, University of Pretoria, 2019

UNIVERSITEIT VAN PRETORIA
UNIVERSITY OF PRETORIA
YUNIBESITHI YA PRETORIA

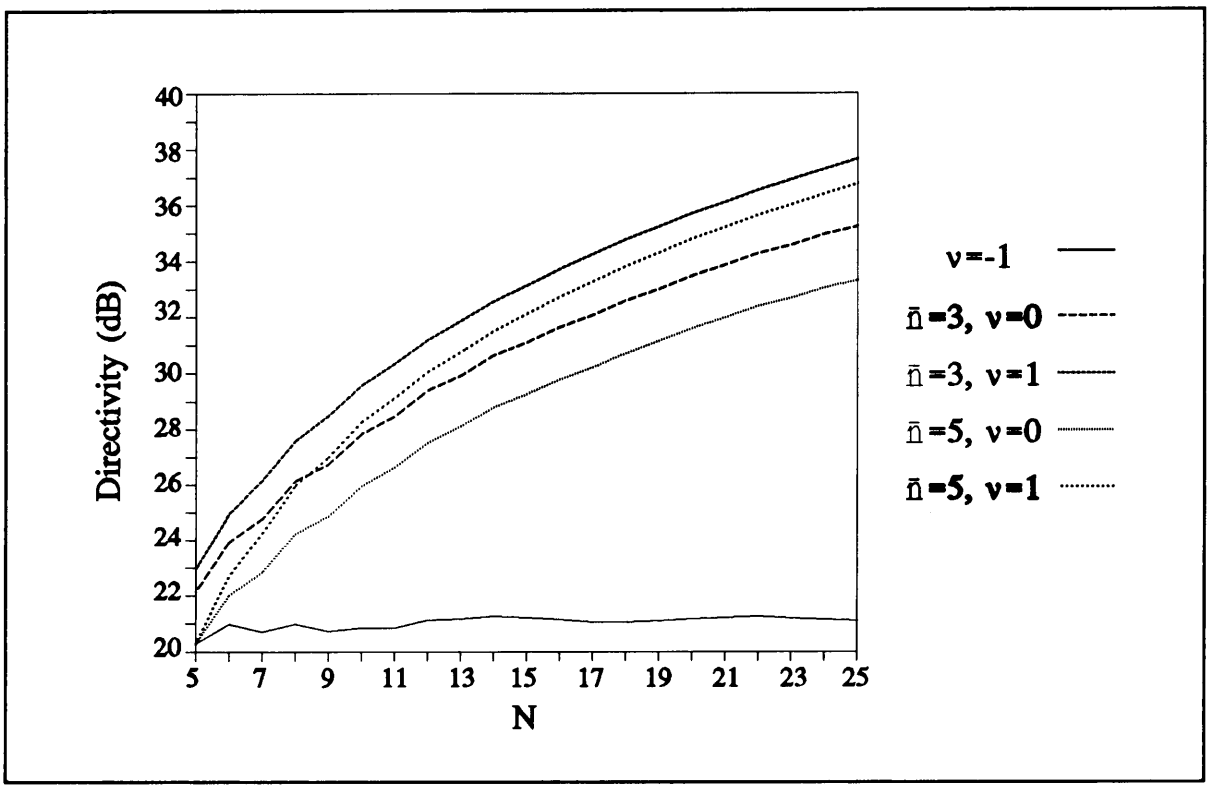

Figure 3.3 Directivity versus N for $SLR=15dB$.

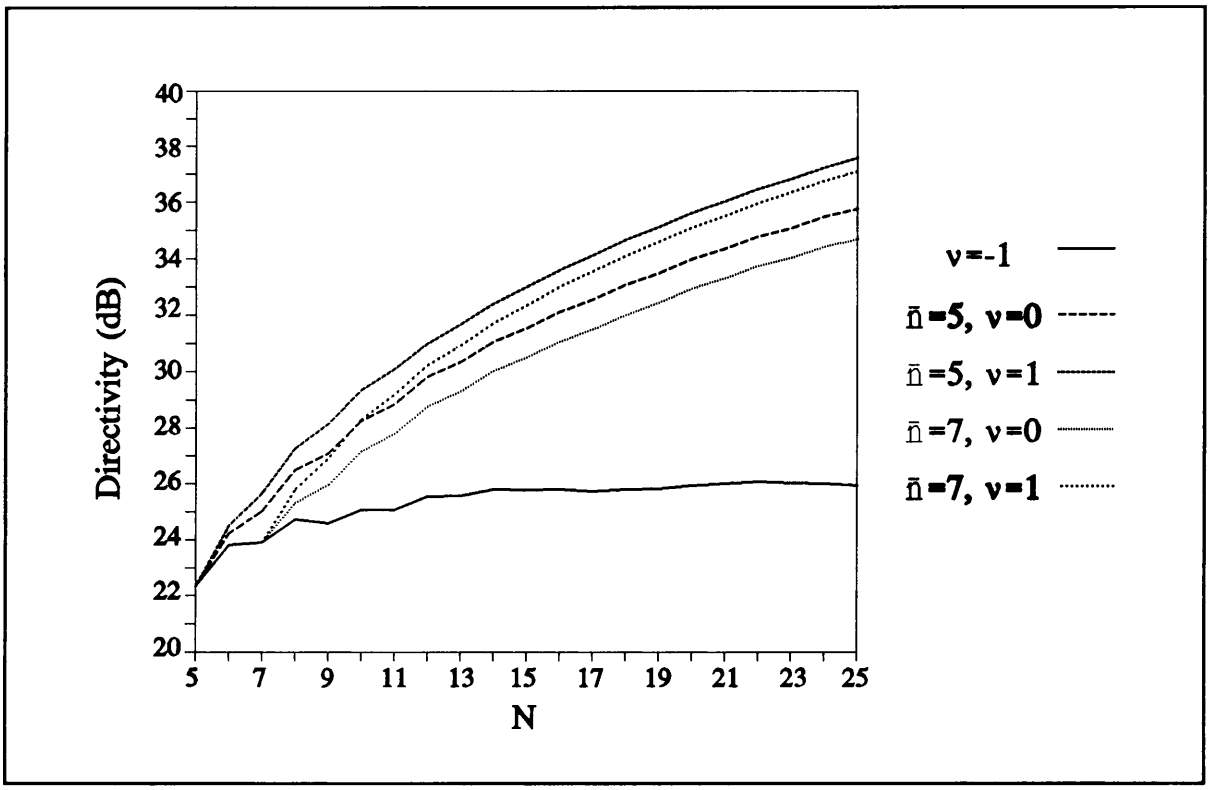

Figure 3.4 Directivity versus N for $SLR=20dB$.

© University of Pretoria Digitised by the Department of Library Services in support of open access to information, University of Pretoria, 2019

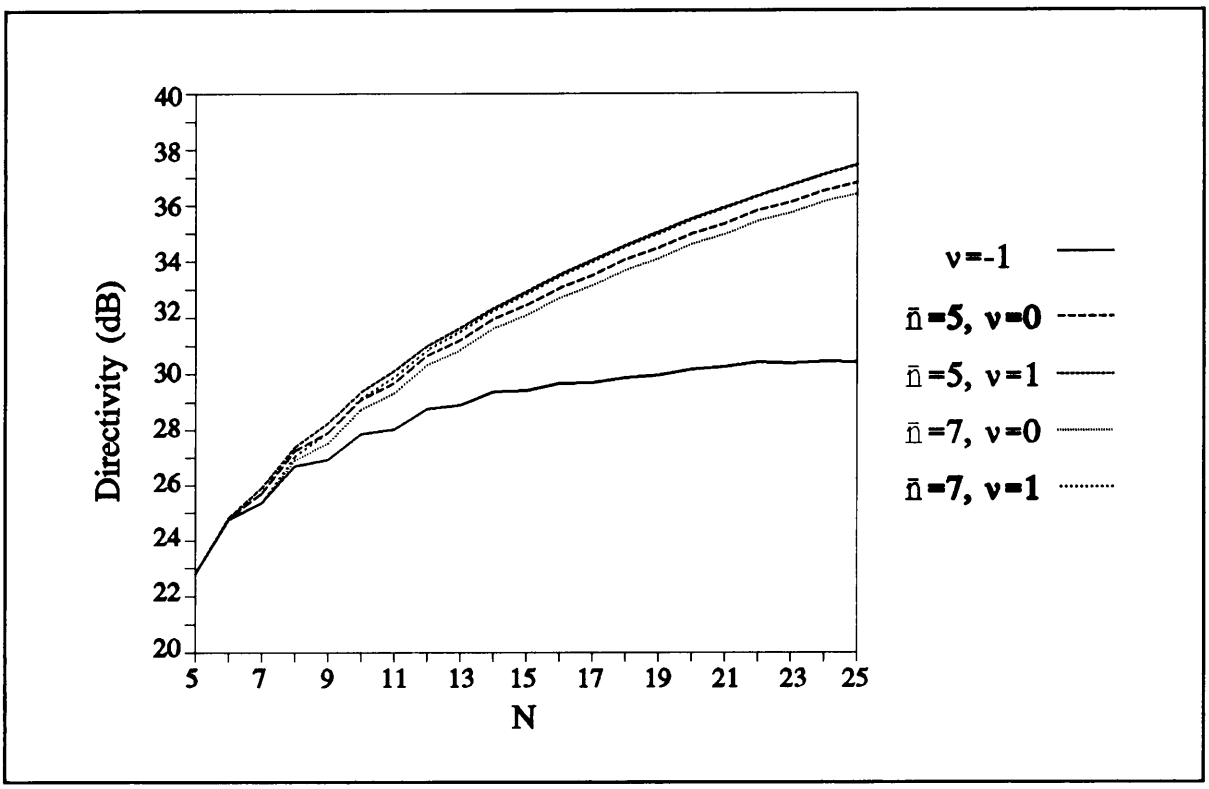

Figure 3.5 Directivity versus N for $SLR=25dB$.

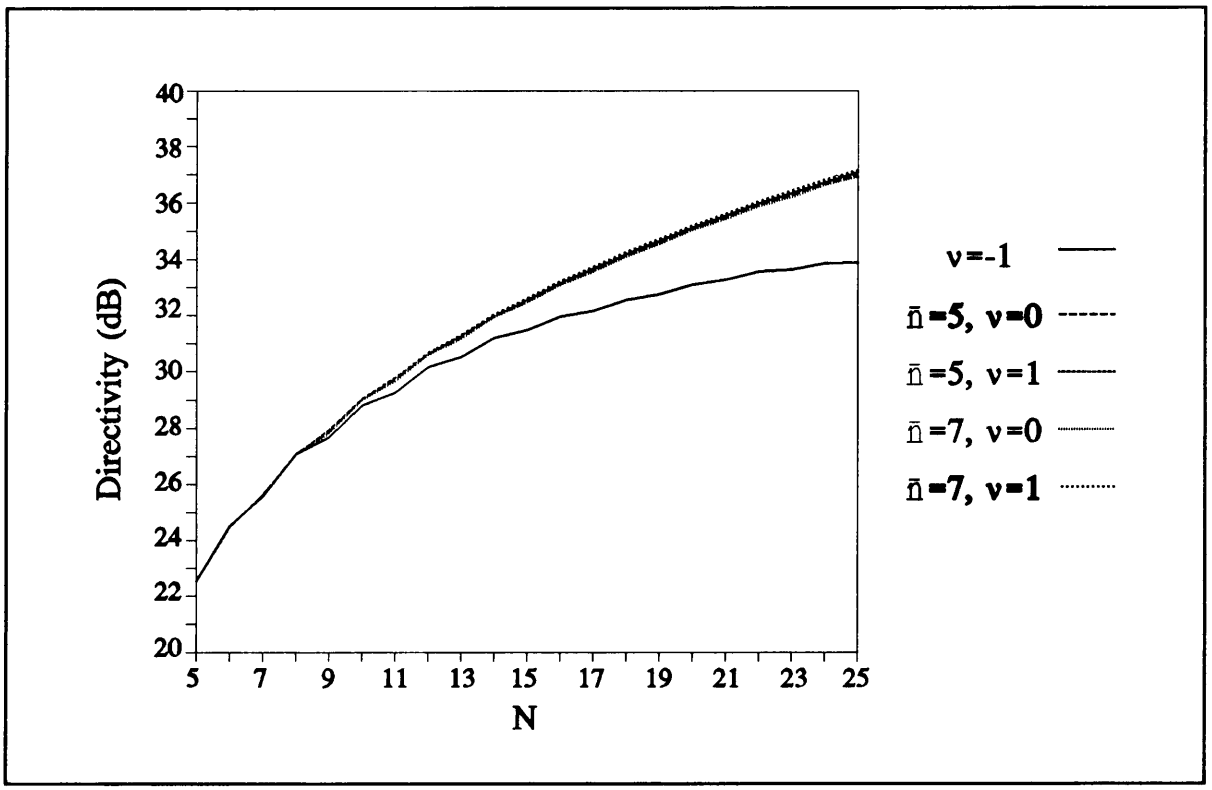

Figure 3.6 Directivity versus N for $SLR=30dB$.

© University of Pretoria Digitised by the Department of Library Services in support of open access to information, University of Pretoria, 2019

Consider an array with $N=15$ and $SLR=20dB$. Because the "parent" distribution of array suffers severely from directivity compression, the advantages of the method can be clearly illustrated. For a given $\bar{n}$ it is evident, from equation (3.13), that an increase in υ will give rise to an increase in σ, and as a result an increase in the first null beamwidth as well. With the beamwidth broadening measured relative to the first null beamwidth of the "parent" Dolph-Chebyshev distribution, in the $\phi=0^\circ$-direction, we can define the beamwidth broadening factor as

$$\tau = \frac{\theta_1}{\theta_1'} = \frac{\sin^{-1}\left(\frac{\psi_1}{kd}\right)}{\sin^{-1}\left(\frac{\psi_1'}{kd}\right)} \tag{3.21}$$

The beamwidth broadening factor versus the taper rate is depicted in Figure 3.7 for various values of $\bar{n}$. The directivity improvement as a function of υ, is shown in Figure 3.8. The influence of $\bar{n}$ on σ is less marked. Indicated in Figures 3.9 and 3.10 are the beamwidth broadening factor and directivity, respectively, as a function of $\bar{n}$, with υ as a parameter. As expected, the beam broadening factor increases for larger values of the taper factor or smaller values of the transition index.

The improvement of the excitation efficiency is also evident in the excitation distribution. The Dolph-Chebyshev distribution, shown in Figure 3.11, has a oscillating behaviour with its peaks at the edge of the array. The distribution of an array with maximum efficiency ($\bar{n}=3$ and $\upsilon=1.0$) is displayed in Figure 3.12. The latter distribution, having its peak is in the centre of the array, tapers of smoothly towards the edge of the array, but then falls of sharply to zero at the corners of the array after a radius of roughly Nd_x.

© University of Pretoria Digitised by the Department of Library Services in support of open access to information, University of Pretoria, 2019

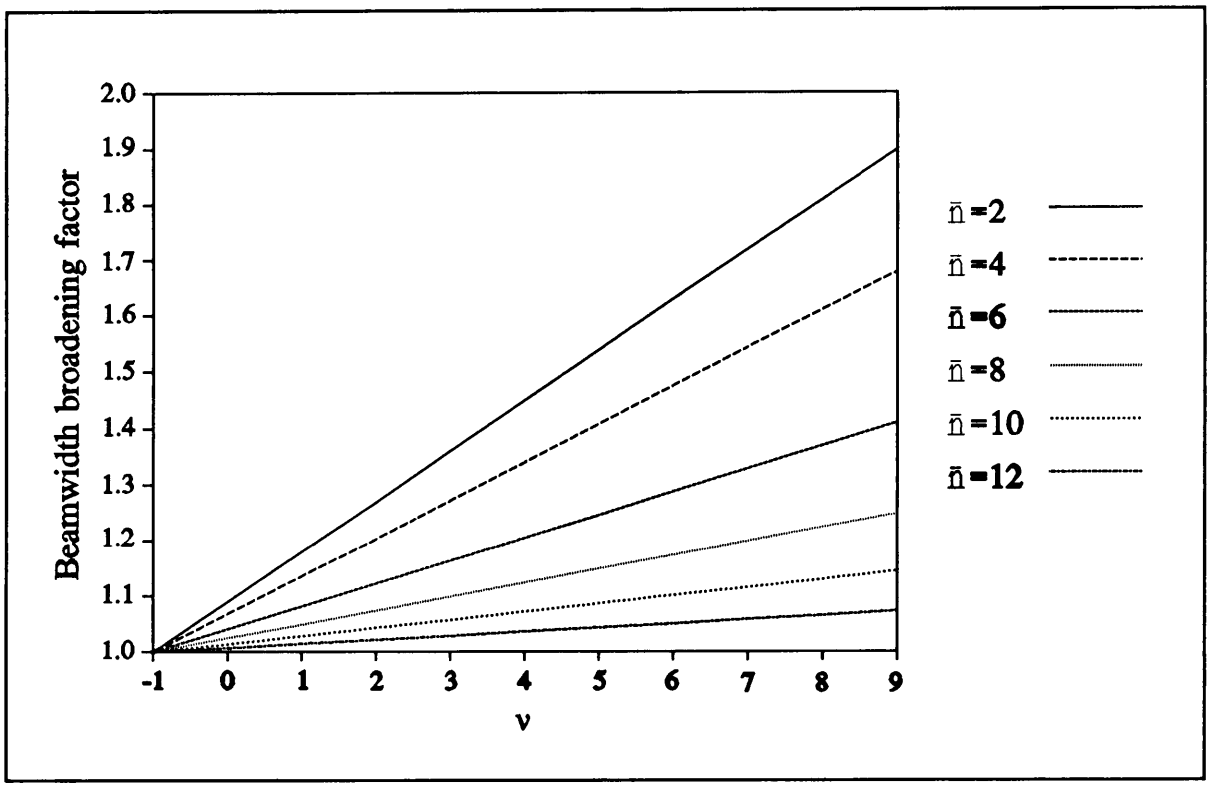

Figure 3.7 Beamwidth broadening factor versus taper rate.

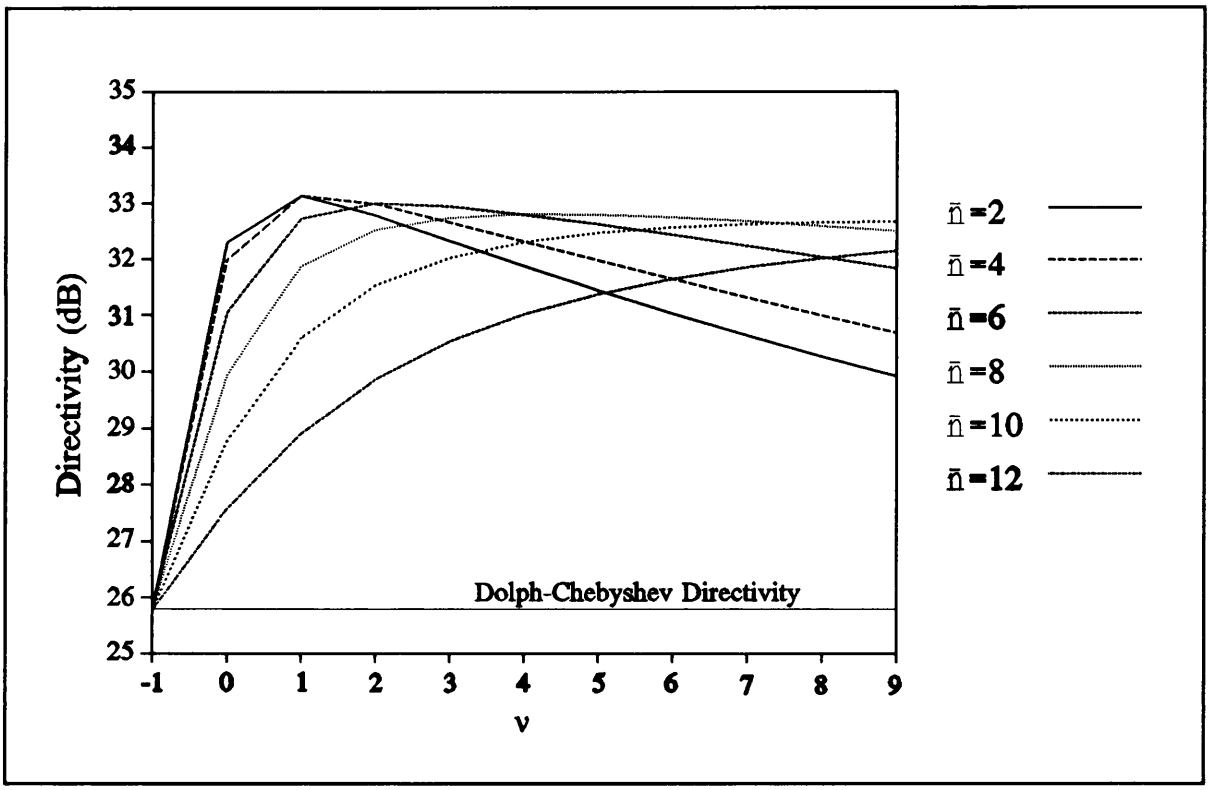

Figure 3.8 Directivity versus taper rate.

© University of Pretoria Digitised by the Department of Library Services in support of open access to information, University of Pretoria, 2019

UNIVERSITEIT VAN PRETORIA
UNIVERSITY OF PRETORIA
YUNIBESITHI YA PRETORIA

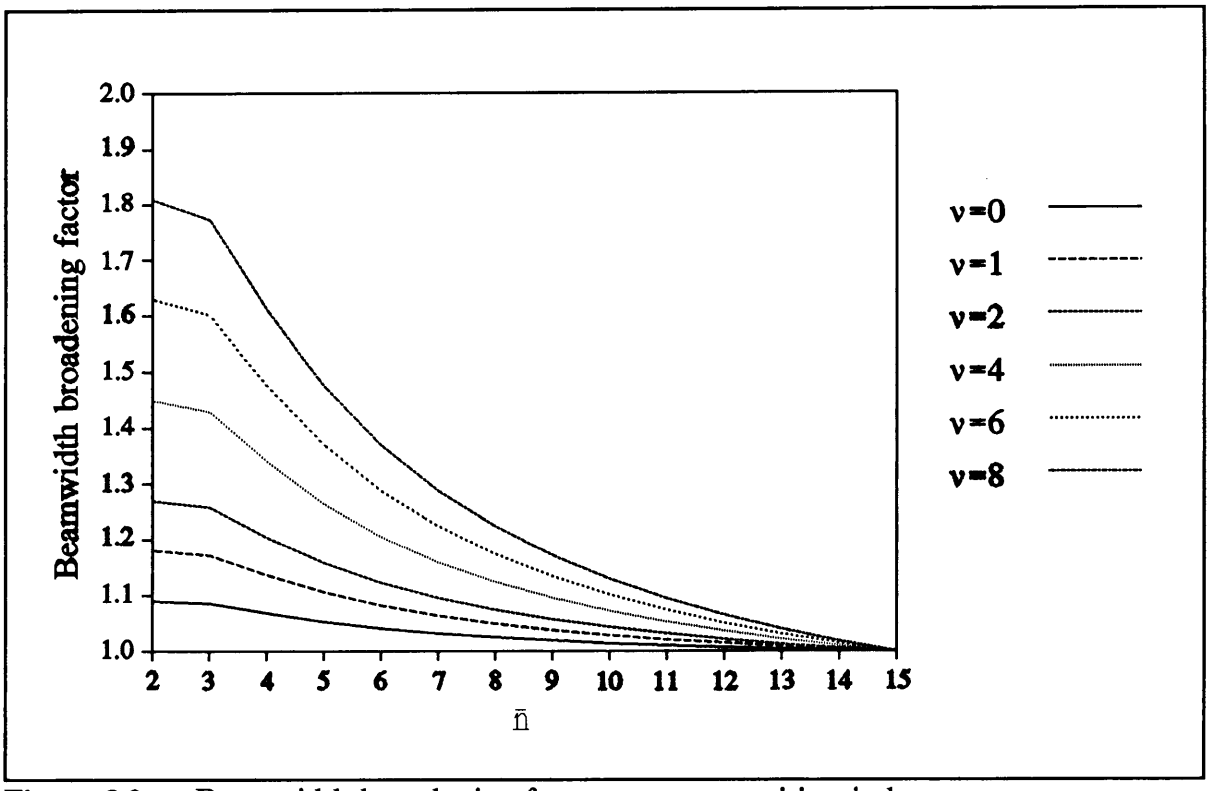

Figure 3.9 Beamwidth broadening factor versus transition index.

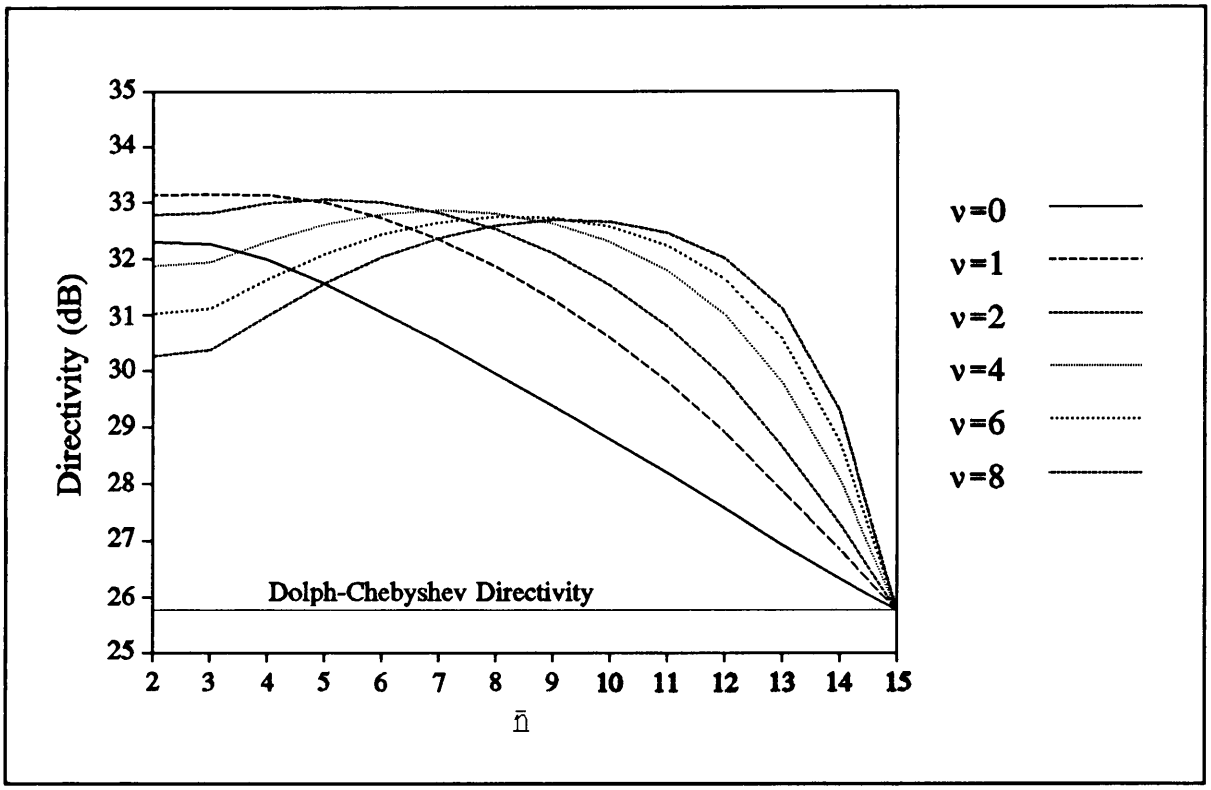

Figure 3.10 Directivity versus transition index.

© University of Pretoria Digitised by the Department of Library Services in support of open access to information, University of Pretoria, 2019

UNIVERSITEIT VAN PRETORIA
UNIVERSITY OF PRETORIA
YUNIBESITHI YA PRETORIA

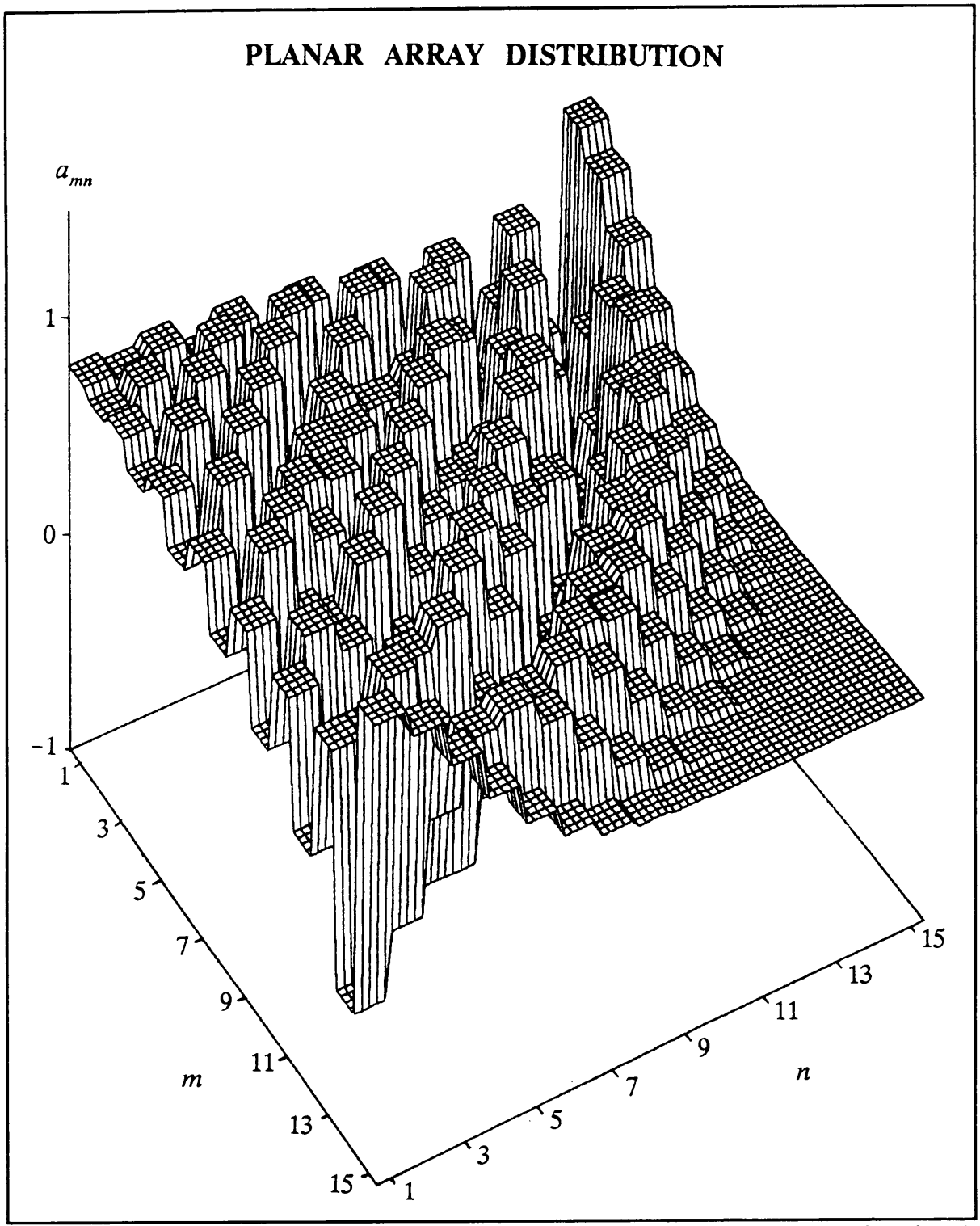

Figure 3.11 Relative amplitudes a_{mn} of the planar Dolph-Chebyshev distribution. (Each "column of sixteen blocks" represents the excitation of a single array element.)

© University of Pretoria Digitised by the Department of Library Services in support of open access to information, University of Pretoria, 2019

UNIVERSITEIT VAN PRETORIA
UNIVERSITY OF PRETORIA
YUNIBESITHI YA PRETORIA

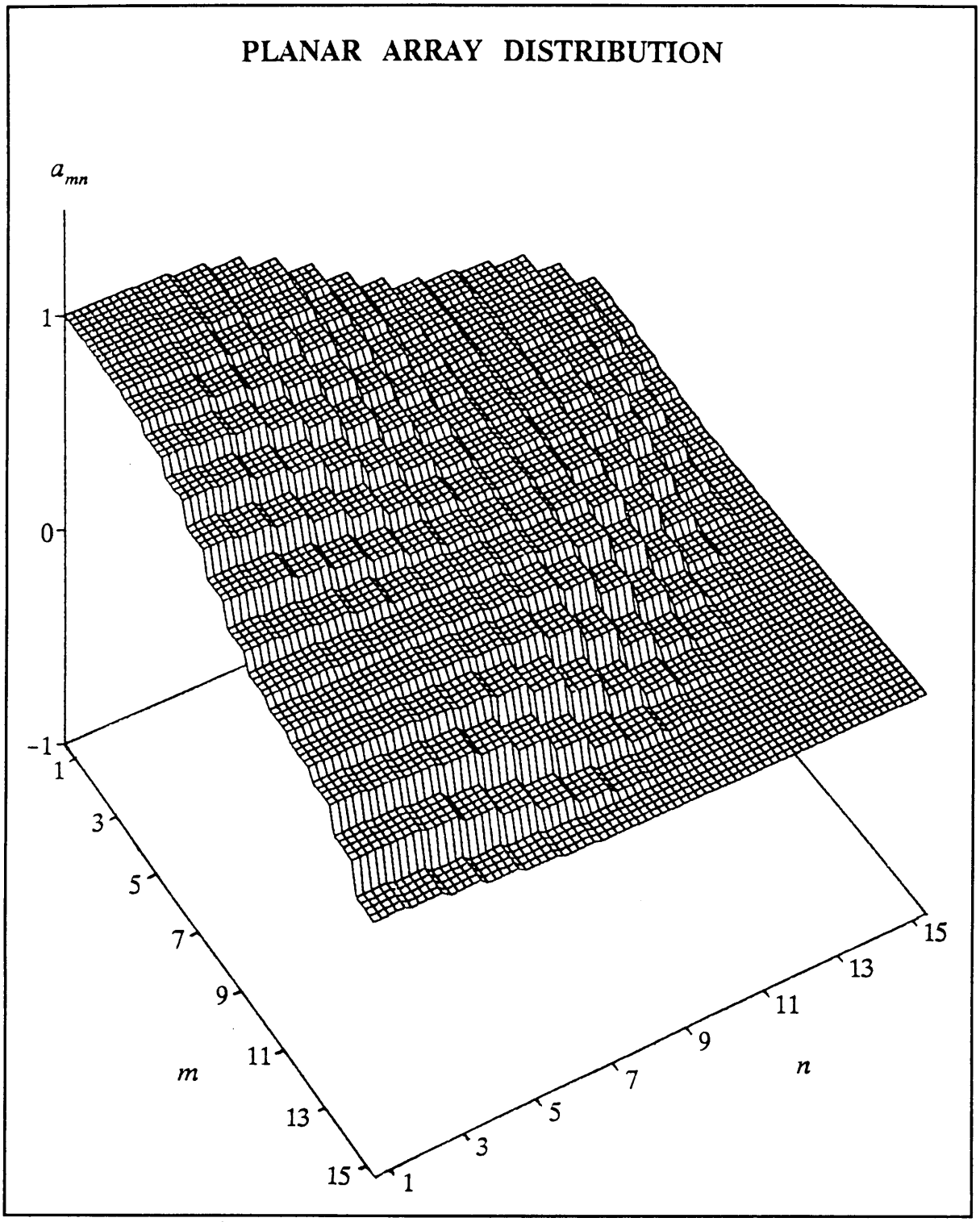

Figure 3.12 Relative amplitudes a_{mn} of the optimum directivity planar distribution. (Each "column of sixteen blocks" represents the excitation of a single array element.)

© University of Pretoria Digitised by the Department of Library Services in support of open access to information, University of Pretoria, 2019

3.2.4 Rectangular Grid Planar Arrays with Circular Boundaries

An added advantage of the generalised planar Villeneuve synthesis method, discussed in Section 3.2.1, is that the excitation of the corner elements is small compared to the other elements. As the sidelobe level envelope taper rate increases the magnitude of the corner elements tend to decrease. In order to obtain an array with a circular boundary all the elements outside the boundary must be lopped off. This will certainly cause some pattern degradation, but if the lopped off elements' excitation are relatively small, this degradation will be minimal. By properly controlling the pattern taper rate ("properly" in the sense that the beamwidth and directivity are little affected) it is possible to ensure that the corner element have excitations that indeed small enough. For the proposes of illustration the circular boundary radius r_b is assumed to be

$$r_b = Nd_x \tag{3.22}$$

The advantages of an increased taper rate is best illustrated by means of an example. Consider a 30 by 30 array ($N=15$) in which $d_x=d_y=\frac{1}{2}\lambda$. The desired pattern is a pencil beam with all sidelobes under -30dB. The array factor of the Dolph-Chebyshev distribution obtained is shown in Figure 3.13. To obtain a circular boundary ($r_b=7.5\lambda$) 46 elements in each quadrant must be lopped off. The degradation of the resulting array factor can be seen from examination of Figure 3.14 and Figure 3.15 (with the floor of the 3D-plot floors at -30dB and -60dB respectively). Figure 3.16 depicts the array factor resulting from a Villeneuve $\bar{n}$-distribution with $\bar{n}=3$. Figures 3.17 and 3.18 display the array factor of the array with elements lopped off to form a circular boundary. From Figure 3.17 it is clear that some of the inner sidelobes are still above -30dB. Increasing the taper rate to $\upsilon=4.0$ ensures that all the sidelobes of the lopped array are just under -30dB. The resulting array factors are shown in Figure 3.19 (full array) and Figure 3.20 (lopped array with circular boundary). The directivity and other important indicators are tabulated in Table 3.1. Observe that the proposed method permits synthesis of a planar array with a circular boundary, and the required sidelobe levels, without the directivity performance being disadvantaged. The latter is due to the correct increasing of the pattern taper (and resulting corner element decrease) through use of the generalised Villeneuve zero shifting and Baklanov transformation.

© University of Pretoria Digitised by the Department of Library Services in support of open access to information, University of Pretoria, 2019

UNIVERSITEIT VAN PRETORIA
UNIVERSITY OF PRETORIA
YUNIBESITHI YA PRETORIA

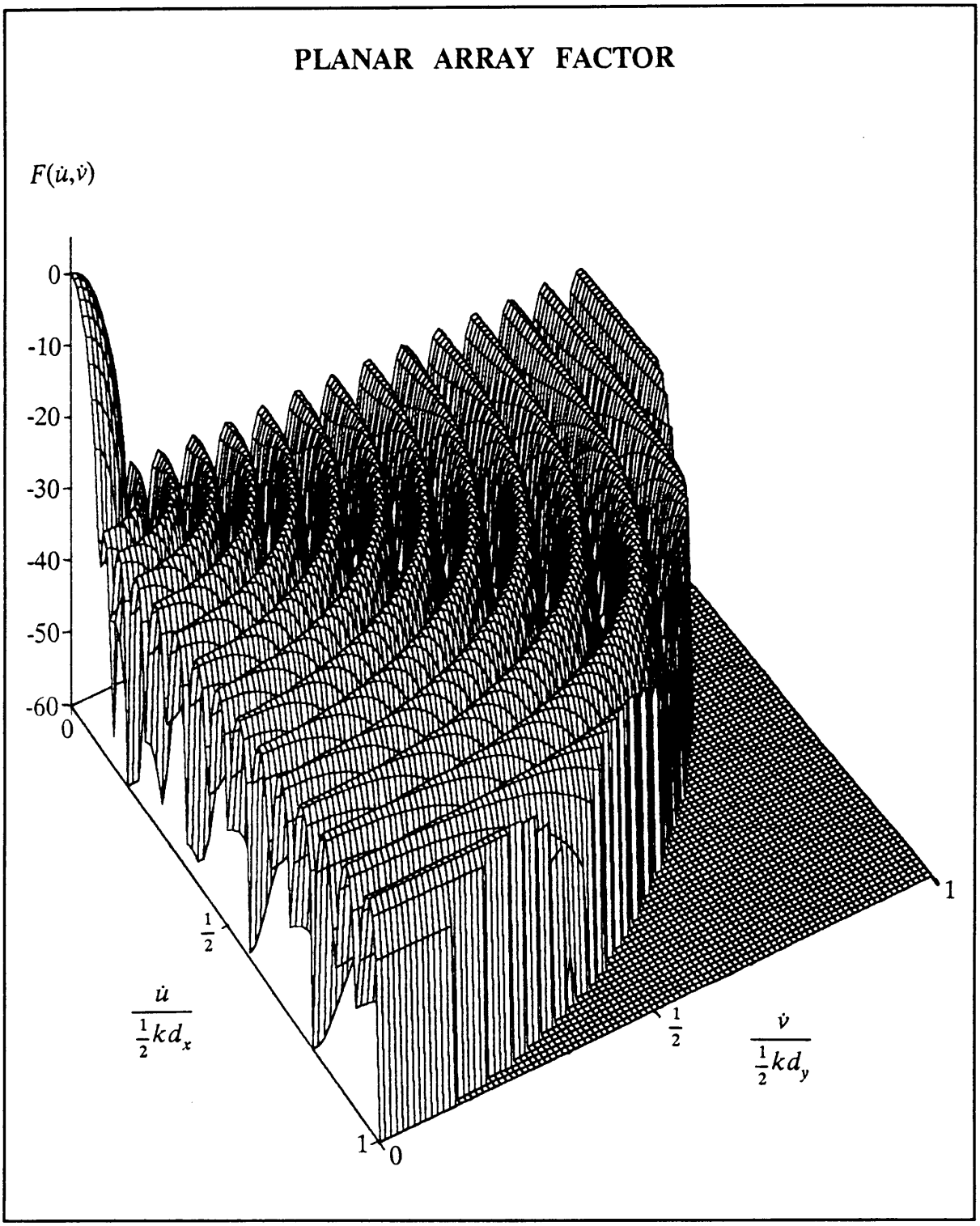

Figure 3.13 Array factor of the full rectangular Dolph-Chebyshev distribution.

© University of Pretoria Digitised by the Department of Library Services in support of open access to information, University of Pretoria, 2019

UNIVERSITEIT VAN PRETORIA
UNIVERSITY OF PRETORIA
YUNIBESITHI YA PRETORIA

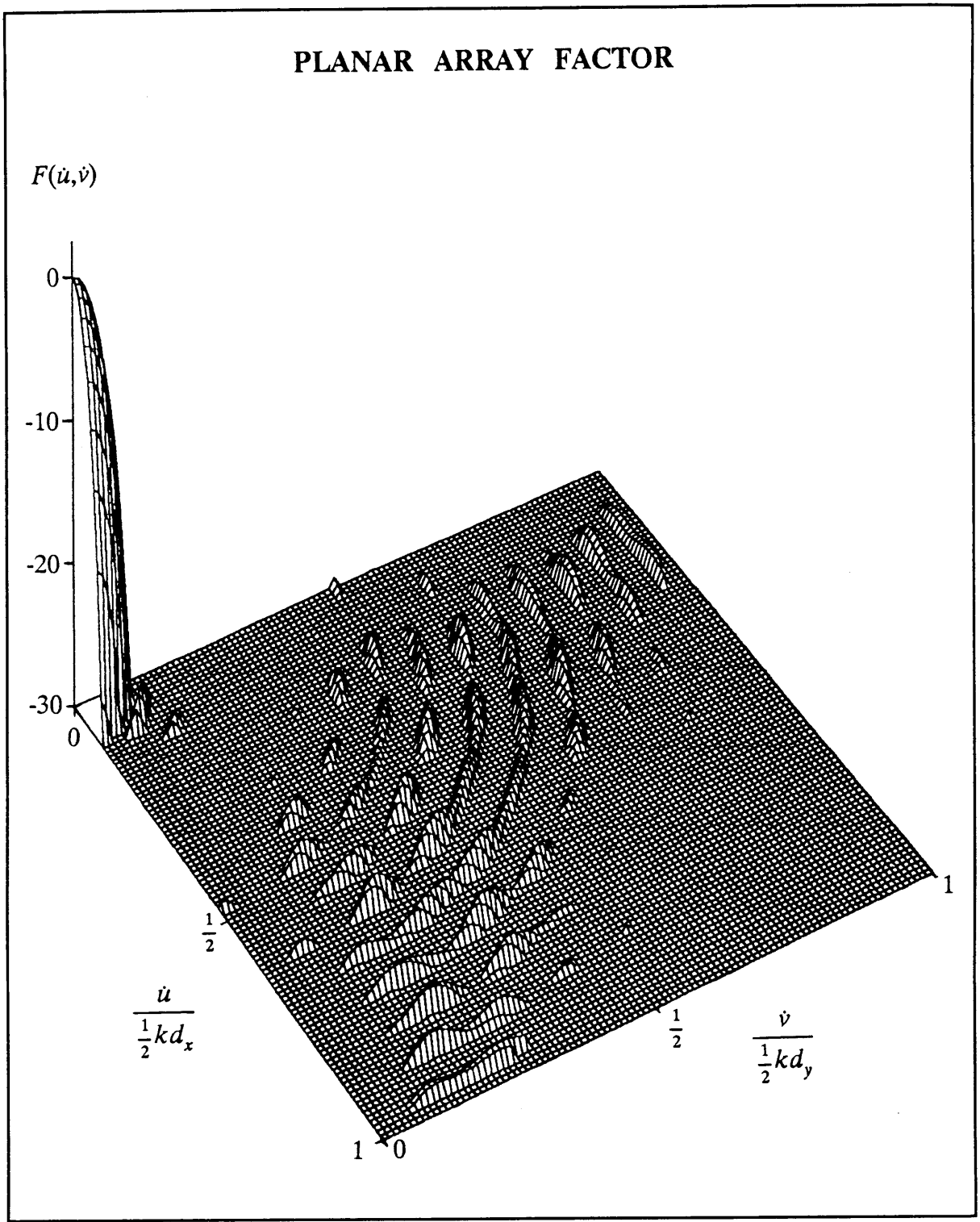

Figure 3.14 Array factor of the Dolph-Chebyshev distribution with 46 elements per quadrant lopped off to form a circular boundary. (3D-plot floor at *-30dB.)*

© University of Pretoria Digitised by the Department of Library Services in support of open access to information, University of Pretoria, 2019

UNIVERSITEIT VAN PRETORIA
UNIVERSITY OF PRETORIA
YUNIBESITHI YA PRETORIA

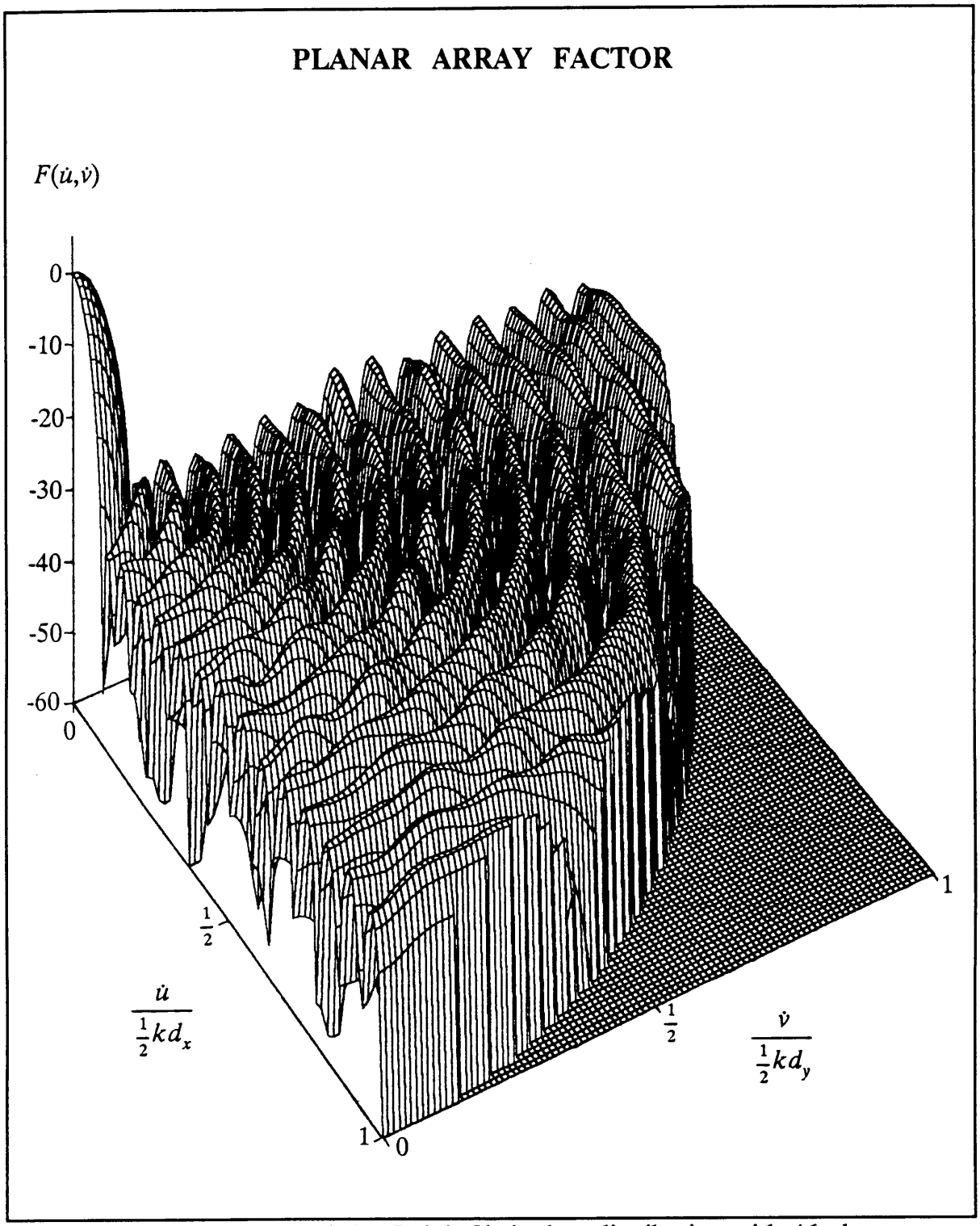

Figure 3.15 Array factor of the Dolph-Chebyshev distribution with 46 elements per quadrant lopped off to form a circular boundary. (3D-plot floor at *-60dB.)*

© University of Pretoria Digitised by the Department of Library Services in support of open access to information, University of Pretoria, 2019

UNIVERSITEIT VAN PRETORIA
UNIVERSITY OF PRETORIA
YUNIBESITHI YA PRETORIA

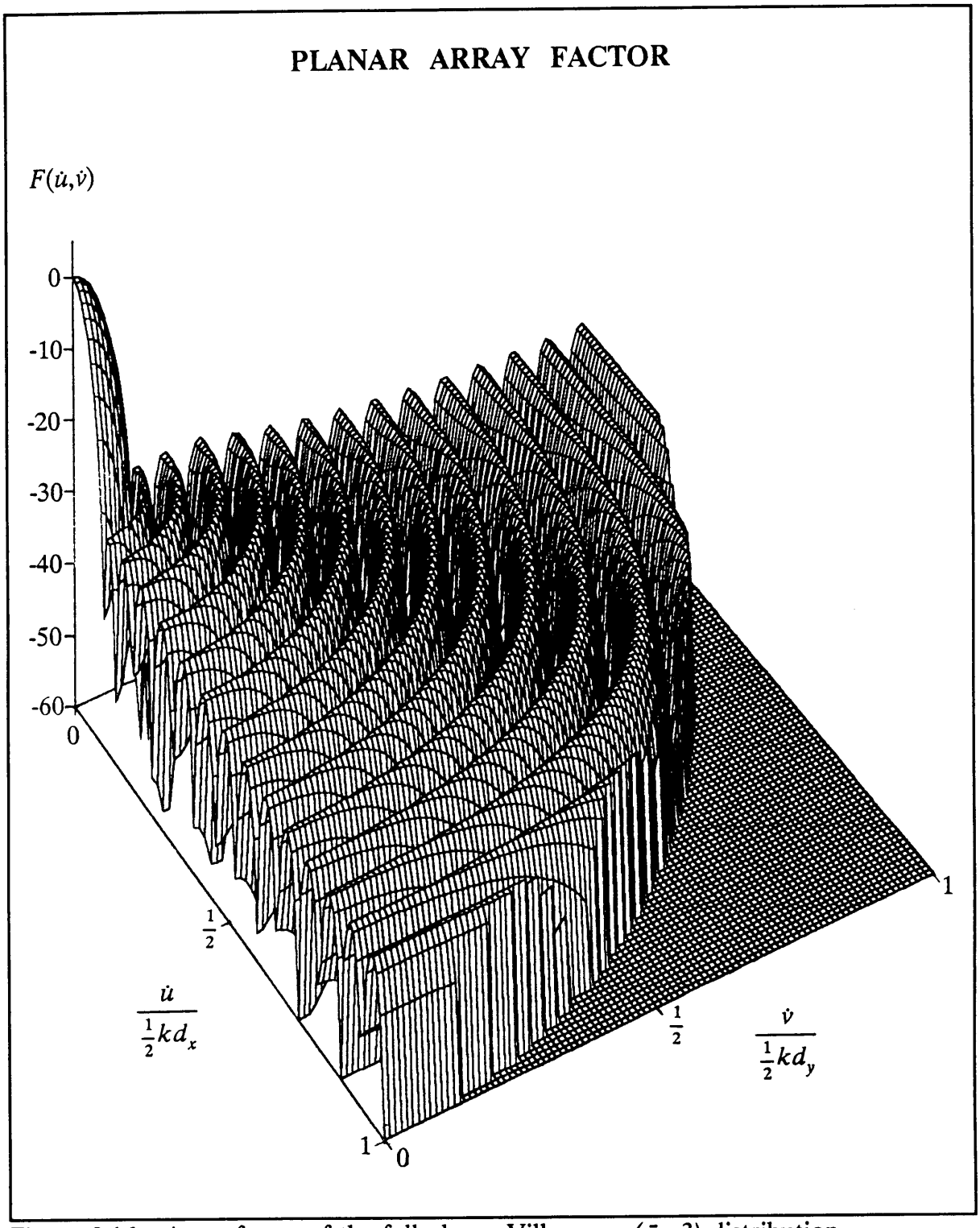

Figure 3.16 Array factor of the full planar Villeneuve ($\bar{n}=3$) distribution.

© University of Pretoria Digitised by the Department of Library Services in support of open access to information, University of Pretoria, 2019

UNIVERSITEIT VAN PRETORIA
UNIVERSITY OF PRETORIA
YUNIBESITHI YA PRETORIA

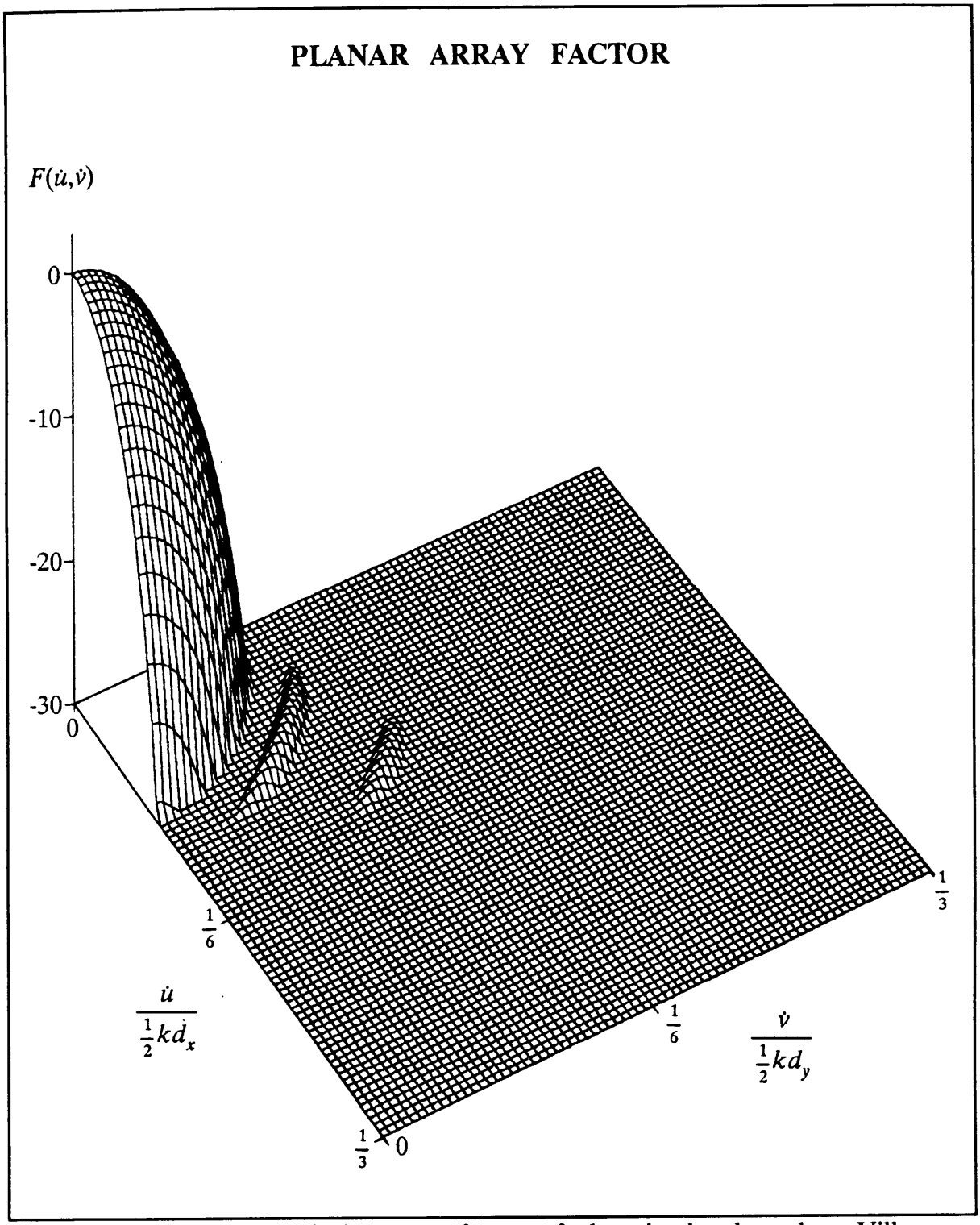

Figure 3.17 A section of the array factor of the circular boundary Villeneuve distribution. (3D-plot floor at *-30dB*)

© University of Pretoria Digitised by the Department of Library Services in support of open access to information, University of Pretoria, 2019

UNIVERSITEIT VAN PRETORIA
UNIVERSITY OF PRETORIA
YUNIBESITHI YA PRETORIA

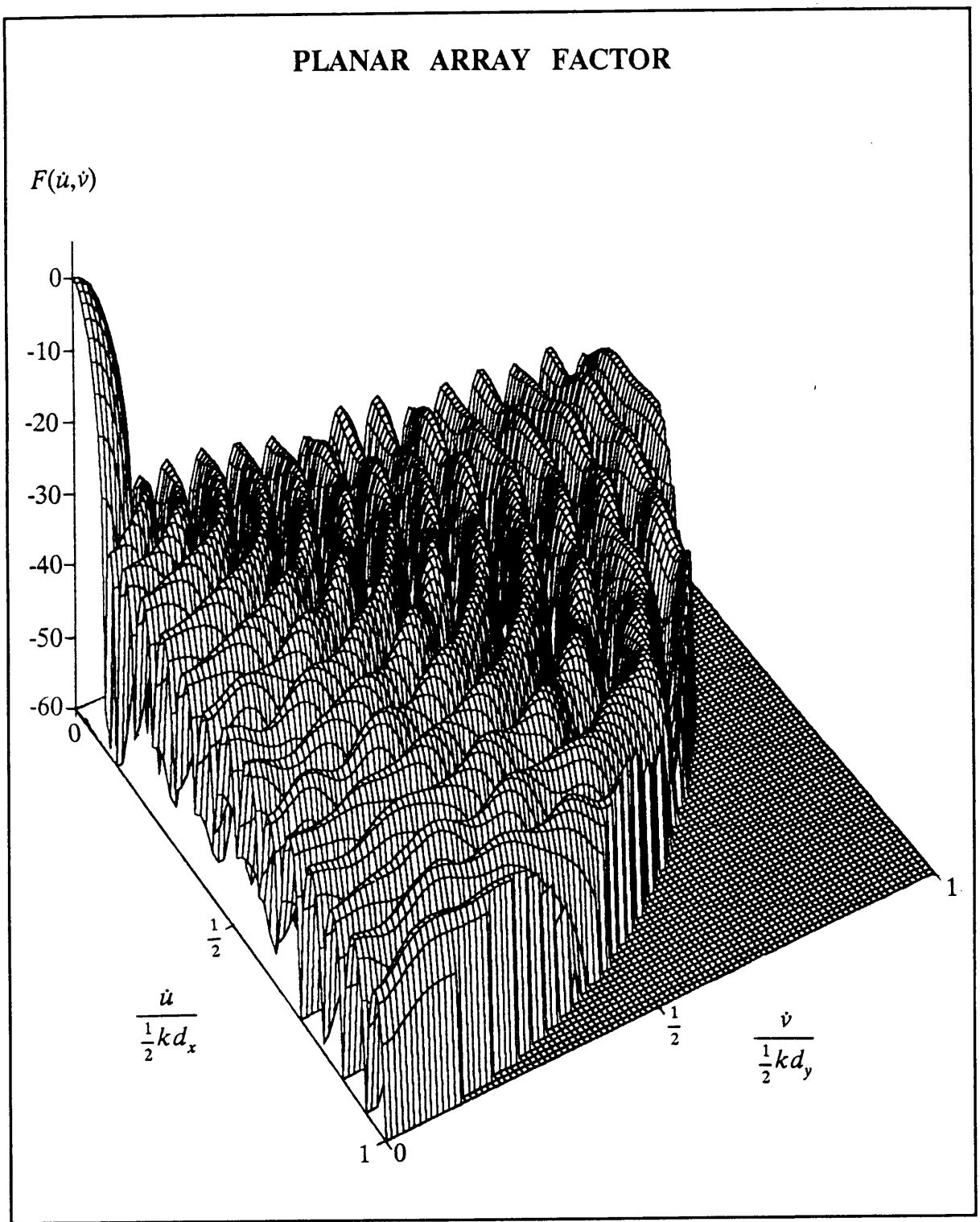

Figure 3.18 Array factor of the circular boundary Villeneuve distribution. (3D-plot floor at *-60dB*)

© University of Pretoria Digitised by the Department of Library Services in support of open access to information, University of Pretoria, 2019

UNIVERSITEIT VAN PRETORIA
UNIVERSITY OF PRETORIA
YUNIBESITHI YA PRETORIA

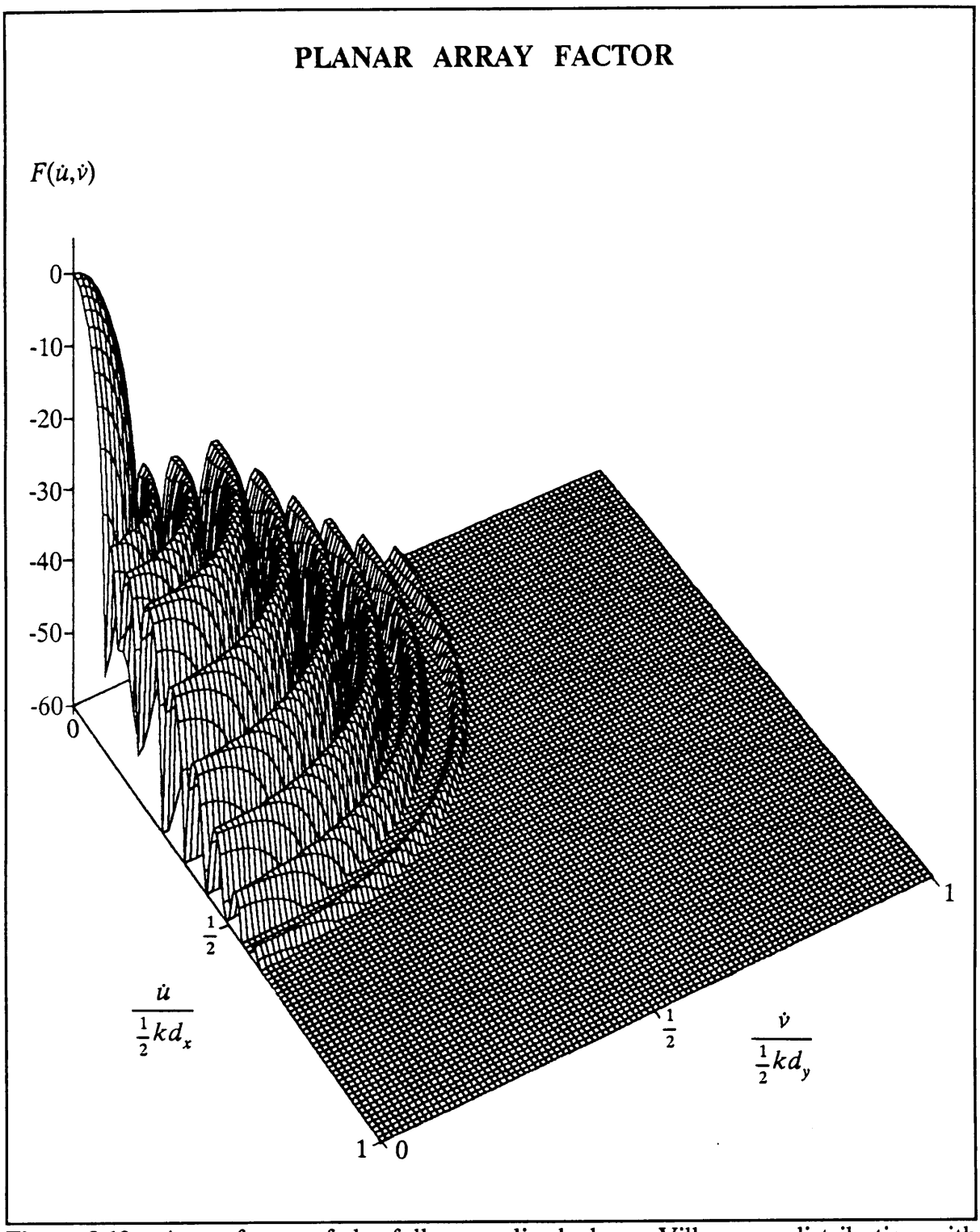

Figure 3.19 Array factor of the full generalised planar Villeneuve distribution with $\bar{n}=3$ and $\upsilon=4.0$.

© University of Pretoria Digitised by the Department of Library Services in support of open access to information, University of Pretoria, 2019

UNIVERSITEIT VAN PRETORIA
UNIVERSITY OF PRETORIA
YUNIBESITHI YA PRETORIA

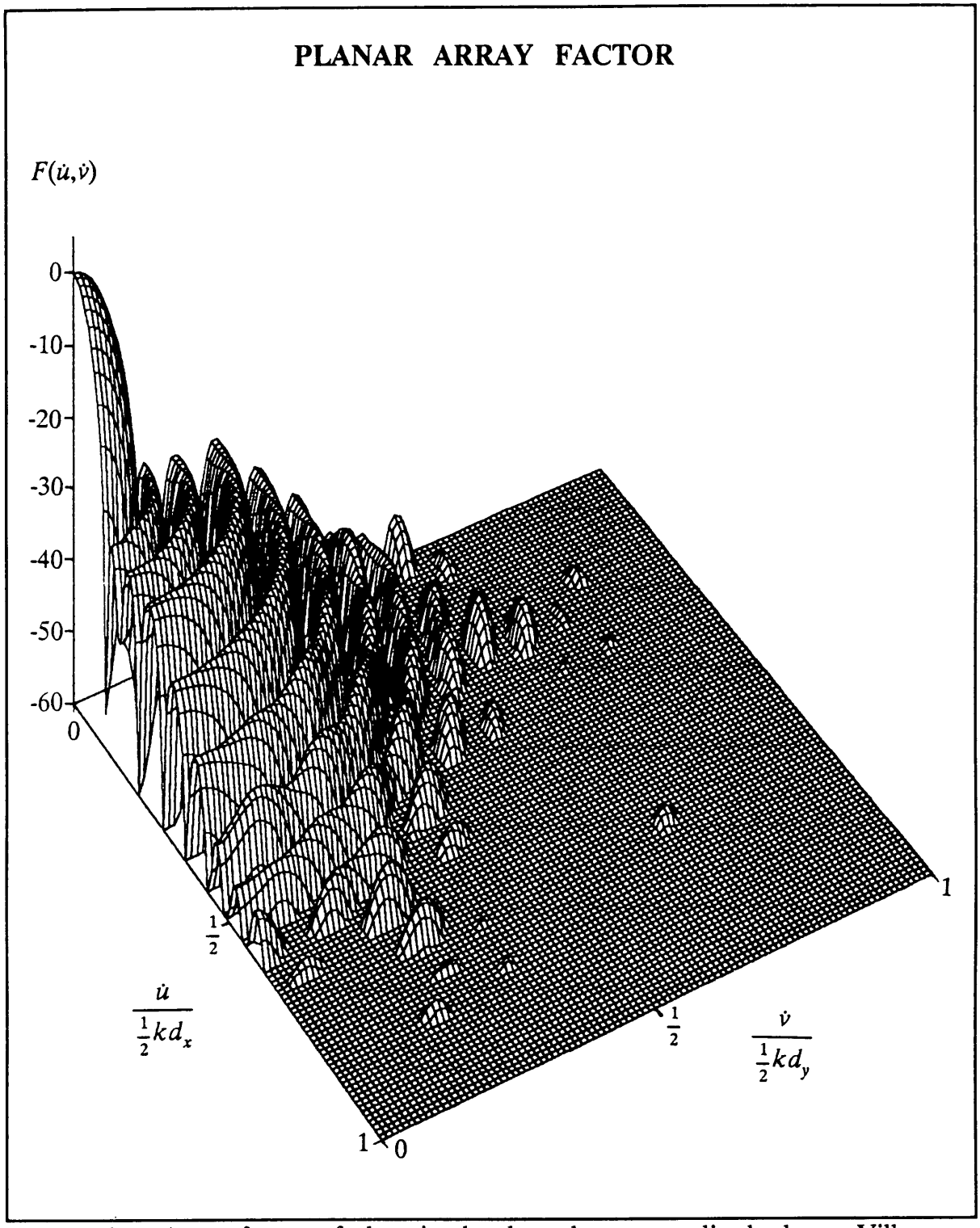

Figure 3.20 Array factor of the circular boundary generalised planar Villeneuve distribution with $\bar{n}=3$ and $\upsilon=4.0$.

© University of Pretoria Digitised by the Department of Library Services in support of open access to information, University of Pretoria, 2019

Figure number	3.12	3.13/4	3.15	3.16/7	3.18	3.19
Transition index $\bar{n}$	-	-	3	3	3	3
Taper rate v	-1.0	-1.0	0.0	0.0	4.0	4.0
Number of elements lopped off	0	46	0	46	0	46
Directivity D (dB)	31.49	31.27	32.52	32.38	32.09	32.05
Biggest element lopped off	-	0.2583	-	0.1969	-	0.0416
Highest sidelobe level (dB)	<-30.00	-27.53	<-30.00	-28.28	<-30.00	<-30.00

Table 3.1 Data relevant to Figures 3.13 to 3.20

3.3 SYNTHESIS OF NEAR-OPTIMUM PLANAR ARRAYS: THE ODD CASE

For completeness, the expressions for the synthesis of a $2N+1$ by $2N+1$ planar array are given here. For such a rectangular array, with symmetry about both the x- and y-axes (2.12) gives the space factor as,

$$F(u,v) = 4\sum_{m=0}^{M}\sum_{n=0}^{N}\zeta_m\,\zeta_n\,a_{mn}\cos(2mu)\cos(2nv) \tag{3.23}$$

with

$$\zeta_i = \begin{cases} \frac{1}{2} & \text{if } i = 0 \\ 1 & \text{if } i \geq 1 \end{cases} \tag{3.24}$$

Since

$$\cos^{2i}x = \frac{1}{2^{2i-1}}\sum_{p=0}^{i}\binom{2i}{i-p}\zeta_{2i}\cos(2px) \tag{3.25}$$

the Baklanov transformation (3.3) can be used to write a general polynomial of degree $2N$, namely

© University of Pretoria Digitised by the Department of Library Services in support of open access to information, University of Pretoria, 2019

$$P_{2N}(w) = \sum_{i=0}^{N} b_{2i} w^{2i} \tag{3.26}$$

to the form

$$\begin{aligned} P_{2N}(u,v) &= \sum_{i=1}^{N} b_{2i} \cos^{2i} u \cos^{2i} v \\ &- \sum_{i=1}^{N} \sum_{k=1}^{i} \sum_{l=1}^{i} \frac{b_{2i}}{4^{2i-2}} \binom{2i}{i-k} \binom{2i}{i-l} \cos(2ku) \cos(2lv) \end{aligned} \tag{3.27}$$

In order for the array factor $F(u,v)$ and the polynomial $P_{2N-1}(u,v)$ are to have the same characteristics, comparison of (3.23) and (3.27) reveals that the element excitations must be given by

$$a_{mn} = \sum_{i=(m,n)}^{N} \frac{b_{2i}}{4^{2i-1}} \binom{2i}{i-m} \binom{2i}{i-n} \tag{3.28}$$

Similar to the even case of Section 3.2, the characteristic polynomial $P_{2N}(w)$ is obtained as follows [6]. Consider a $2N+1$ element linear array. The $2N$ zeros of the parent Dolph-Chebyshev array factor, for a given SLR, are

$$\psi_{\pm n} = \pm 2\cos^{-1}\left\{\frac{1}{u_0} \cos\left[\frac{(2n-1)\pi}{4N}\right]\right\} \qquad n = 1,2,.....,N \tag{3.29}$$

in which

$$u_0 = \cosh\left[\frac{1}{2N} \ln\left(SLR + \sqrt{SLR^2 - 1}\right)\right] \tag{3.30}$$

The zeros of a $2N+1$ element uniformly excited array are at

$$\psi_{\pm n}^{0} = \frac{\pm 2n\pi}{2N-1} \qquad n = 1,2,.....,N \tag{3.31}$$

Let the array factor zeros be adjusted in the same manner as in the even case,

© University of Pretoria Digitised by the Department of Library Services in support of open access to information, University of Pretoria, 2019

UNIVERSITEIT VAN PRETORIA
UNIVERSITY OF PRETORIA
YUNIBESITHI YA PRETORIA

$$\psi'_{\pm n} = \begin{cases} \sigma\,\psi_{\pm n} & |n| \le \bar{n} \\ \psi_{\pm n} + (v+1)\left(\psi'_{\pm n} - \psi_{\pm n}\right) & |n| \ge \bar{n} \end{cases} \tag{3.32}$$

with the dilation factor σ

$$\sigma = \frac{1}{\psi_{\bar{n}}}\left[\psi_{\bar{n}} + (v+1)\left(\psi^0_{\bar{n}} - \psi_{\bar{n}}\right)\right] \tag{3.33}$$

The zeros are transformed from the ψ-plane to the w-plane by

$$w = \cos\left(\frac{\psi}{2}\right) \tag{3.34}$$

to obtain the characteristic polynomial. Because of symmetry, all the zeros are in pairs, each pair having the same magnitude but alternating signs. This will cause the characteristic polynomial to have only even non-zero coefficients, eg. b_{2i}.

3.4 CONCLUSIONS

The generalised Villeneuve distribution linear array synthesis method has been extended to the planar array case by means of a modified Baklanov transformation. The generalised Villeneuve distribution for planar arrays developed in this chapter enables the direct synthesis of discrete array distributions for high efficiency patterns of arbitrary sidelobe levels and envelope taper. The synthesis method is extremely rapid; consequently, design trade-off studies are feasible. For a set number of elements and sidelobe ratio, the values of the transition index and the taper rate for a specific application will depend on the relative importance of farther-out sidelobe levels and the excitation efficiency (or directivity) desired. Parametric studies of the distribution's performance have been conducted; such curves of directivity versus element number for planar arrays do not appear to be available elsewhere in the literature. It has also been shown how the generalised planar Villeneuve distribution can be used for the synthesis of planar arrays with a circular boundaries, without the directivity performance being disadvantaged.

© University of Pretoria Digitised by the Department of Library Services in support of open access to information, University of Pretoria, 2019

UNIVERSITEIT VAN PRETORIA
UNIVERSITY OF PRETORIA
YUNIBESITHI YA PRETORIA

3.5 REFERENCES

[1] C.L.Dolph, "A current distribution for broadside arrays which optimises the relationship between beam width and side-lobe level", *Proc. IRE*, Vol.34, pp.335-348, June 1946.

[2] T.T. Taylor, "Design of line-source antennas for narrow beamwidth and low sidelobes", *IRE Trans. Antennas Propagat.*, Vol.AP-3, pp.16-28, Jan.1955.

[3] D.R.Rhodes, "On the Taylor distribution", *IEEE Trans. Antennas Propagat.*, Vol.AP-32, pp.143-145, Jan.1972.

[4] D.R.Rhodes, *Synthesis of Planar Antenna Sources*, London: Clarendon Press, 1974.

[5] A.T.Villeneuve, "Taylor patterns for discrete arrays", *IEEE Trans. Antennas Propagat.*, Vol.AP-32, No.10, pp.1089-1093, Oct.1984.

[6] D.A.McNamara, "Generalised Villeneuve n-distribution", *IEE Proc.*, Pt.H, Vol.136, No.3, pp.245-249, June 1989.

[7] Y.V.Baklanov, "Chebyshev distribution of current for a planar array of radiators", *Radio Eng. Electron. Phys. (USSR)*, Vol.11, pp.640-642, 1966.

[8] F.I.Tseng and D.K.Cheng, "Optimum scannable planar arrays with an invariant side lobe level", *Proc. IEEE*, Vol.56, No.11, pp.1771-1778, Nov.1968.

[9] R.S.Elliott, "Synthesis of rectangular planar arrays for sum patterns with ring side lobes of arbitrary topography", *Radio Science*, Vol.12, pp.653-657, 1977.

[10] Y.U.Kim and R.S.Elliott, "Extensions of the Tseng-Cheng pattern synthesis technique", *J. Electromagn. Waves Applic.*, Vol.2, No.3/4, pp.255-268, 1988.

© University of Pretoria Digitised by the Department of Library Services in support of open access to information, University of Pretoria, 2019

UNIVERSITEIT VAN PRETORIA
UNIVERSITY OF PRETORIA
YUNIBESITHI YA PRETORIA

CHAPTER 4

A TECHNIQUE FOR THE SYNTHESIS OF PLANAR ARRAYS WITH ARBITRARY PATTERN CONTOURS

4.1 INTRODUCTORY REMARKS

There is considerable interest in the problem of designing an antenna, to be placed on a satellite, that will beam electromagnetic waves of uniform strength onto a specified portion of the earth's surface while causing negligible radiation to reach the remainder of the earth's surface. In order to best utilise the limited spacecraft transmitter power and reduce possible interference problems with other coverage areas, the ideal antenna would have uniform gain over the coverage region and no radiation elsewhere. Such shaped beams are said to have a *contoured footprint*. The fact that a real antenna is of finite size, along with several other practical limitations, means that there will be some sidelobe radiation outside the defined irregularly shaped coverage region.

The McClellan transformation, used in signal processing in the design of two-dimensional digital filters [1], is adapted and extended to planar (two dimensional) array synthesis. The method developed here for the synthesis of planar arrays with prescribed contour beams, uses the McClellan transformation and its generalisation to decouple the synthesis problem into two separate problems; the synthesis of a linear array prototype and the determination of the transform coefficients. The transformation method is a powerful approach since it utilizes the vast resources of the already very well developed

© University of Pretoria Digitised by the Department of Library Services in support of open access to information, University of Pretoria, 2019

linear array synthesis techniques. The number of transform coefficients is also much smaller than the number of elements in the array. With this technique the time to design a planar array is modest, as a result very large arrays can readily be designed and trade-off studies can be conducted. In Section 4.2 we will discuss the application of the transform in the synthesis of planar arrays with quadrantal symmetric space factors. In Section 4.3 the transform method will be extended to allow for centro-symmetric radiation patterns. Section 4.4 will be devoted to the contour approximation problem, and simple expressions for the calculation of the transform coefficients for circular and elliptical footprint patterns will be presented. In Section 4.5 application of the technique is examined by a number of specific examples.

4.2 SYNTHESIS OF PLANAR ARRAYS FOR THE CASE OF QUADRANTAL SYMMETRY

4.2.1 Introduction

All the analytical expressions used in this section, although previously defined in Chapter 2, will be repeated for convenience. We first consider contoured footprints that are symmetric about both the x- and y-axes. Such contours can be generated by planar arrays with excitations that have quadrantal symmetry. Furthermore, the array lattice is assumed to be rectangular, although the spacings d_x and d_y need not be equal. In addition, the array is assumed to have a rectangular boundary; that is, no elements have been removed from the lattice in order to alter the boundary shape.

4.2.2 Planar Arrays with $2M+1$ by $2N+1$ Elements

Under the above assumptions and the following substitutions,

$$\begin{aligned} u &= kd_x(\sin\theta\cos\phi - \sin\theta_0\cos\phi_0) \\ v &= kd_y(\sin\theta\sin\phi - \sin\theta_0\sin\phi_0) \end{aligned} \tag{4.1}$$

with d_x, d_y the interelement spacings and θ_0, ϕ_0 the pointing direction of the main beam, the $2M+1$ by $2N+1$ planar array space factor becomes, from (2.12),

© University of Pretoria Digitised by the Department of Library Services in support of open access to information, University of Pretoria, 2019

$$F(u,v) = 4\sum_{m=0}^{M}\sum_{n=0}^{N}\zeta_m\zeta_n a_{mn}\cos(mu)\cos(nv)$$

$$\text{where } \zeta_i = \begin{cases} \frac{1}{2} & \text{if } i = 0 \\ 1 & \text{if } i \geq 1 \end{cases} \tag{4.2}$$

Next consider a $2Q+1$ element linear array (which will be referred to as the *prototype linear array*), also with symmetrical excitation. By using the substitution

$$\psi = kd(\sin\theta - \sin\theta_0) \tag{4.3}$$

with d the inter element spacing and θ_0 the main beam pointing direction, the prototype linear array factor is, from (2.4), given by

$$F(\psi) = a_0 + 2\sum_{q=1}^{Q} a_q \cos(q\psi) \tag{4.4}$$

With the use of the recurrence relation [11: p.17]

$$\cos^q x = \sum_{i=0}^{q} g_{iq}\cos(ix)$$

$$\text{with } g_{iq} = \begin{cases} \frac{1}{2^q} & \text{if } i = o \text{ and } q \text{ is even} \\ \frac{1}{2^{q-1}}\binom{q}{\frac{1}{2}(q-i)} & \text{if } i \text{ and } q \text{ both even or } i \text{ and } q \text{ both odd} \\ 0 & \text{if } i \text{ even and } q \text{ odd or } i \text{ odd and } q \text{ even} \end{cases} \tag{4.5}$$

the linear array factor (4.4) can be written as

$$F(\psi) = \sum_{q=0}^{Q} b_q \cos^q\psi \tag{4.6}$$

The original McClellan's transform [1] is a transformation of a one-dimensional FIR filter into a two-dimensional FIR filter by means of the substitution of variables. In the array context, a prototype linear array is transformed into a planar array by means of the substitution of variables,

© University of Pretoria Digitised by the Department of Library Services in support of open access to information, University of Pretoria, 2019

$$\cos\psi = H(u,v) = t_{00} + t_{01}\cos v + t_{10}\cos u + t_{11}\cos u\cos v \tag{4.7}$$

in which

$$|H(u,v)| \leq 1 \tag{4.8}$$

Next consider a transformation [2] which is a generalised form of the original McClellan transformation, and which converts a symmetrical prototype linear array factor into a quadrantal symmetric planar array factor,

$$\cos\psi = H(u,v) = \sum_{i=0}^{I}\sum_{j=0}^{J} t_{ij}\cos(iu)\cos(jv) \tag{4.9}$$

in which t_{ij} are real coefficients. The order of the transformation is determined by the largest of I and J.

Substitution of (4.9) into (4.6) gives an expression for $F(\psi)$ in terms of the two variables u and v, that is $F(u,v)$, as

$$F(u,v) = \sum_{q=0}^{Q} b_q\left[\sum_{i=0}^{I}\sum_{j=0}^{J} t_{ij}\cos(iu)\cos(jv)\right]^q \tag{4.10}$$

The application of the recurrence relation (4.5) a second time then allows (4.10) to be re-written in the form

$$F(u,v) = \sum_{m=0}^{M}\sum_{n=0}^{N} c_{mn}\cos(mu)\cos(nv) \tag{4.11}$$

with $M=QI$ and $N=QJ$. Comparison of (4.11) with the planar array space factor (4.2) shows that the planar array element excitation is

$$a_{mn} = \frac{c_{mn}}{\zeta_m \zeta_n} \tag{4.12}$$

A recursive formula for computing the b_q in (4.6) from the prototype linear array coefficients of (4.4) is given in Appendix B.2. Recursion relations for the c_{mn} of (4.12) in terms of b_q are given in Appendix B.3. Although it is not easy to write these formulas in a mathematically elegant fashion, the recursive formulas are ideally suited for

© University of Pretoria Digitised by the Department of Library Services in support of open access to information, University of Pretoria, 2019

computation.

On those contours defined by $H(u,v)=constant$, $F(u,v)$ must be constant. These contours are controlled by the parameters t_{ij}. The value associated with a particular contour depends only on the excitation coefficients of the prototype linear array and is equal to $F(\psi)$ with $\psi=arccos[H(u,v)]$. The synthesis problem has thus been reduced to two smaller and more easily solvable problems; the synthesis of a linear array and the selection of a set of transformation parameters.

If the desired accuracy or detailed shape of the contours cannot be employed using a first order transformation ($I=J=1$) in the form of (4.7), one can use a higher order transformation as in (4.9). The coefficients of the transformation are obtained using a constrained approximation or optimisation technique. The use of a higher order transformation will mean that I and J increase, with a resultant increase in the size of the final planar array, proportional to I in the x-direction and J in the y-direction. The size of the prototype linear array used is dependent on the sidelobe level, the beamwidth and amount of coverage area gain ripple allowable.

4.2.3 Planar Arrays with $2M$ by $2N$ Elements

Under the assumptions mentioned in Section 4.2.1 and the substitutions:

$$\begin{aligned} \dot{u} &= \frac{1}{2}u = \frac{1}{2}kd_x(\sin\theta\cos\phi - \sin\theta_0\cos\phi_0) \\ \dot{v} &= \frac{1}{2}v = \frac{1}{2}kd_y(\sin\theta\sin\phi - \sin\theta_0\sin\phi_0) \end{aligned} \tag{4.13}$$

the $2M$ by $2N$ planar array space factor becomes, from (2.13),

$$F(\dot{u},\dot{v}) = 4\sum_{m=1}^{M}\sum_{n=1}^{N} a_{mn}\cos[(2m-1)\dot{u}]\cos[(2n-1)\dot{v}] \tag{4.14}$$

Consider a $2Q$ element prototype linear array, also with symmetrical excitation. Using the substitution

$$\dot{\psi} = \frac{1}{2}\psi = \frac{1}{2}kd(\sin\theta - \sin\theta_0) \tag{4.15}$$

the prototype linear array factor (2.3) becomes

© University of Pretoria Digitised by the Department of Library Services in support of open access to information, University of Pretoria, 2019

$$F(\dot{\psi}) = 2\sum_{q=1}^{Q} a_q \cos[(2q-1)\dot{\psi}] \tag{4.16}$$

The recurrence relation [11: p.17]

$$[\cos x]^{(2q-1)} = \sum_{i=1}^{q} \frac{1}{2^{2q-2}} \binom{2q-1}{q-i} \cos[(2i-1)x] \tag{4.17}$$

allows us to write the linear array factor (4.16) in the form

$$F(\dot{\psi}) = \sum_{q=1}^{Q} b_q [\cos\dot{\psi}]^{2q-1} \tag{4.18}$$

The general transformation which converts the symmetrical prototype linear array pattern into a quadrantal symmetric planar array pattern is,

$$\cos\dot{\psi} = H(\dot{u},\dot{v}) = \sum_{i=1}^{I}\sum_{j=1}^{J} t_{ij}\cos[(2i-1)\dot{u}]\cos[(2j-1)\dot{v}] \tag{4.19}$$

in which t_{ij} are real coefficients.

Substitution of (4.19) into (4.18) gives an expression for $F(\dot{\psi})$ in terms of the two variables $\dot{u}$ and $\dot{v}$, that is $F(\dot{u},\dot{v})$, as

$$F(\dot{u},\dot{v}) = \sum_{q=1}^{Q} b_q \left[\sum_{i=1}^{I}\sum_{j=1}^{J} t_{ij}\cos[(2i-1)\dot{u}]\cos[(2j-1)\dot{v}]\right]^{(2q-1)} \tag{4.20}$$

By applying the recurrence relation (4.17) again, (4.20) can be written in the same form as a planar array factor,

$$F(\dot{u},\dot{v}) = \sum_{m=1}^{M}\sum_{n=1}^{N} c_{mn}\cos[(2m-1)\dot{u}]\cos[(2n-1)\dot{v}] \tag{4.21}$$

with $M=(2I-1)(2Q-1)$ and $N=(2J-1)(2Q-1)$. Comparison of (4.21) with the planar array space factor (4.14) shows that the planar array element excitation simply is

$$a_{mn} = c_{mn} \tag{4.22}$$

Again on those contours defined by $H(\dot{u},\dot{v})=constant$, which are controlled by the

© University of Pretoria Digitised by the Department of Library Services in support of open access to information, University of Pretoria, 2019

parameters t_{ij}, $F(\dot{u},\dot{v})$ must be constant. Unlike the case in Section 4.2.2, the use of the first order transformation is limited to near circular footprint contours. The use of higher order transformation will mean a increase I and J and hence the size of the final planar array along with them. This increase in planar array size is proportional to $2I-1$ in the x-direction and $2J-1$ in the y-direction, which is more rapid than the case in Section 4.2.2. Thus the use of this synthesis technique for planar arrays with even number of elements in the x- and y-directions, is limited to meanly high directivity, low sidelobe applications.

4.2.4 Planar Arrays with $2M$ by $2N+1$ Elements

Under the assumptions mentioned in Section 4.2.1 and substitutions in (4.13) the $2M$ by $2N+1$ planar array factor can be written as

$$F(\dot{u},\dot{v}) = 4\sum_{m=1}^{M}\sum_{n=0}^{N} \zeta_n a_{mn} \cos[(2m-1)\dot{u}]\cos[2n\dot{v}] \tag{4.23}$$

Next consider the general transformation

$$\cos\dot{\psi} = H(\dot{u},\dot{v}) = \sum_{i=1}^{I}\sum_{j=0}^{J} t_{ij}\cos[(2i-1)\dot{u}]\cos[2j\dot{v}] \tag{4.24}$$

in which t_{ij} are real coefficients. The prototype linear array is a $2Q$ element array, with symmetrical excitation. Substitution of the transformation (4.24) into the prototype linear array radiation pattern (4.18) gives

$$F(\dot{u},\dot{v}) = \sum_{q=1}^{2Q-1} b_q \left[\sum_{i=1}^{I}\sum_{j=0}^{J} t_{ij}\cos[(2i-1)\dot{u}]\cos[2j\dot{v}]\right]^{(2q-1)} \tag{4.25}$$

The use of the recurrence relation (4.17) permits (4.25) to written in the same form as the planar array factor,

$$F(\dot{u},\dot{v}) = \sum_{m=1}^{M}\sum_{n=0}^{N} c_{mn}\cos[(2m-1)\dot{u}]\cos[2n\dot{v}] \tag{4.26}$$

with $M=(2I-1)(2Q-1)$ and $N=2IQ$. Comparison of the two expressions shows that the element excitation is

© University of Pretoria Digitised by the Department of Library Services in support of open access to information, University of Pretoria, 2019

$$a_{mn} = \frac{c_{mn}}{\zeta_n} \tag{4.27}$$

This case suffers from the same limitations as the case with the array consisting of $2M$ by $2N$ elements, thus its use is limited.

4.2.5 Relationship to the Baklanov Transformation Planar Array Synthesis Method.

Baklanov [8] proposed a synthesis procedure for broadside, square arrays that will produce a Dolph-Chebyshev pattern in any cross section. The procedure was extended by Tseng and Cheng [9] to scannable planar arrays. Kim and Elliott [10] extended the method to include flattop beams and arbitrary sidelobe levels.

For an odd number of elements in each row and column in the planar array (the odd case), the procedure is as follows. With the substitution

$$w = \cos\dot{\psi} \tag{4.28}$$

with $\dot{\psi}$ is defined in (4.7), the space factor of an linear array with $2Q+1$ symmetrically excited elements, can be written as polynomial of order $2Q$,

$$F(w) = P_{2Q}(w) = \sum_{q=0}^{Q} b_{2q} w^{2q} \tag{4.29}$$

After using the following transformation, proposed by Baklanov [8],

$$\cos\dot{\psi} = w = w_0 \cos\dot{u} \cos\dot{v} \tag{4.30}$$

with $\dot{u}$ and $\dot{v}$ defined in (4.13), the polynomial (space factor) becomes

$$P_{2Q}(\dot{u},\dot{v}) = \sum_{q=0}^{Q} a_{2q} w_0^{2q} [\cos\dot{u} \cos\dot{v}]^{2q} \tag{4.31}$$

where w_0 and the coefficients a_{2q} are determined from a Chebyshev polynomial of order $2Q$ [9]. The factor w_0 and the coefficients a_{2q} can be combined to form b_{2q} [10] as

© University of Pretoria Digitised by the Department of Library Services in support of open access to information, University of Pretoria, 2019

UNIVERSITEIT VAN PRETORIA
UNIVERSITY OF PRETORIA
YUNIBESITHI YA PRETORIA

$$b_{2q} = a_{2q} w_0^{2q} \tag{4.32}$$

The Baklanov transformation now is

$$\cos\dot{\psi} = w = \cos\dot{u}\cos\dot{v} \tag{4.33}$$

and the polynomial becomes

$$P_{2Q}(\dot{u},\dot{v}) = \sum_{q=0}^{Q} b_{2q}[\cos\dot{u}\cos\dot{v}]^{2q} \tag{4.34}$$

Kim and Elliott [10] used these coefficients, which are determined from a linear array excitation, in their extension of the Baklanov synthesis method. These b_{2q} coefficients are essentially the same as the b_q coefficients in the technique proposed in this chapter. After implementing the Baklanov transformation (4.33) and by using the recurrence relations (4.5) the polynomial P_{2Q} have the same form as a planar radiation pattern.

To make a comparison between the original McClellan transformation (4.7) and the Baklanov transformation (4.33) the latter must be written in terms of ψ, u and v. The polynomial can be written in terms of w^2 as

$$P_{2Q}(w) = \sum_{q=0}^{Q} b_{2q}[w^2]^q \tag{4.35}$$

with

$$\begin{aligned} w^2 = \cos^2\dot{\psi} &= \frac{1}{2} + \frac{1}{2}\cos 2\dot{\psi} \\ &= \frac{1}{2} + \frac{1}{2}\cos\psi \end{aligned} \tag{4.36}$$

From the Baklanov transformation (4.33) w^2 is

$$\begin{aligned} w^2 = \cos^2\dot{u}\cos^2\dot{v} &= \left[\frac{1}{2} + \frac{1}{2}\cos 2\dot{u}\right]\left[\frac{1}{2} + \frac{1}{2}\cos 2\dot{v}\right] \\ &= \left[\frac{1}{2} + \frac{1}{2}\cos u\right]\left[\frac{1}{2} + \frac{1}{2}\cos v\right] \end{aligned} \tag{4.37}$$

Comparison between (4.36) and (4.37) shows that

© University of Pretoria Digitised by the Department of Library Services in support of open access to information, University of Pretoria, 2019

UNIVERSITEIT VAN PRETORIA
UNIVERSITY OF PRETORIA
YUNIBESITHI YA PRETORIA

$$\cos\psi = -\frac{1}{2} + \frac{1}{2}\cos v + \frac{1}{2}\cos u + \frac{1}{2}\cos u\cos v \qquad (4.38)$$

Thus, for the odd case the Baklanov transformation is equivalent to a special case of the newly developed method, namely: the original (first order, $I=J=1$) McClellan transformation with $-t_{00}=t_{01}=t_{10}=t_{11}=½$.

For an even number of elements in each row and column, the Baklanov transformation is once again equivalent to a special case of method developed here; namely the first order transformation with $t_{11}=½$, as can easily be seen form a comparison of (4.19) and (4.33)

Planar array synthesis with the Baklanov transformation gives only "near" circular contours. To obtain elliptical contours, the interelement spacings d_x and d_y have to be adjusted. However, care should be taken to avoid grating lobes. Kim and Elliott proposed a generalisation of the Baklanov transformation [10: equation (16)]. This transformation produces "near" elliptical inner contours. To obtain elliptical contours with a different major axis to minor axis ratio, p and q of [10: equation (16)] must be changed. This will also change the number of elements of the array. Neither of these two methods can be extended to synthesise arbitrary contours. Neither a change in interelement spacing nor a change in the number of array elements can be tolerated when synthesising reconfigurable arrays.

4.3 SYNTHESIS OF PLANAR ARRAY WITH FOR THE CASE OF CENTRO-SYMMETRY

By centro-symmetry is meant symmetry of the beam contour, about the broadside direction, in any constant ϕ pattern plane. Such contours can be generated by planar arrays with excitations a_{mn} that are a superposition of a set of excitations a^c_{mn} symmetric about the x- and y-axes and a set of excitations a^s_{mn} asymmetric about the x- and y-axes. Again, the array lattice and boundary is assumed to be rectangular, although the spacings d_x and d_y need not be equal. The transformation will be extended only to the case of an odd number of elements in both the x- and y-directions of the planar array.

© University of Pretoria Digitised by the Department of Library Services in support of open access to information, University of Pretoria, 2019

Using the substitutions of (4.1), the array factor of a $2M+1$ by $2N+1$ planar array is (2.11)

$$F(u,v) = \sum_{m=-M}^{M} \sum_{n=-N}^{N} a_{mn} e^{j(mu+nv)} \tag{4.39}$$

The element excitation a_{mn} is a superposition of a_{mn}^c and a_{mn}^s where

$$a_{mn}^c = a_{-mn}^c = a_{-m-n}^c = a_{m-n}^c \tag{4.40a}$$

and

$$\begin{aligned} a_{mn}^s &= 0 && \text{if } m=0 \text{ or } n=0 \\ a_{mn}^s &= -a_{-mn}^s = a_{-m-n}^s = -a_{m-n}^s && \text{otherwise} \end{aligned} \tag{4.40b}$$

Using these excitations, the array factor (4.39) becomes

$$F(u,v) = \sum_{m=0}^{M} \sum_{n=0}^{N} \left[\zeta_m \zeta_n a_{mn}^c \cos(mu)\cos(nv) - a_{mn}^s \sin(mu)\sin(nv) \right] \tag{4.41}$$

The transformation for the centro-symmetric case is [2]

$$\cos(\psi) = H(u,v) = \sum_{i=0}^{I} \sum_{j=0}^{J} t_{ij} \cos(iu)\cos(jv) + \sum_{i=1}^{I} \sum_{j=1}^{J} s_{ij} \sin(iu)\sin(jv) \tag{4.42}$$

in which t_{ij} and s_{ij} are real coefficients. Substitution of (4.42) into (4.6) gives

$$F(u,v) = \sum_{q=0}^{Q} b_q \left[\sum_{i=0}^{I} \sum_{j=0}^{J} t_{ij} \cos(iu)\cos(jv) + \sum_{i=1}^{I} \sum_{j=1}^{J} s_{ij} \sin(iu)\sin(jv) \right]^q \tag{4.43}$$

Application of the recurrence relation (4.5) in (4.43) yields

$$F(u,v) = \sum_{m=0}^{M} \sum_{n=0}^{N} \left[c_{mn}^c \cos(mu)\cos(nv) + c_{mn}^s \sin(mu)\sin(nv) \right] \tag{4.44}$$

with $M=QI$ and $N=QJ$. Comparison of (4.44) with the planar array factor (4.41) yields

© University of Pretoria Digitised by the Department of Library Services in support of open access to information, University of Pretoria, 2019

$$a_{mn}^{c} = \frac{c_{mn}^{c}}{\zeta_m \zeta_n} \tag{4.45a}$$

and

$$a_{mn}^{s} = -c_{mn}^{s} \tag{4.45b}$$

The final array excitation is thus

$$\begin{aligned} a_{mn} &= a_{mn}^{c} + \kappa_m \kappa_n a_{mn}^{s} \\ &= \frac{c_{mn}^{c}}{\zeta_m \zeta_n} - \kappa_m \kappa_n c_{mn}^{s} \end{aligned} \tag{4.46}$$

$$\begin{aligned} for \quad m &= -M, -(M-1), \ldots, -1, 0, 1, \ldots, M \\ n &= -N, -(N-1), \ldots, -1, 0, 1, \ldots, N \end{aligned}$$

with $\kappa_i = sign(i)$

Recursive formulas for computing c_{mn}^{c} and c_{mn}^{s} are given in Appendix B.4. On those contours defined by $H(u,v) = constant$, $F(u,v)$ must be constant on equal to $F(\psi)$ with $\psi = arccos[H(u,v)]$. These contours are controlled by the parameters t_{ij} and s_{ij}. The synthesis problem has thus been reduced to two smaller and easily solvable problems; the synthesis of a linear array and the selection of a set of transformation parameters.

Again, a higher order transformation can be used if the desired accuracy or detailed shape of the contours cannot be achieved using with a first order transformation. This increase in order will cause a proportional increase in the final array size. The coefficients of the transformation are obtained using a constrained approximation or optimisation technique.

4.4 THE CONTOUR APPROXIMATION PROBLEM.

4.4.1 Introduction

The isopotential contours of transformation $H(u,v)$ are controlled by the transformation coefficients t_{ij} and s_{ij}. This section will be devoted to the problem of

© University of Pretoria Digitised by the Department of Library Services in support of open access to information, University of Pretoria, 2019

choosing the transformation parameters t_{ij} and s_{ij} so that the ψ=*constant* contours produced by the transformation $H(u,v)$ in the uv-plane have some desired shape. In footprint pattern planar array synthesis it will usually be sufficient to control the shape of a single contour, namely the halfpower (-3dB) contour or the contour of the first null. In same other cases, such as high directivity, narrow beam arrays, it may be advantageous to constrain the shape of all the contours.

4.4.2 Simple formulas for Scaling Factors

Visible space is the region where $0 \le \theta \le \pi$ and $0 \le \phi \le 2\pi$. From the definition of u and v in (4.1) a elliptical disc, with major axis kd_x and minor axis kd_y, constitutes visible space in the uv-plane [12]. The transformation mapping ψ into the uv-plane is

$$\cos(\psi) = H(u,v) = \sum_{i=0}^{I}\sum_{j=0}^{J} t_{ij}\cos(iu)\cos(jv) + \sum_{i=1}^{I}\sum_{j=1}^{J} s_{ij}\sin(iu)\sin(jv) \qquad (4.47)$$

in which t_{ij} and s_{ij} are real coefficients. It is clear from the definition of $H(u,v)$ that, in order to map the visible space of ψ into the visible space in the uv-plane, the following constraint must be imposed on $H(u,v)$,

$$|H(u,v)| \le 1 \quad for \quad \sqrt{\left(\frac{u}{kd_x}\right)^2 + \left(\frac{v}{kd_y}\right)^2} \le 1 \qquad (4.48)$$

Here lies the difference between the in the application of the transformation method in array synthesis and digital filter design [2, 5]. In the digital filter design case the transformation, $H_D(u,v)$, maps ψ into a square area, $0 \le u,v \le \pi$, in the uv-plane. Thus the constraint imposed on $H_D(u,v)$ [2, 5] is

$$|H_D(u,v)| \le 1 \quad for \ 0 \le u,v \le \pi \qquad (4.49)$$

The transform parameters are found using a optimization technique or approximation to fit the desired shape of the target contour. The solution, however, usually does not satisfy the condition in (4.48) and scaling is therefore necessary. The following linear scaling scheme can be employed [2, 5]

$$H'(u,v) = C_1 H(u,v) - C_2 \qquad (4.50)$$

© University of Pretoria Digitised by the Department of Library Services in support of open access to information, University of Pretoria, 2019

where

$$C_1 = \frac{2}{H_{max} - H_{min}} \tag{4.51a}$$

and

$$C_2 = C_1 H_{max} - 1 \tag{4.51b}$$

H_{max} and H_{min} are the maximum and minimum values of $H(u,v)$ which usually have to be found numerically. Obviously this scaling does not change the shape of the contours defined by $H(u,v)=constant$. $H'(u,v)$ is then used instead of $H(u,v)$ as the transformation. All that changes is the original ψ associated with a specific contour, namely

$$\psi' = \arccos(C_1 \cos\psi - C_2) \tag{4.52}$$

4.4.3 Approximation of Circular Contours

The following first order transformation coefficients gives near circular contours

$$-t_{00} = t_{01} = t_{10} = t_{11} = \frac{1}{2} \tag{4.53}$$

Studying the contour plot of $H(u,v)$, Figure 4.1, reviles that the contours for low values of ψ (close to the origin of the uv-plane) are approximately circular but deviate considerably from circular contours as ψ increases. At $\psi=\pi$ the contour is a square. The maximum deviation from the ideal circular behaviour is at $\phi=45°$ (or where $u=v$). An advantage of this transformation is the linear array factor is preserved along the u-axis ($v=0$) and v-axis ($u=0$). In other words, both the collapsed distributions planar array are identical to the prototype linear array distribution. As the shape of the contours in the sidelobe region is not important, this transformation can be used for narrow beamwidth applications.

© University of Pretoria Digitised by the Department of Library Services in support of open access to information, University of Pretoria, 2019

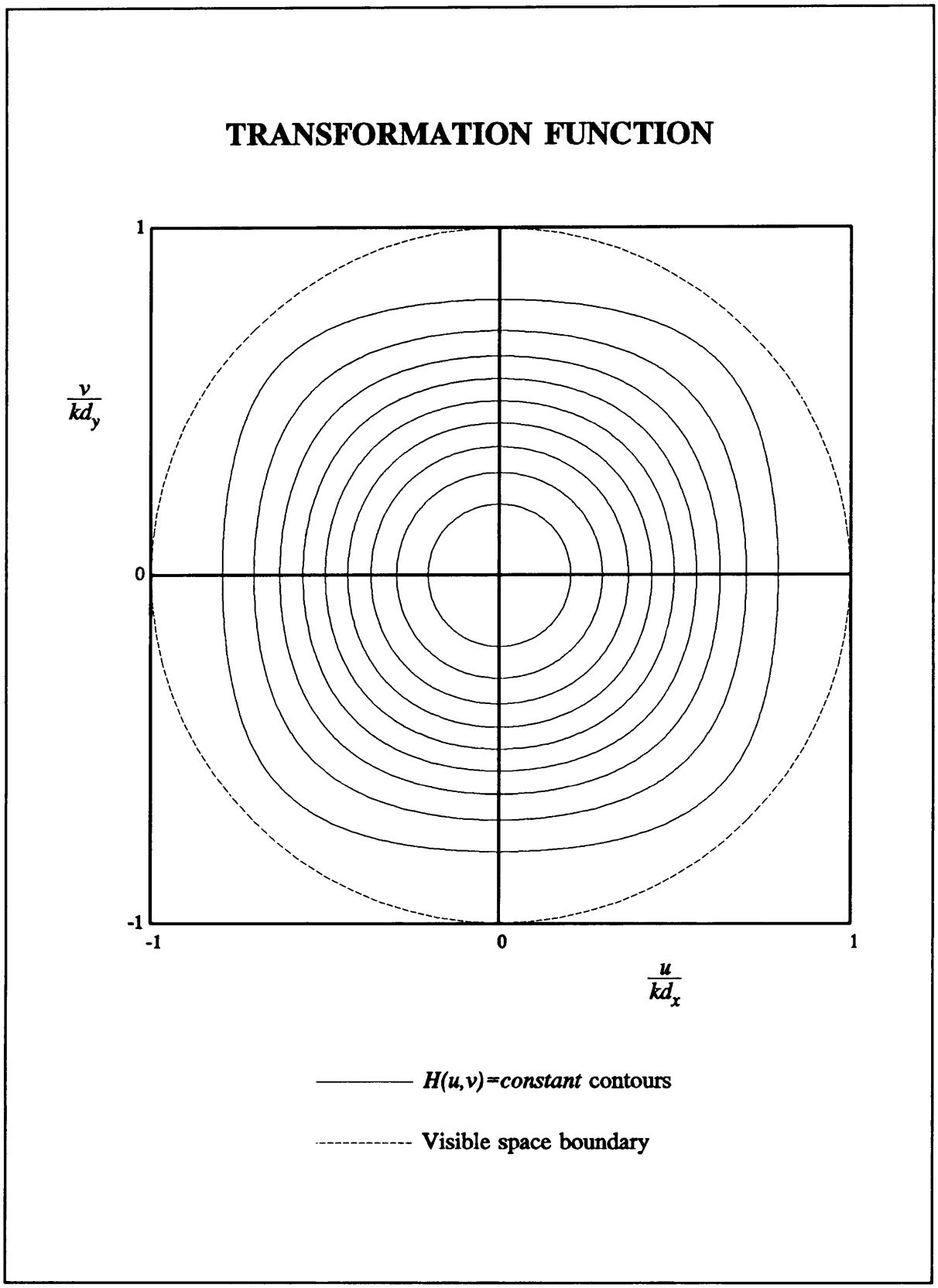

Figure 4.1 Contour plot of $H(u,v)$ with $t_{00}=t_{01}=t_{10}=t_{11}=½$

© University of Pretoria Digitised by the Department of Library Services in support of open access to information, University of Pretoria, 2019

The following analytical procedure can used to determine the coefficients t_{ij} of a first order transformation (4.7) to obtain a circular contour [7], at a certain value of ψ_0, with a high degree of accuracy. We want to map ψ_0 to a circular contour with radius u_0. Thus:

1. The transformation must be symmetric in u and v, thus

$$t_{01} = t_{10} \tag{4.54}$$

2. The origin of the prototype linear array factor ($\psi=0$) must map into the origin of the planar array factor ($u=v=0$), thus (4.7) becomes

$$t_{00} + 2t_{10} + t_{11} = 1 \tag{4.55}$$

3. The point ψ_0 must be mapped to the point u_0 on the u-axis ($v=0$), so that (4.7) becomes

$$t_{00} + t_{10} + (t_{10} + t_{11})\cos(u_0) = \cos(\psi_0) \tag{4.56}$$

4. Because the maximum deviation from the circular contour appear on the diagonal with $\phi=45°$, it may be possible to improve the contour by forcing the appropriate point on this diagonal to be on the circular contour, thus $\psi=\psi_0$ maps to $(u,v)=(u_0/\sqrt{2},\ u_0/\sqrt{2})$. Substituting these values into (4.7) gives

$$t_{00} + 2t_{10}\cos\left(\frac{u_0}{\sqrt{2}}\right) + t_{11}\cos^2\left(\frac{u_0}{\sqrt{2}}\right) = \cos(\psi_0) \tag{4.57}$$

After solving these simultaneous equations (4.54) to (4.57) we obtain

$$t_{00} = 1 - X\left[1 - 2\cos\left(\frac{u_0}{\sqrt{2}}\right) + \cos^2\left(\frac{u_0}{\sqrt{2}}\right) - \cos u_0\right] \tag{4.58a}$$

$$t_{01} = t_{10} = X\left[\cos^2\left(\frac{u_0}{\sqrt{2}}\right) - \cos u_0\right] \tag{4.58b}$$

and

$$t_{11} = X\left[1 - 2\cos\left(\frac{u_0}{\sqrt{2}}\right) + \cos u_0\right] \tag{4.58c}$$

© University of Pretoria Digitised by the Department of Library Services in support of open access to information, University of Pretoria, 2019

wherein

$$X = \frac{1 - \cos\psi_0}{\left[1 - \cos u_0\right]\left[1 - \cos\left(\frac{u_0}{\sqrt{2}}\right)\right]^2} \tag{4.59}$$

These transformation coefficients may need scaling. The use of these expressions are illustrated in Example #1 in Section 4.5.2. The design objective of the example is to have a circular contour at $\theta=25°$.

4.4.4 Approximation of Elliptical Contours [7]

By approximating *cos(x)* by its truncated power series in *x* [11: p.111]

$$\cos x = 1 - \frac{x^2}{2} + \frac{x^4}{24} \tag{4.60}$$

and neglecting all the higher order terms, the first order transformation (4.7) can be written as

$$1 - \frac{\psi^2}{2} + \frac{\psi^4}{24} = \left(t_{00} + t_{01} + t_{10} + t_{11}\right) - \frac{1}{2}\left(p_1 u^2 + p_2 v^2\right) + \frac{1}{24}\left(p_1 u^4 + 6t_{11}u^2v^2 + p_2 v^4\right) \tag{4.61}$$

wherein

$$p_1 = t_{10} + t_{11} \tag{4.62a}$$

and

$$p_2 = t_{01} + t_{11} \tag{4.62b}$$

For "low frequencies" (i.e $u, v \ll 1$) the u^4, v^4 and u^2v^2 terms can be neglected. However, for "higher frequencies" these terms represent a deviation from the elliptical contour. Let us define a deviation function as

$$D(u,v) = p_1 u^4 + 6t_{11}u^2v^2 + p_2 v^4 \tag{4.63}$$

© University of Pretoria Digitised by the Department of Library Services in support of open access to information, University of Pretoria, 2019

As usual the origin of the prototype linear array factor must be mapped into the origin of the planar array factor, that is

$$t_{00} + t_{01} + t_{10} + t_{11} = 1 \tag{4.64}$$

Using (4.63) and (4.64), (4.61) can be written as

$$\psi^2\left(1 - \frac{\psi^2}{12}\right) = p_1 u^2 + p_2 v^2 - \frac{1}{12} D(u,v) \tag{4.65}$$

Let ψ_0 of the prototype array factor map into a elliptical contour of major axis a and minor axis b,

$$\frac{u^2}{a^2} + \frac{v^2}{b^2} = 1 \tag{4.66}$$

By using (4.66) the deviation function $D(u,v)$ on this elliptical contour can be written in terms of u as,

$$D_0(u,v) = u^4\left[p_1 + \left(\frac{b}{a}\right)^4 p_2 - 6\left(\frac{b}{a}\right)^2 t_{11}\right] - u^2\left[2b^2\left(\frac{b}{a}\right)^2 p_2 - 6b^2 t_{11}\right] \tag{4.67}$$

For (4.65) to describe an elliptical contour, $D_0(u,v)$ should be free of the fourth-order term u^4. This requires that

$$p_1 + \left(\frac{a}{b}\right)^4 p_2 - 6\left(\frac{b}{a}\right)^2 t_{11} = 0 \tag{4.68}$$

Using (4.68) to eliminate u^4, form $D_0(u,v)$, D_0 becomes a function of only u^2,

$$D_0(u,v) = u^2 b^2\left[\left(\frac{a}{b}\right)^2 p_1 - \left(\frac{b}{a}\right)^2 p_2\right] + b^4 p_2 \tag{4.69}$$

When setting $\psi = \psi_0$ and inserting (4.69) into (4.65) we obtain a mapping of ψ_0 to an elliptical contour the in the uv-plane as

$$\left[\psi_0^2\left(1 - \frac{\psi_0^2}{12}\right) + \frac{b^4}{12} p_2\right] = u^2\left[\left(1 - \frac{a^2}{12}\right) + \frac{b^2}{12}\left(\frac{b}{a}\right)^2 p_2\right] + v^2 p_2 \tag{4.70}$$

© University of Pretoria Digitised by the Department of Library Services in support of open access to information, University of Pretoria, 2019

UNIVERSITEIT VAN PRETORIA
UNIVERSITY OF PRETORIA
YUNIBESITHI YA PRETORIA

By comparing (4.66) and (4.70) term by term we find

$$a^2 = \frac{\psi_0^2\left(1 - \frac{\psi_0^2}{12}\right) + p_2\frac{b^4}{12}}{p_1\left(1 - \frac{a^2}{12}\right) + p_2\frac{b^2}{12}\left(\frac{b}{a}\right)^2} \tag{4.71a}$$

and

$$b^2 = \frac{\psi_0^2\left(1 - \frac{\psi_0^2}{12}\right) + p_2\frac{b^4}{12}}{p_2} \tag{4.71b}$$

Equations (4.71a) and (4.71b) allow us to solve for

$$p_1 = t_{10} + t_{11} = \left(\frac{\psi_0}{a}\right)^2 \frac{\left(1 - \frac{\psi_0^2}{12}\right)}{\left(1 - \frac{a^2}{12}\right)} \tag{4.72a}$$

and

$$p_2 = t_{01} + t_{11} = \left(\frac{\psi_0}{b}\right)^2 \frac{\left(1 - \frac{\psi_0^2}{12}\right)}{\left(1 - \frac{b^2}{12}\right)} \tag{4.72b}$$

By back substituting p_1 and p_2 into (4.68) we obtain

$$t_{11} = \frac{1}{6}\psi_0^2\left(1 - \frac{\psi_0^2}{12}\right)\left[\frac{1}{a^2\left(1 - \frac{b^2}{12}\right)} + \frac{1}{b^2\left(1 - \frac{b^2}{12}\right)}\right] \tag{4.73}$$

The procedure to determine the transformation coefficients is as follows: First, calculate t_{11} from (4.73); then calculate t_{01} and t_{10} by using (4.72a) and (4.72b); lastly t_{00} is obtained from (4.64). It should be emphasized that these approximate solutions for t_{ij} attempts to preserve only the footprint elliptical contour in (4.66). However, examination of (4.73) reveals that, as long as the major and minor axes of other contours are much smaller than $\sqrt{12}$, t_{ij} will transform the prototype linear array pattern into ellipses where $\psi < \sqrt{12}$. The approximation works well with all ratios $a/b > 1$. Its use is

© University of Pretoria Digitised by the Department of Library Services in support of open access to information, University of Pretoria, 2019

illustrated in Example #2 of Section 4.5.2.

4.4.5 Elliptical Contours Approximation Using the Scaling-Free Transform

If we assume here that the scaling is to preserve the prototype linear array factor on the u-axis, a scaling free transformation can be written as

$$H(u,v) = -T_{01} + T_{01}\cos v + T_{10}\cos u + (1 - T_{10})\cos u \cos v \tag{4.74}$$

in which

$$T_{ij} = \frac{t_{ij}}{t_{10} + t_{11}} \tag{4.75}$$

are the scaled coefficients.

If we use (4.74) instead of (4.7), a parallel procedure as in Section 4.4.4 results in the following three equations,

$$1 + \left(\frac{b}{a}\right)^4 P - 6\left(\frac{b}{a}\right)^2 T = 0 \tag{4.76a}$$

$$a^2 = \frac{\psi_0^2\left(1 - \frac{\psi_0^2}{12}\right) + P\frac{b^4}{12}}{1 - \frac{a^2}{12} + P\frac{b^2}{12}\left(\frac{b}{a}\right)^2} \tag{4.76b}$$

and

$$b^2 = \frac{\psi_0^2\left(1 - \frac{\psi_0^2}{12}\right) + P\frac{b^4}{12}}{P} \tag{4.76c}$$

in which

$$T = 1 - T_{10} \tag{4.77a}$$

and

© University of Pretoria Digitised by the Department of Library Services in support of open access to information, University of Pretoria, 2019

UNIVERSITEIT VAN PRETORIA
UNIVERSITY OF PRETORIA
YUNIBESITHI YA PRETORIA

$$P = T_{01} + T_{11} \tag{4.77b}$$

Note that (3.76b) is always true due the assumption about scaling in which $\psi_0 = a$. From (4.76a) and (4.76c) the approximation solution is

$$T_{10} = 1 - \frac{1}{6}\left[\left(\frac{a}{b}\right)^2 + \frac{1 - \frac{a^2}{12}}{1 - \frac{b^2}{12}}\right] \tag{4.78a}$$

and

$$T_{01} = \left(\frac{a}{b}\right)^2\left[\frac{1 - \frac{a^2}{12}}{1 - \frac{b^2}{12}}\right] + T_{10} - 1 \tag{4.78b}$$

The scaling-free approximate solutions for T_{ij} attempts to preserve only the footprint elliptical contour in (4.66). Examination of (4.78a) and (4.78b) reveals that as long as the major and minor axes of other contours are much smaller than $\sqrt{12}$, T_{ij} will produce elliptical contours where $\psi < \sqrt{12}$. Because of the preservation of the prototype linear array on the u-axis $H(kd_x, 0) = -1$. However, if the ratio a/b is smaller than roughly 1.3 (1.20 at $\theta = 5°$ and 1.27 at $\theta = 25°$ to be more exact) the value $H(kd_x, 0) = -1$ is not the minimum value of $H(u,v)$. Thus for a/b ratios of less than 1.3 the approximation of Section 4.4.4 is recommended. For ratios $a/b > 1.3$ the approximation of Section 4.4.4 and the scaling-free approximation produce similar results, thus the scaling-free approximation is recommended. The scaling-free approximation is illustrated in Example #2 of Section 4.5.2.

4.4.6 Contour Approximation by Constrained Optimization

If the contour in the uv-plane can be written as a analytical function i.e.

$$\frac{u}{a} + \frac{v}{b} = 1 \tag{4.79}$$

one variable can be written in terms of the other, say v in terms of u, as

© University of Pretoria Digitised by the Department of Library Services in support of open access to information, University of Pretoria, 2019

UNIVERSITEIT VAN PRETORIA
UNIVERSITY OF PRETORIA
YUNIBESITHI YA PRETORIA

$$v = f(u) \tag{4.80}$$

Using a first order transformation we can solve v in terms of ψ, u and the mapping variables as

$$v = G(\psi,u,t_{00},t_{01},t_{10},t_{11}) = \arccos\left[\frac{\cos\psi - t_{00} - t_{10}\cos u}{t_{01} + t_{11}\cos u}\right] \tag{4.81}$$

We can define an error function

$$E_1(u) = G(\psi_0,u,t_{ij}) - f(u) \tag{4.82}$$

where ψ_0 is the cutoff point of the prototype. Imposing the usual constraint namely, the origin of the prototype linear array must map onto the origin of the uv-plane, gives

$$\sum_{i=0}^{I}\sum_{j=0}^{J} t_{ij} = 1 \tag{4.83}$$

This allow one variable to be constrained as a function of the other three (in the first order case). The parameters t_{ij} can then be chosen to minimize the error function $E_1(u)$. There are two difficulties with this formulation, firstly nonlinear optimization routine must be used and secondly an explicit relation for G can only be found for first order transformations.

The problem can be reformulated as linear approximation problem. The error function can be defined as

$$E_2(u) = \cos\psi_0 - \sum_{i=0}^{I}\sum_{j=0}^{J} t_{ij}\cos(iu)\cos[j f(u)] \tag{4.84}$$

Using the constraint (4.83) one variable can be written as a function of the others, resulting in one less parameter to be optimized. Linear optimization routines can be used and any order transformation can be accommodated. The transformation parameters obtained with these methods will usually need scaling.

An alternative procedure for the design of contours of any shape follows. The algorithm can design one or more contours at once and it can be used with transformations of any order. Let us state the procedure for a one contour mapping.

© University of Pretoria Digitised by the Department of Library Services in support of open access to information, University of Pretoria, 2019

Assume that we want to map the point ψ_0 to a contour $u=f(\phi)$ and $v=g(\phi)$. A set of error equations can then be formed on some set of discrete samples, as

$$e(\phi_k) = \cos\psi_0 - \left\{ \sum_{i=0}^{I}\sum_{j=0}^{J} t_{ij}\cos[f(\phi_k)]\cos[g(\phi_k)] + \sum_{i=0}^{I}\sum_{j=0}^{J} s_{ij}\sin[f(\phi_k)]\sin[g(\phi_k)] \right\} \tag{4.85}$$

We can then minimize

$$E_3 = \max_k |e[f(\phi_k)]| \tag{4.86}$$

or

$$E_4 = \sum_k e^2[f(\phi_k)] \tag{4.87}$$

subject to equality constraints of the form

$$\sum_{i=0}^{I}\sum_{j=0}^{J} t_{ij}\cos(iu)\cos(jv) + \sum_{i=0}^{I}\sum_{j=0}^{J} s_{ij}\sin(iu)\sin(jv) = \xi \tag{4.88}$$

and inequality constraints of the form

$$\left| \sum_{i=0}^{I}\sum_{j=0}^{J} t_{ij}\cos(iu)\cos(jv) + \sum_{i=0}^{I}\sum_{j=0}^{J} s_{ij}\sin(iu)\sin(jv) \right| \le 1 \tag{4.89}$$

The quantity E_3 can be minimized by linear programming or if the inequality constraints (4.89) are not present E_4 can be optimized using least squares techniques. The advantage of this method is that no analytical function for the contour shape is needed.

The transformation design problem can also be stated in the same form as the design problem for two-dimensional equiripple digital filters. The transformation coefficients can be obtained from the impulse response coefficients of a $2I+1$ by $2I+1$ digital filter. Although it may seem that we end up where we started, the number of unknowns is drastically reduced. Fast and efficient algorithms exist [12, 13] to determine the impulse response such small digital filters. For a complete discussion of these methods see reference [2].

© University of Pretoria Digitised by the Department of Library Services in support of open access to information, University of Pretoria, 2019

4.5 APPLICATION OF THE TRANSFORMATION METHOD

4.5.1 Introduction

The newly developed synthesis method is illustrated at the hand of six examples. The first four examples, contained in Section 4.5.2, all possess quadrantal symmetric array factors. The first example utilises the circular contour approximation expressions derived in Section 4.4.3. An space factor with elliptical contours is presented in Example #2. Application of both the elliptical approximation methods (Section 4.4.4 and Section 4.4.5) are illustrated. The use of higher order transformations are shown with the third and fourth examples. Section 4.5.3 presents two centro-symmetric examples, Example #5 with a first order transformation and Example #6 with a second order transformation.

4.5.2 Planar Array with Quadrantal Symmetry

Example #1:

To illustrate the synthesis method step by step let us assume the following design requirements:

1. A *25* by *25* element planar array with interelement spacing $d_x = d_y = \frac{1}{2}\lambda$.
2. A flat-top main beam with maximum peak to peak ripple of *0.5dB*.
3. Main beam must have a circular footprint contour at the first null.
4. A first null beamwidth of 50°.
5. All sidelobes below *-30dB*

Step #1: Determine the transformation parameters.

A first order transformation would be sufficient. The transformation parameters are determined by using approximate expression derived in Section 4.4.3. With the values

$$u_0 = \psi_0 = \pi \sin(\theta) = 1.327694$$

© University of Pretoria Digitised by the Department of Library Services in support of open access to information, University of Pretoria, 2019

the result of the simple formula in (4.58) and then (4.55) is

$$t_{00} = -0.664339$$
$$t_{01} = 0.664339$$
$$t_{10} = 0.664339$$
$$t_{11} = 0.353661$$

Step #2: Preform Scaling.

The minimum value of $H(u,v)$ was found to be

$$H_{min} = -1.299566 \quad at \; u = v = \frac{\pi}{\sqrt{2}}$$

thus necessitating scaling. The scaling coefficients calculated with equation (4.51) is

$$C_1 = 0.869729$$
$$C_2 = -0.130271$$

The θ value of the prototype linear array corresponding to the design contour is

$$\theta' = 22.9358°$$

Thus, the first null beamwidth θ_{FNBW} of the prototype linear array must be

$$\theta^{L}_{FNBW} = 2\theta' = 45.8716°$$

The scaled transformation parameters determined with expression (4.50) are

$$t_{00} = -0.431869$$
$$t_{01} = 0.562140$$
$$t_{10} = 0.562140$$
$$t_{11} = 0.307589$$

A contour plot of $H'(u,v)$ is shown Figure 4.2. The contours are spaced at intervals of *0.2*.

© University of Pretoria Digitised by the Department of Library Services in support of open access to information, University of Pretoria, 2019

Step #3: Prototype linear array synthesis.

Because a first order transformation is employed, a prototype linear array with *25* elements is needed. Other requirements are: a flat-top main beam shape with a maximum ripple of *0.5dB*, $SLR = 30dB$ and a first null beamwidth as determined above. The prototype array can be synthesised with the method of Orchard, Elliott and Stern [15]. With six zeros of the unit circle the first null beamwidth is

$$\theta_{FNBW}^{L} = 45.0498^{\circ}$$

which is slightly narrower than the design objective, but adequate for present purposes.

Step #4: Computation of the planar distribution.

The planar elements excitations can now be computed through implementation of the algorithm presented in Appendix B.2.

A contour plot of the resulting array factor is depicted in Figure 4.3 and a three-dimensional plot of the first (or north-east) quadrant is shown in Figure 4.4.

Example #2:

This example illustrates the use of the approximation of elliptical contours of Section 4.4.4 and Section 4.4.5. Assume the following design requirements:

1. A *25* by *25* element planar array with interelement spacing $d_x = d_y = \frac{1}{2}\lambda$.
2. A flat-top main beam with maximum peak to peak ripple of *0.5dB*.
3. A first null beamwidth of 24° in the *x*-direction.
4. Main beam must have a elliptical footprint contour at the first null, with a major to minor axis ratio of *1:2*, thus a first null beamwidth of 48° in the *y*-direction.
5. All sidelobes below *-30dB*

A first order transformation with the transformation parameters calculated by using approximate expression derived in either Section 4.4.4 or Section 4.4.5,

© University of Pretoria Digitised by the Department of Library Services in support of open access to information, University of Pretoria, 2019

UNIVERSITEIT VAN PRETORIA
UNIVERSITY OF PRETORIA
YUNIBESITHI YA PRETORIA

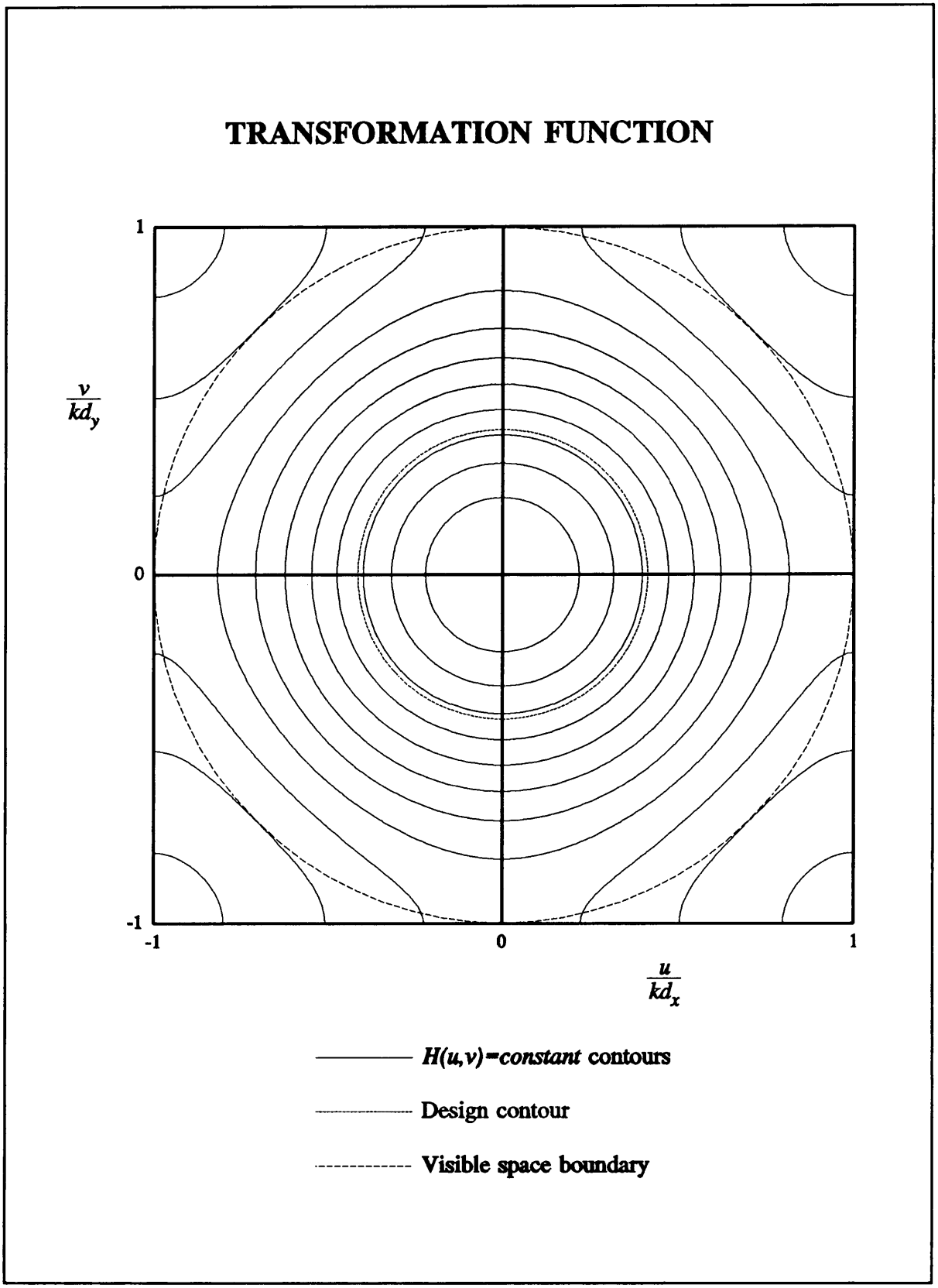

Figure 4.2 Example #1. Contour plot of the transformation function.

© University of Pretoria Digitised by the Department of Library Services in support of open access to information, University of Pretoria, 2019

UNIVERSITEIT VAN PRETORIA
UNIVERSITY OF PRETORIA
YUNIBESITHI YA PRETORIA

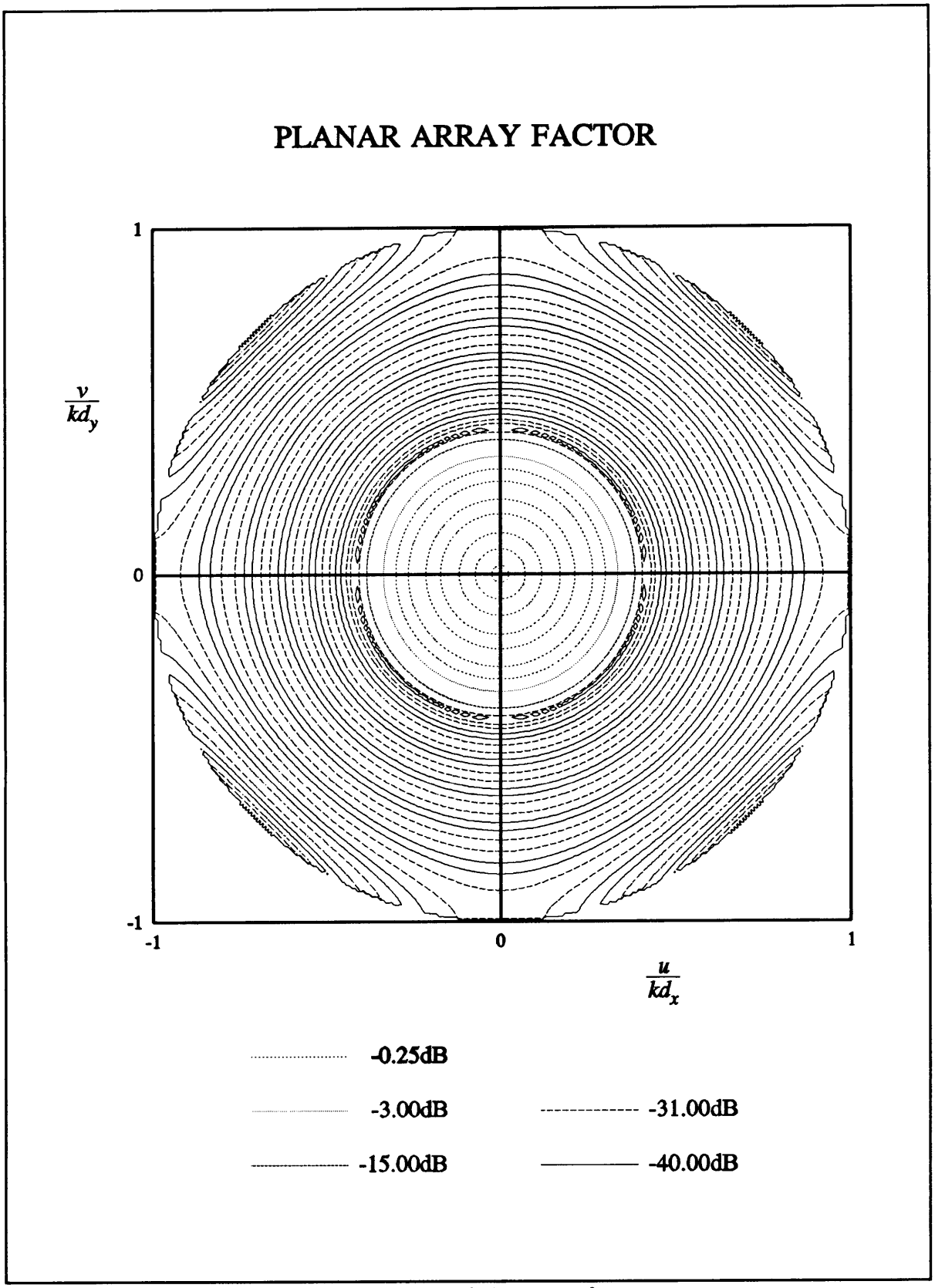

Figure 4.3 Example #1. Contour plot of the array factor.

© University of Pretoria Digitised by the Department of Library Services in support of open access to information, University of Pretoria, 2019

UNIVERSITEIT VAN PRETORIA
UNIVERSITY OF PRETORIA
YUNIBESITHI YA PRETORIA

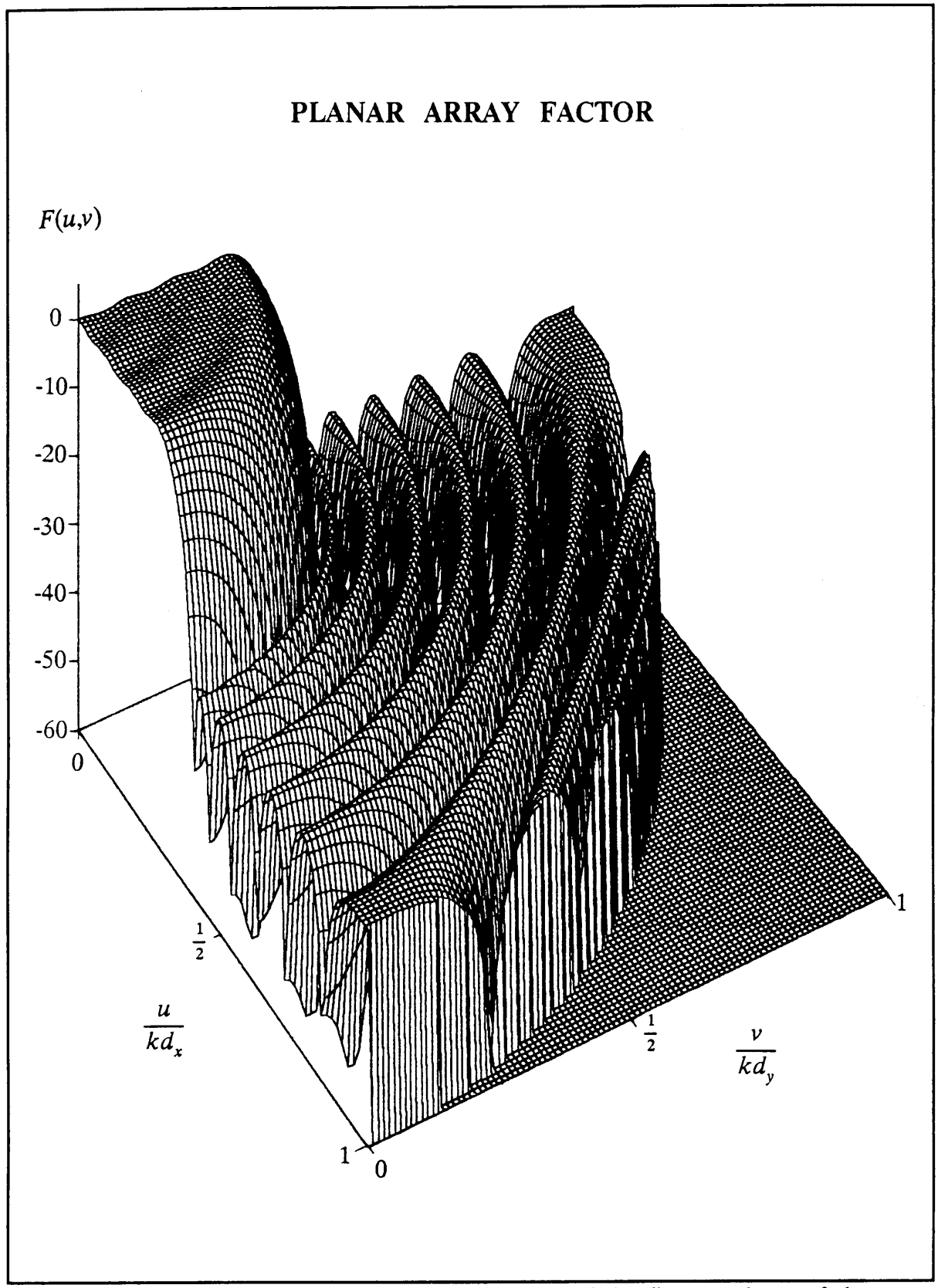

Figure 4.4 Example #1. Three-dimensional plot of the first quadrant of the array factor.

© University of Pretoria Digitised by the Department of Library Services in support of open access to information, University of Pretoria, 2019

would be sufficient. Using the values

$$\theta = 12°$$
$$a = \pi \sin(\theta) = 0.653174$$
$$b = \pi \sin(2\theta) = 1.306348$$

the scaling-free elliptical approximation (4.78) gives

$$T_{01} = -0.062088$$
$$T_{10} = 0.770394$$

If $\psi_0 = 0.653174$ is used in calculating the transformation coefficients with the procedure in Section 4.4.4, the resulting coefficients are

$$t_{00} = -0.062088$$
$$t_{01} = 0.062088$$
$$t_{10} = 0.770394$$
$$t_{11} = 0.229606$$

In this case scaling is not necessary. A close investigation of the two sets of transformation coefficients proves that they are identical. If any other value ψ_0 is selected, the transformation coefficients would differ from those above. In general scaling would then be necessary. However, the scaled coefficients will always be equal the values above and the prototype θ'-value associated with the contour will be very close to $12°$. A contour plot of the transformation is shown Figure 4.5. The contours are spaced at intervals of 0.2.

As a first order transformation is employed, the number of elements needed in the prototype linear array is 25. Using Orchard's [15] method two zeros of the unit circle proved to be sufficient. The first null beamwidth of the prototype linear array is

$$\theta_{FNBW}^{L} = 24.1154°$$

which is slightly broader than the design objective. The planar distribution is then computation with the algorithm in Appendix B.2. The resulting planar array factor is shown in Figure 4.6 (a contour plot) and Figure 4.7 (a three-dimensional plot of the first quadrant).

© University of Pretoria Digitised by the Department of Library Services in support of open access to information, University of Pretoria, 2019

UNIVERSITEIT VAN PRETORIA
UNIVERSITY OF PRETORIA
YUNIBESITHI YA PRETORIA

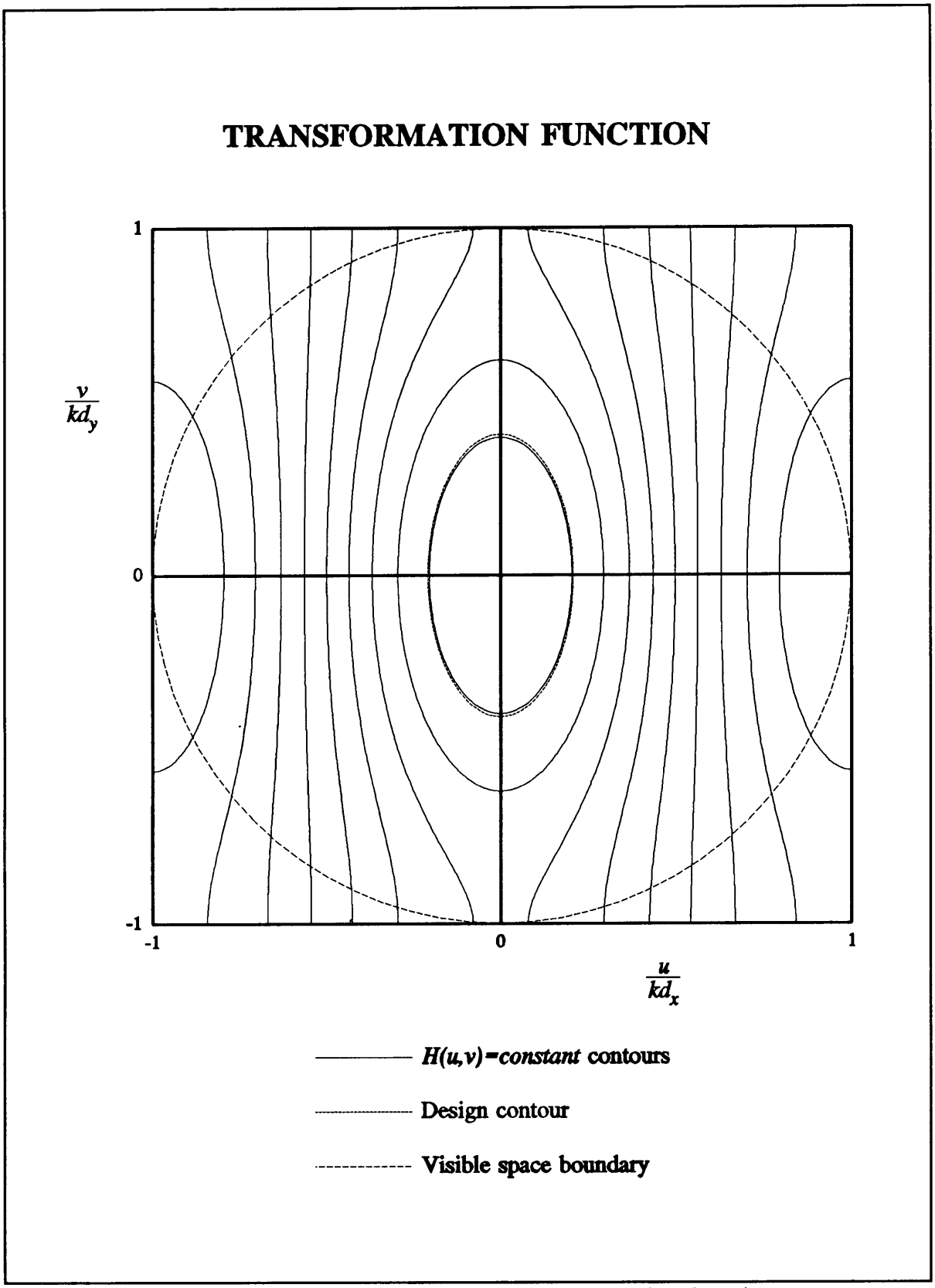

Figure 4.5 Example #2. Contour plot of the transformation function.

© University of Pretoria Digitised by the Department of Library Services in support of open access to information, University of Pretoria, 2019

UNIVERSITEIT VAN PRETORIA
UNIVERSITY OF PRETORIA
YUNIBESITHI YA PRETORIA

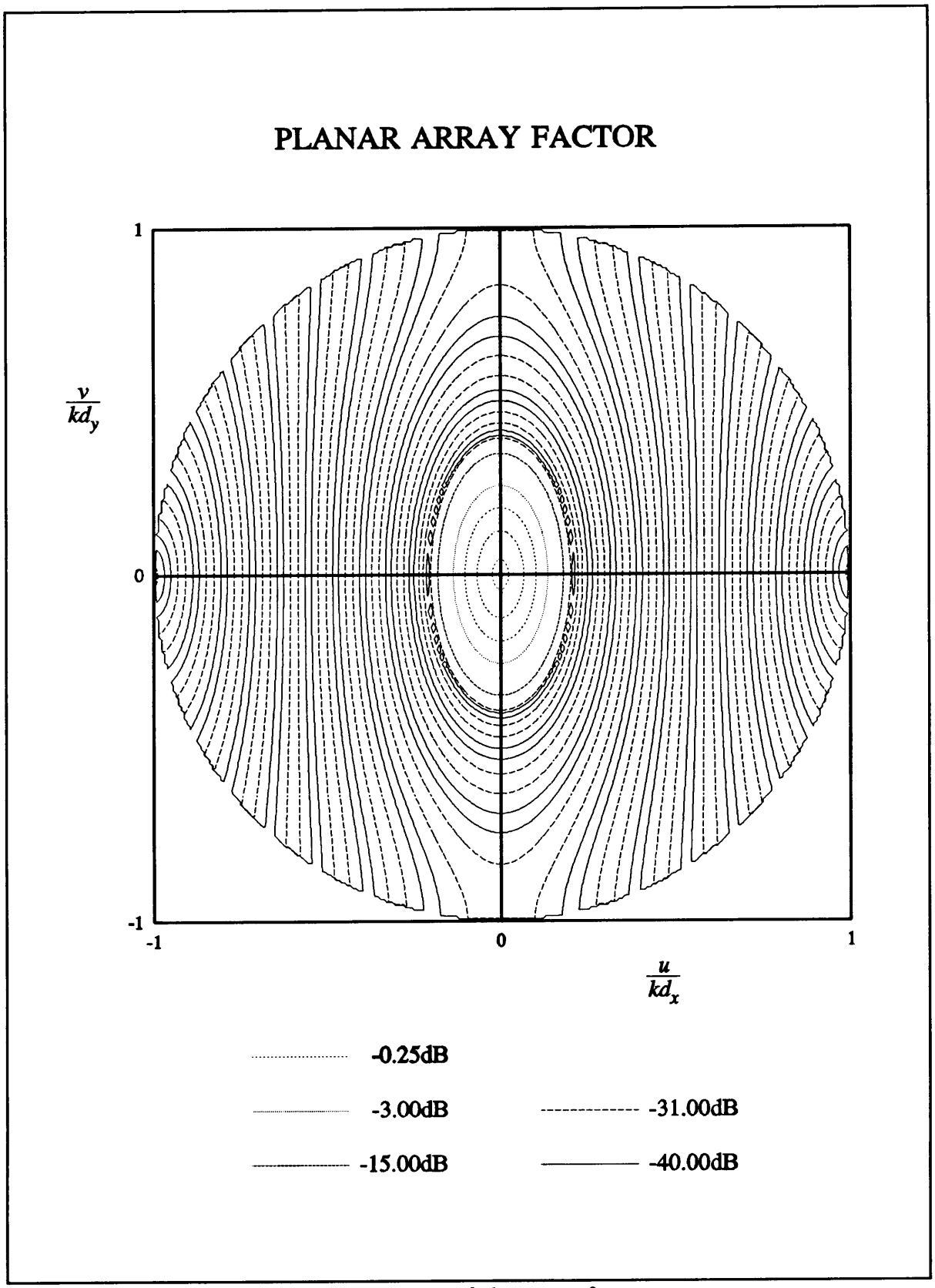

Figure 4.6 Example #2. Contour plot of the array factor.

© University of Pretoria Digitised by the Department of Library Services in support of open access to information, University of Pretoria, 2019

UNIVERSITEIT VAN PRETORIA
UNIVERSITY OF PRETORIA
YUNIBESITHI YA PRETORIA

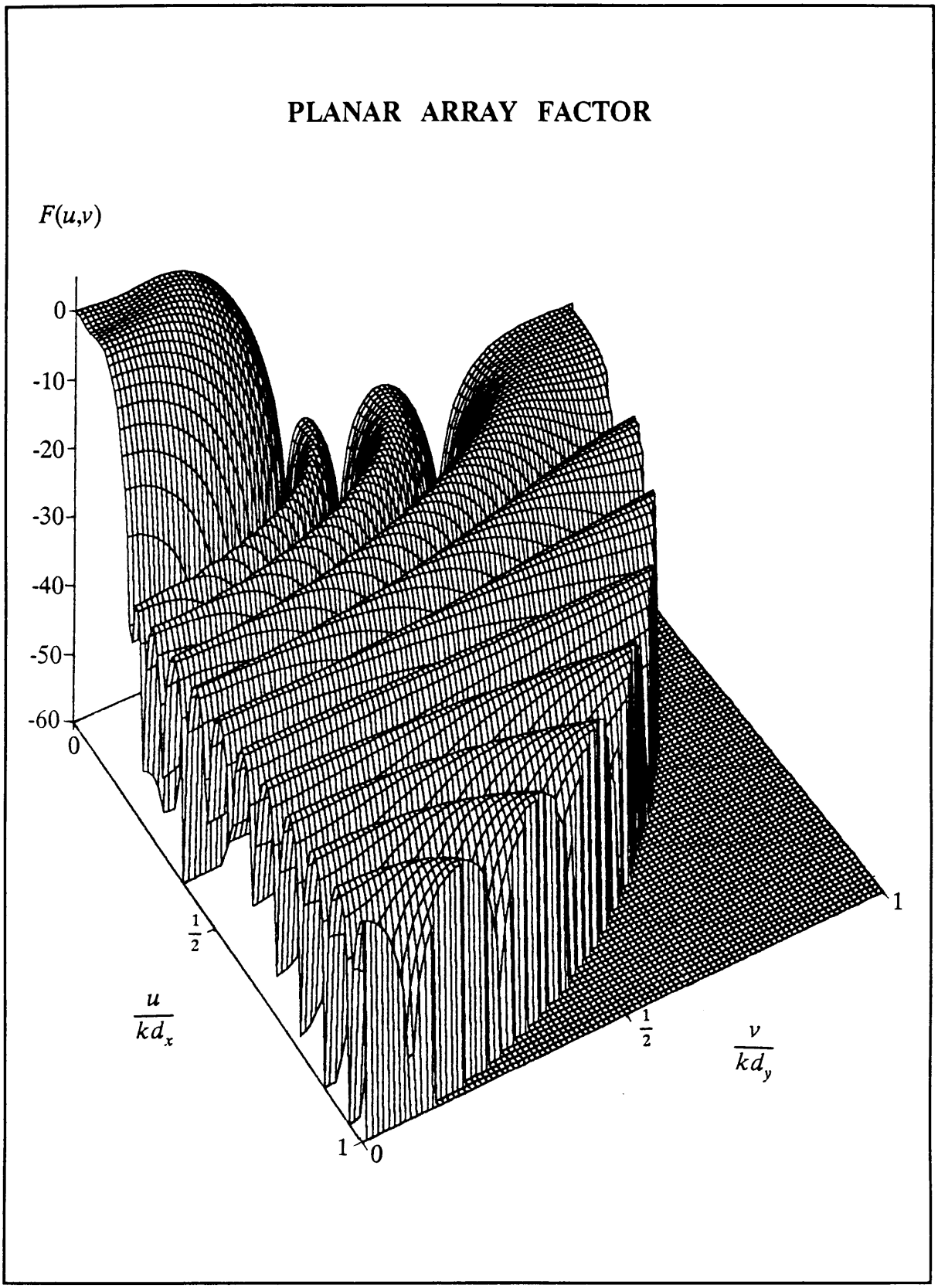

Figure 4.7 Example #2. Three-dimensional plot of the first quadrant of the array factor.

© University of Pretoria Digitised by the Department of Library Services in support of open access to information, University of Pretoria, 2019

Example #3:

A square-shaped main beam is desired. To obtain a such a beam shape require a second order transformation. Mersereau et al. [2] derived such a transformation from a *5* by *5* optimal two dimensional digital filter with square-shaped passband and stopband region. The transformation is square-shaped in the region $23.6° \leq \theta \leq 36.9°$. The transformation coefficients are tabulated in Table 4.1. A contour plot of $H(u,v)$, with the contours are spaced at intervals of *0.2*, is shown Figure 4.8.

i / j	0	1	2
0	-0.43121	0.30365	0.005325
1	0.30365	0.68633	0.008787
2	0.005325	0.008787	0.10836

Table 4.1 Transformation coefficients t_{ij} of Example #3

The prototype linear array factor has a flat-top shaped main beam with a maximum allowable ripple of *0.5dB*, a sidelobe level of *-20dB* and a first null beamwidth near $90°$. The *17* element array with six zeros of the unit circle is sufficient, the first null is at $\theta = 31.03°$.

Assume the interelement spacing $d_x = d_y = \frac{1}{2}\lambda$. The planar elements excitations can now be computed with the algorithm presented in Appendix B.2. The resulting planar array is an array with *33* by *33* elements. The array factor is presented in Figures 4.9 and 4.10.

Example #4:

To obtain a diamond beam shape, required for this example, a third order transformation is needed. Mersereau et al. [2] derived such a transformation from a *7* by *7* optimal two dimensional digital filter with diamond-shaped passband and stopband region. The transformation is diamond-shaped in the region $23.6° \leq \theta \leq 36.9°$. The transformation coefficients are tabulated in Table 4.2. A contour plot of $H(u,v)$ is presented in Figure 4.11.

© University of Pretoria Digitised by the Department of Library Services in support of open access to information, University of Pretoria, 2019

UNIVERSITEIT VAN PRETORIA
UNIVERSITY OF PRETORIA
YUNIBESITHI YA PRETORIA

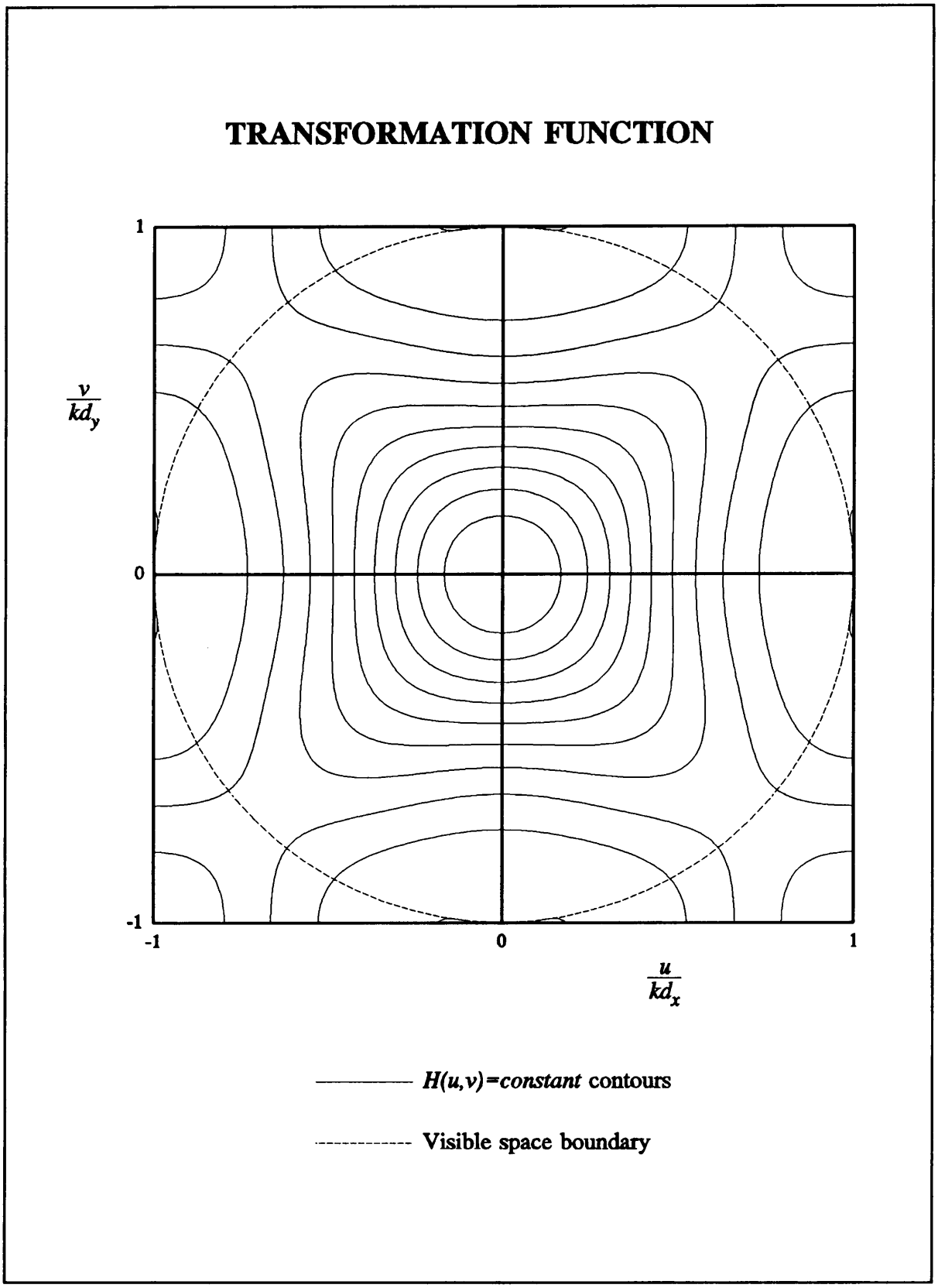

Figure 4.8 Example #3. Contour plot of the transformation function.

© University of Pretoria Digitised by the Department of Library Services in support of open access to information, University of Pretoria, 2019

UNIVERSITEIT VAN PRETORIA
UNIVERSITY OF PRETORIA
YUNIBESITHI YA PRETORIA

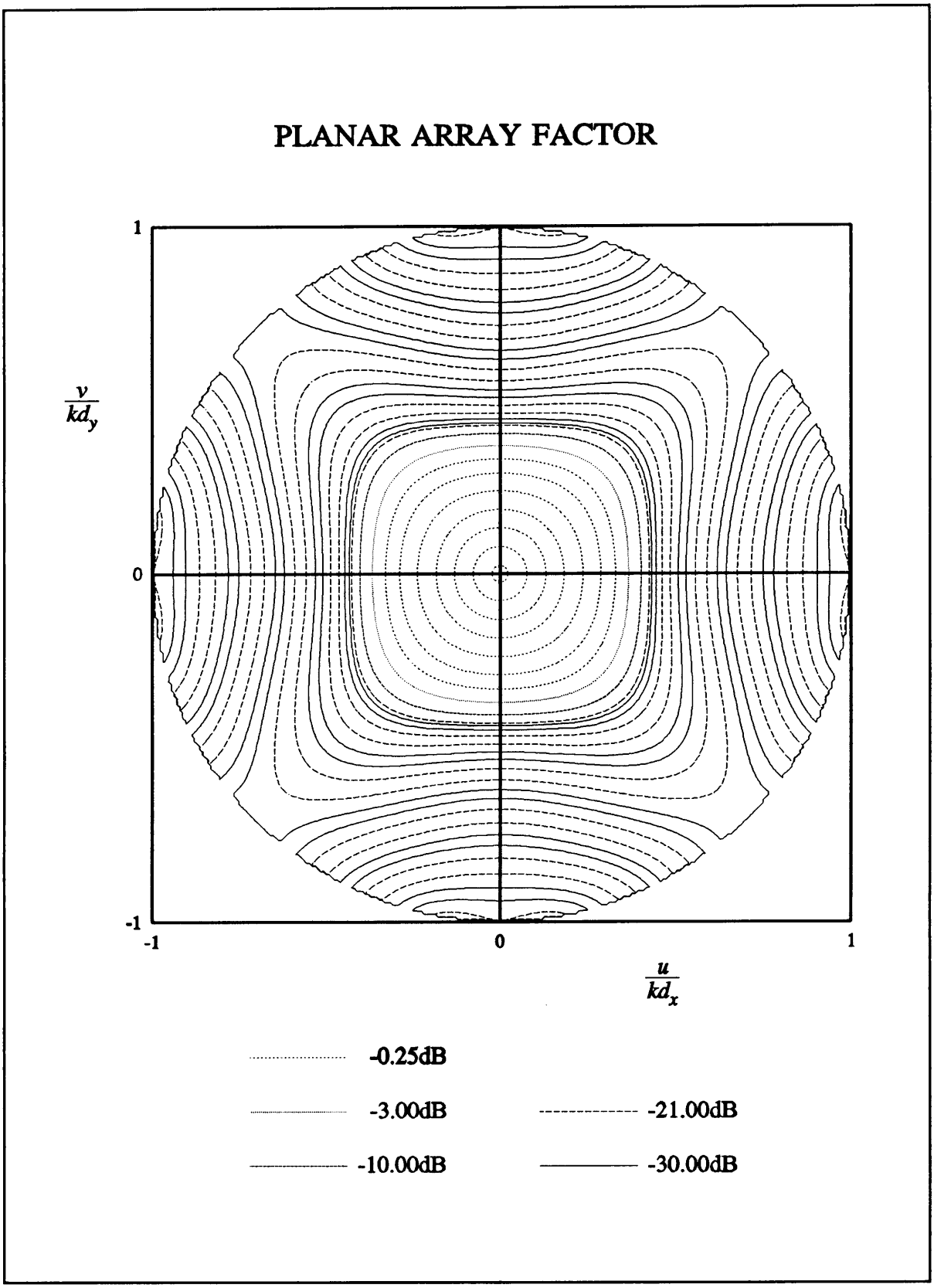

Figure 4.9 Example #3. Contour plot of the array factor.

© University of Pretoria Digitised by the Department of Library Services in support of open access to information, University of Pretoria, 2019

UNIVERSITEIT VAN PRETORIA
UNIVERSITY OF PRETORIA
YUNIBESITHI YA PRETORIA

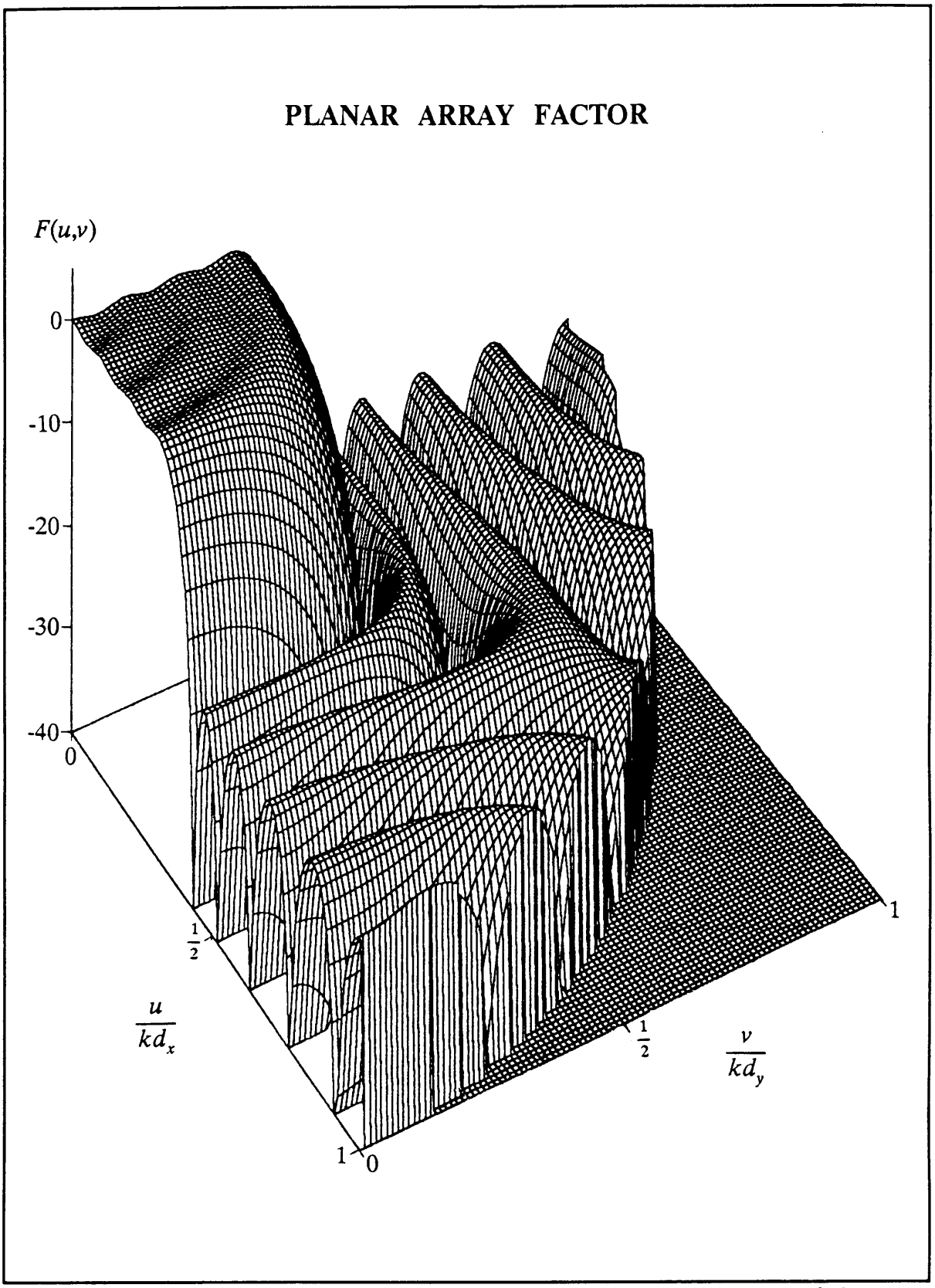

Figure 4.10 Example #3. Three-dimensional plot of the first quadrant of the array factor.

© University of Pretoria Digitised by the Department of Library Services in support of open access to information, University of Pretoria, 2019

UNIVERSITEIT VAN PRETORIA
UNIVERSITY OF PRETORIA
YUNIBESITHI YA PRETORIA

i/j	0	1	2	3
0	-0.55078	0.31577	0.14760	0.04362
1	0.31577	0.50364	0.20770	0.001693
2	0.14760	0.20770	0.097659	-0.18861
3	0.04362	0.001693	-0.18861	-0.12855

Table 4.2 Transformation coefficients t_{ij} of Example #4

The prototype linear array used for this example is the same as the one used in Example #3. Assume the interelement spacing $d_x=d_y=\frac{1}{2}\lambda$. The planar elements excitations can now be computed with the algorithm presented in Appendix B.2. The resulting planar array is an array with *49* by *49* elements. The array factor is shown in Figures 4.12 and 4.13.

4.5.3 Planar Array with Centro-Symmetry

Example #5:

This example illustrate the inclusion of anti-symmetric components. The same transformation coefficients as in Example #2 are used, but an anti-symmetric component $s_{11}sin(u)sin(v)$ is added. The transformation coefficients are

$$t_{00} = -0.062088$$
$$t_{01} = 0.062088$$
$$t_{10} = 0.770394$$
$$t_{11} = 0.229606$$
$$s_{11} = 0.250000$$

No scaling is not necessary. A contour plot of $H(u,v)$ is shown Figure 4.14. As usual the contours are spaced at intervals of *0.2*. The contours are clearly centro-symmetric.

The prototype linear array used is the *25* element array used in Example #2. The planar elements excitations can now be computed through implementation of the algorithm presented in Appendix B.3. A contour plot and a three-dimensional plot of the resulting array factor are depicted in Figures 4.15 and 4.16 respectively.

Although the collapsed distributions of Example #2 and this example are identical, the contours are destictively different.

© University of Pretoria Digitised by the Department of Library Services in support of open access to information, University of Pretoria, 2019

UNIVERSITEIT VAN PRETORIA
UNIVERSITY OF PRETORIA
YUNIBESITHI YA PRETORIA

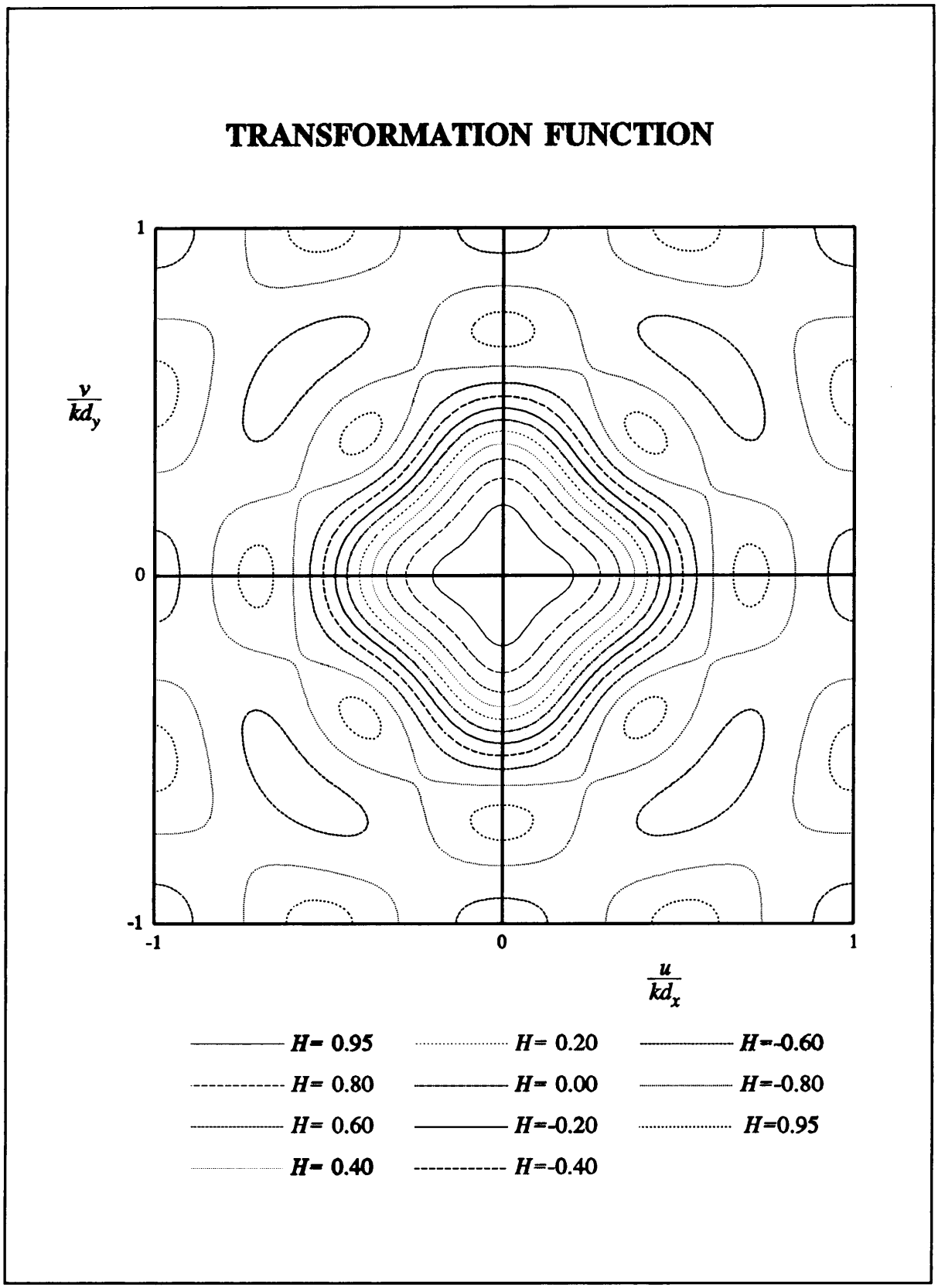

Figure 4.11 Example #4. Contour plot of the transformation function.

© University of Pretoria Digitised by the Department of Library Services in support of open access to information, University of Pretoria, 2019

UNIVERSITEIT VAN PRETORIA
UNIVERSITY OF PRETORIA
YUNIBESITHI YA PRETORIA

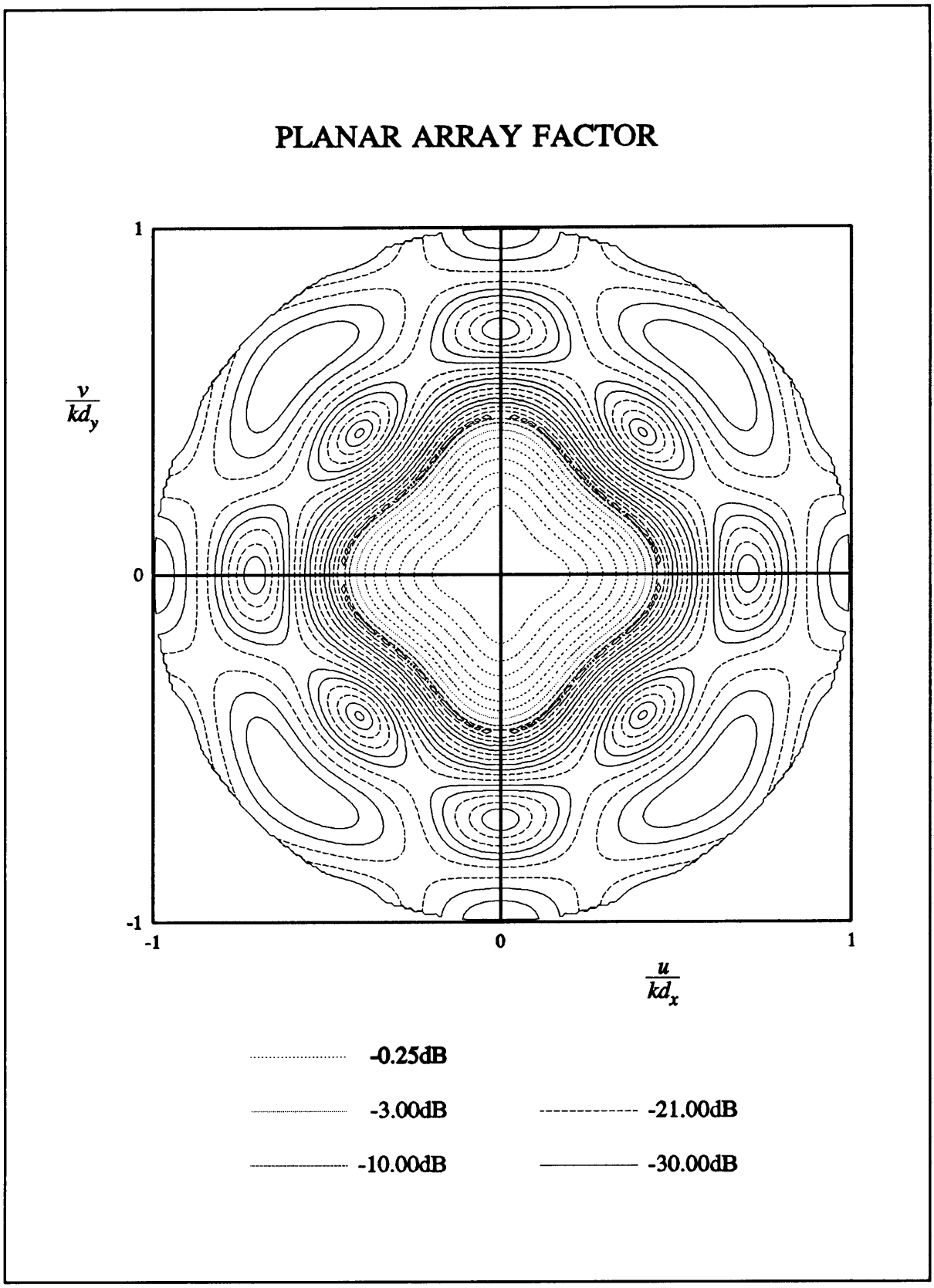

Figure 4.12 Example #4. Contour plot of the array factor.

© University of Pretoria Digitised by the Department of Library Services in support of open access to information, University of Pretoria, 2019

UNIVERSITEIT VAN PRETORIA
UNIVERSITY OF PRETORIA
YUNIBESITHI YA PRETORIA

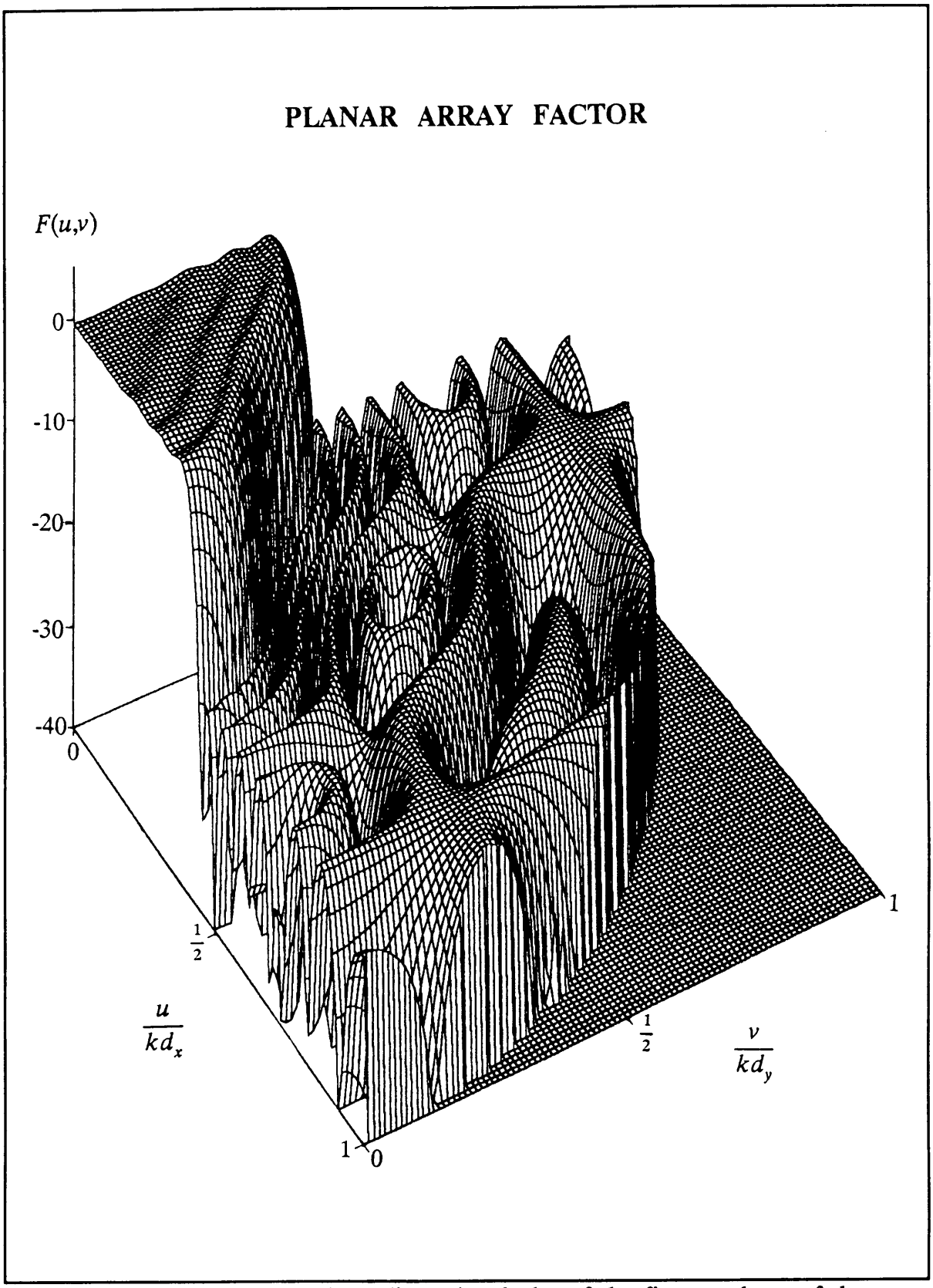

Figure 4.13 Example #4. Three-dimensional plot of the first quadrant of the array factor.

© University of Pretoria Digitised by the Department of Library Services in support of open access to information, University of Pretoria, 2019

UNIVERSITEIT VAN PRETORIA
UNIVERSITY OF PRETORIA
YUNIBESITHI YA PRETORIA

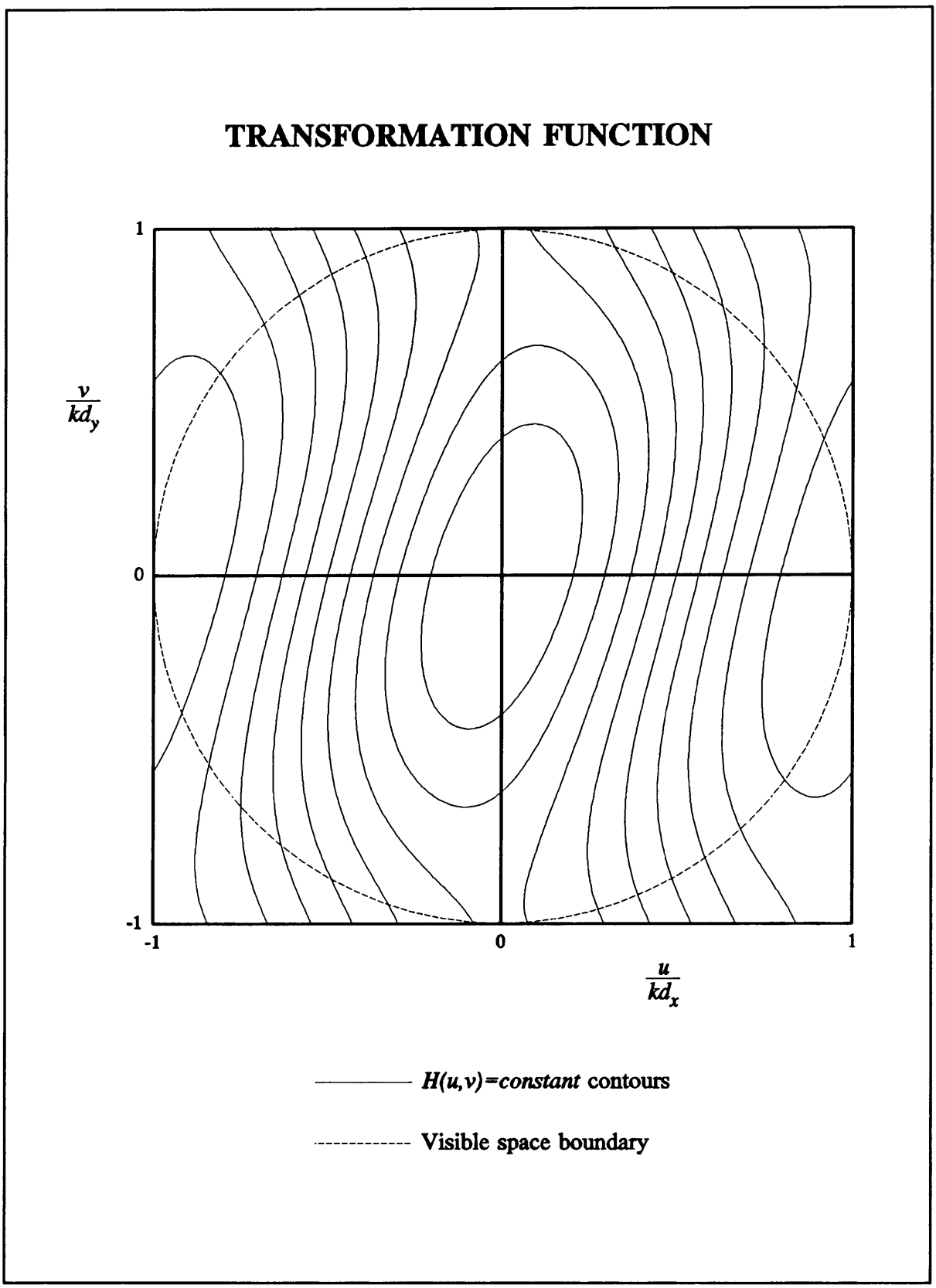

Figure 4.14 Example #5. Contour plot of the transformation function.

© University of Pretoria Digitised by the Department of Library Services in support of open access to information, University of Pretoria, 2019

UNIVERSITEIT VAN PRETORIA
UNIVERSITY OF PRETORIA
YUNIBESITHI YA PRETORIA

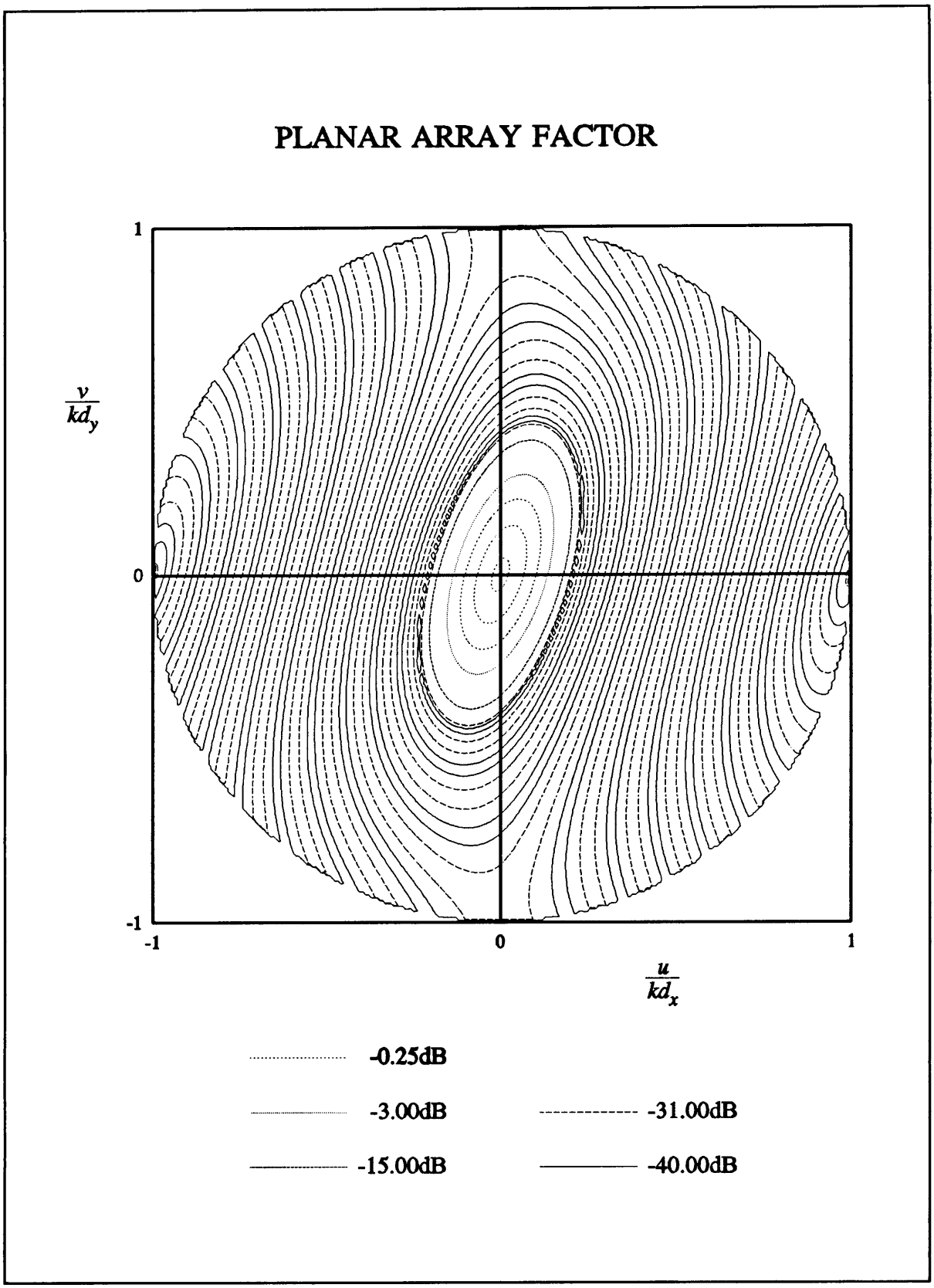

Figure 4.15 Example #5. Contour plot of the array factor.

© University of Pretoria Digitised by the Department of Library Services in support of open access to information, University of Pretoria, 2019

UNIVERSITEIT VAN PRETORIA
UNIVERSITY OF PRETORIA
YUNIBESITHI YA PRETORIA

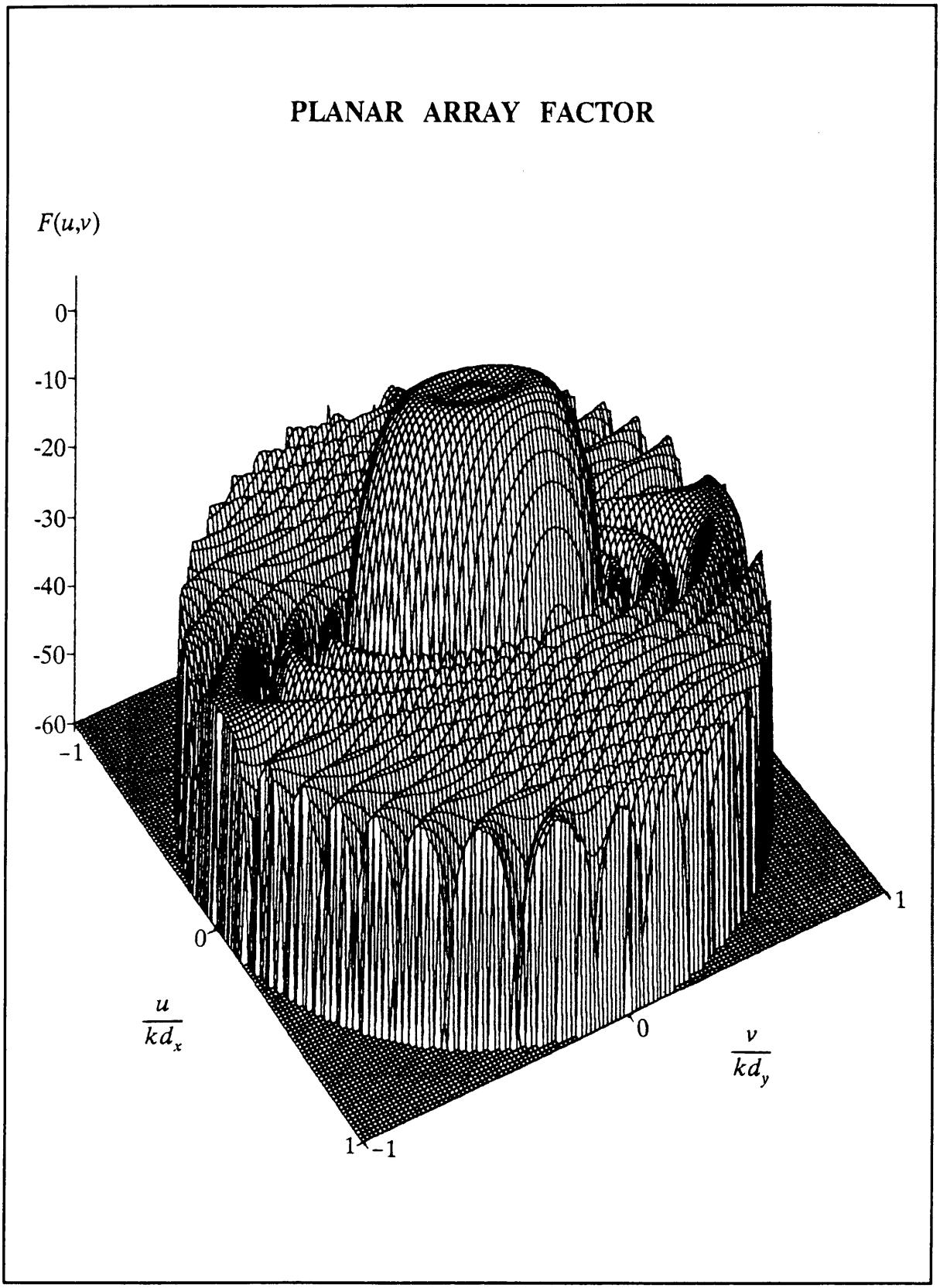

Figure 4.16 Example #5. Three-dimensional plot of the array factor.

© University of Pretoria Digitised by the Department of Library Services in support of open access to information, University of Pretoria, 2019

UNIVERSITEIT VAN PRETORIA
UNIVERSITY OF PRETORIA
YUNIBESITHI YA PRETORIA

Example #6:

This example illustrate the a higher order centro-symmetric footprint pattern. The transformation coefficients are tabulated in Table 4.3.

i/j	0	1	2
0	-0.35121 0.00000	0.29365 0.00000	0.005325 0.00000
1	0.29365 0.00000	0.62630 -0.10000	0.008787 0.25000
2	0.005325 0.00000	0.008787 0.00000	0.10836 -0.08000

Table 4.3 Transformation coefficients t_{ij} (top of each cell) and s_{ij} (bottom of each cell) for Example #6.

A contour plot of $H(u,v)$ is presented Figure 4.17, in which the contours are spaced at intervals of *0.2*.

This example uses the same prototype linear as Example #3. The planar elements excitations can now be computed through implementation of the algorithm presented in Appendix B.3. A contour plot and a three-dimensional plot of the resulting array factor are shown in Figures 4.18 and 4.19 respectively.

4.6 CONCLUSIONS

A discrete synthesis technique that produces planar arrays with contoured beams has been proposed in this chapter. The synthesis technique developed here utilises a transformation that divides the problem into two decoupled sub-problems. In the antenna array context, one sub-problem consists of a linear array synthesis, for which there exist powerful methods for determining appropriate element excitations. The other involves the determination of certain coefficients of the transformation in order to achieve the required footprint contours. The number coefficients which are needed depends on the complexity of the desired contour, but is very small in comparison to the

© University of Pretoria Digitised by the Department of Library Services in support of open access to information, University of Pretoria, 2019

UNIVERSITEIT VAN PRETORIA
UNIVERSITY OF PRETORIA
YUNIBESITHI YA PRETORIA

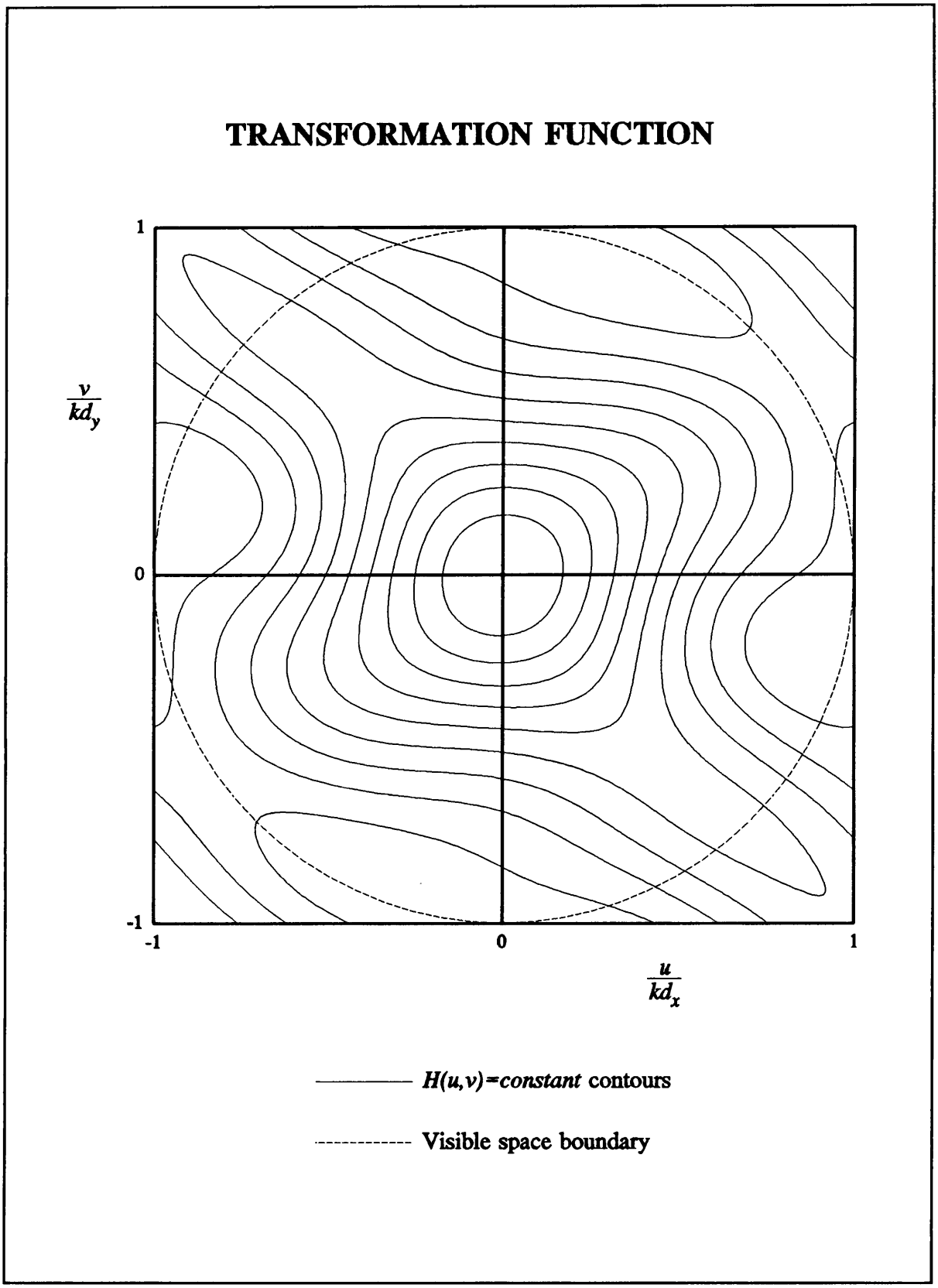

Figure 4.17 Example #6. Contour plot of the transformation function.

© University of Pretoria Digitised by the Department of Library Services in support of open access to information, University of Pretoria, 2019

UNIVERSITEIT VAN PRETORIA
UNIVERSITY OF PRETORIA
YUNIBESITHI YA PRETORIA

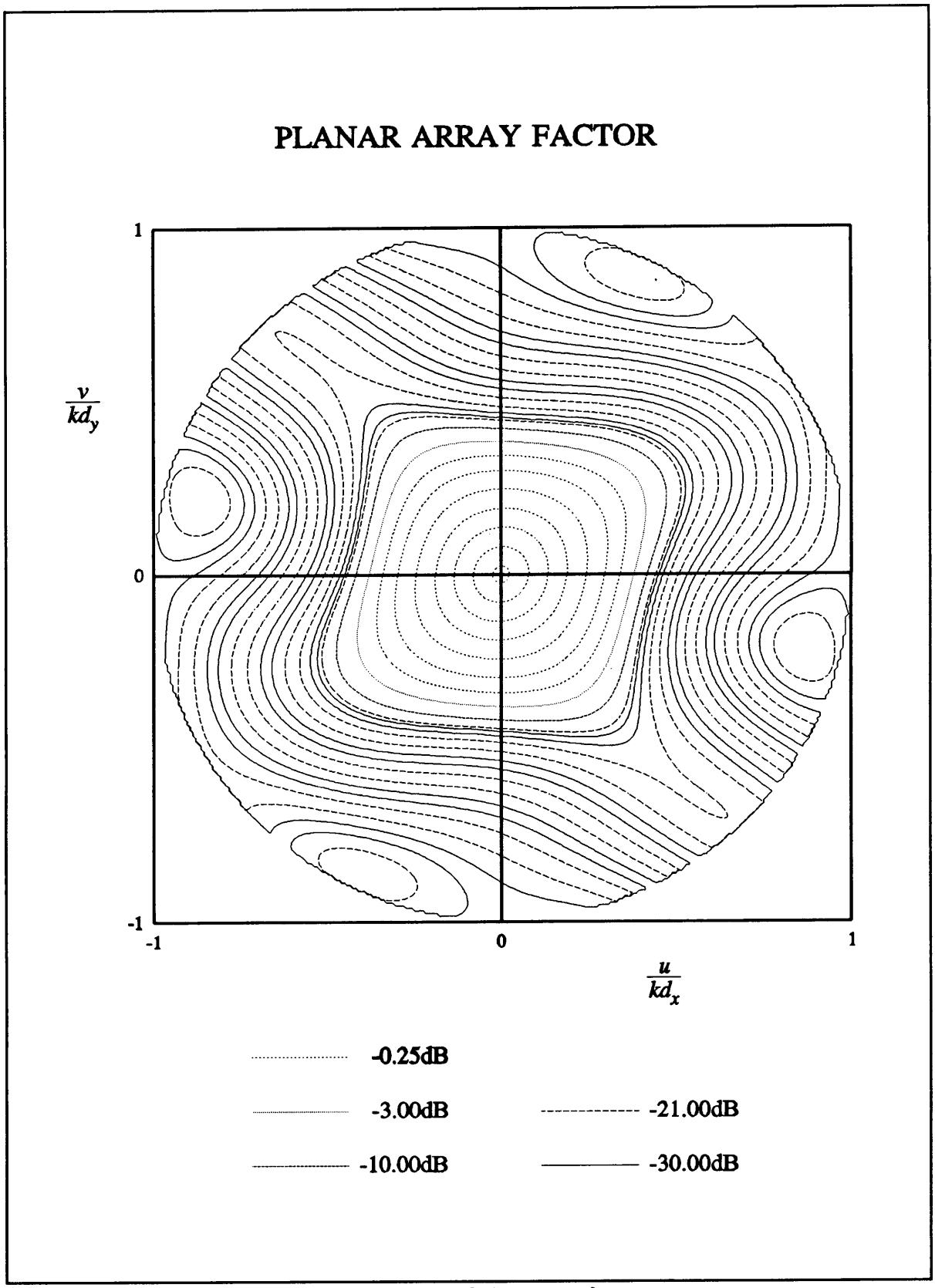

Figure 4.18 Example #6. Contour plot of the array factor.

© University of Pretoria Digitised by the Department of Library Services in support of open access to information, University of Pretoria, 2019

UNIVERSITEIT VAN PRETORIA
UNIVERSITY OF PRETORIA
YUNIBESITHI YA PRETORIA

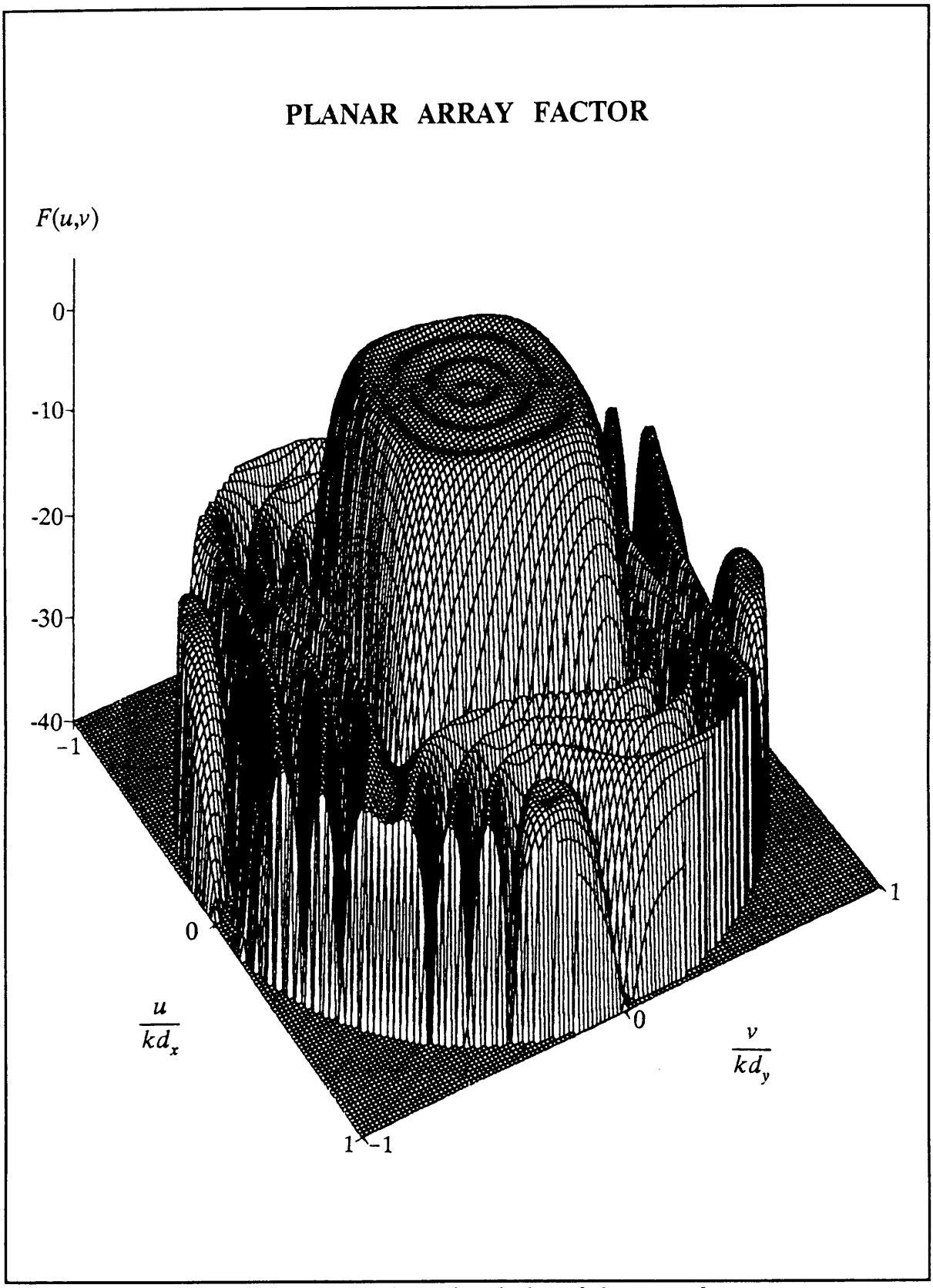

Figure 4.19 Example #6. Three-dimensional plot of the array factor.

© University of Pretoria Digitised by the Department of Library Services in support of open access to information, University of Pretoria, 2019

UNIVERSITEIT VAN PRETORIA
UNIVERSITY OF PRETORIA
YUNIBESITHI YA PRETORIA

number of planar array elements. The size required for this prototype linear array depends on the number of transformation coefficients used and the planar array size. Simple formulas then determine the final planar array excitations from the information forthcoming from the above two sub-problem solutions. Among the advantages of the technique are that it can be used to synthesise very large arrays and yet the time required to perform such a synthesis is relatively short. Simple formulas for the calculation of the transform coefficients for circular and elliptical contours were derived, and the more general contour problem discussed. The method can be used to produce elliptical footprint contours of arbitrary major to minor axis ratios, something that has to yet been achieved by alternative direct methods for uniformly spaced planar arrays.

© University of Pretoria Digitised by the Department of Library Services in support of open access to information, University of Pretoria, 2019

UNIVERSITEIT VAN PRETORIA
UNIVERSITY OF PRETORIA
YUNIBESITHI YA PRETORIA

4.7 REFERENCES

[1] J.H.McClellan, "The design of two-dimensional digital filters by transformation", *Proc. 7th Ann. Princeton Conf. on Information Sciences and Systems*, p.247-251, 1973.

[2] R.M.Mersereau, W.F.G.Mecklenbräuker and T.F.Quatieri Jr, "McClellan transformation for two-dimensional digital filtering: I - Design", *IEEE Trans. Circuits Syst.*, Vol.CAS-23, No.7, p.405-414, July 1976.

[3] R.M.Mersereau, "The design of arbitary 2-D zero-phase FIR filters using transformations", *IEEE Trans. Circuits Syst.*, Vol.CAS-27, No.2, pp142-144, Feb.1980.

[4] D.T.Nguyen and M.N.S.Swamy, "Scaling-free McClellan tranform for 2-D digital filters", *Electron. Lett.*, Vol.21, No.5, p.176-178, Feb. 1985.

[5] D.T.Nguyen and M.N.S.Swamy, "Formulas for parameter scaling in the McClellan tranform", *IEEE Trans. Circuits Syst.*, Vol.CAS-33, No.1, p.108-109, Jan.1986.

[6] D.T.Nguyen and M.N.S.Swamy, "Approximation design of 2-D digital filters with elliptical magnitude response of arbitrary orientation", *IEEE Trans. Circuits Syst.*, Vol.CAS-33, No.6, p.597-603, June 1986.

[7] S.N.Hazra and M.S.Reddy, "Design of circularly symmetric low-pass two-dimetional FIR digital filters using transformation", *IEEE Trans. Circuits Syst.*, Vol.CAS-33, No.10, p.1022-1026, Oct.1986.

[8] Y.V.Baklanov, "Chebyshev distribution of current for a planar array of radiators", *Radio Eng. Electron. Phys. (USSR)*, Vol.11, p.640-642, 1966.

[9] F.I.Tseng and D.K.Cheng, "Optimum scannable planar arrays with an invariant side lobe level", *Proc.IEEE*, Vol.56, No.11, p.1771-1778, Nov.1968.

[10] Y.U.Kim and R.S.Elliott, "Extensions of the Tseng-Cheng pattern synthesis technique", *J. Electromagn. Waves Applic.*, Vol.2, No.3/4, p.255-268, 1988.

[11] M.R.Spiegel, *Mathematical Handbook of Formulas and Tables*, New York: McGraw-Hill, 1968

[12] D.R.Rhodes, *Synthesis of Planar Antenna Sources*, London: Clarendon Press, 1974.

[13] Y.Kamp and J.P.Thiran, "Chebyshev approximation for two-dimensional nonrecursive digital filters", *IEEE Trans. Circuits Syst.*, Vol.CAS-22, No.3, p.208-218, March 1975.

© University of Pretoria Digitised by the Department of Library Services in support of open access to information, University of Pretoria, 2019

UNIVERSITEIT VAN PRETORIA
UNIVERSITY OF PRETORIA
YUNIBESITHI YA PRETORIA

[14] R.M.Mersereau, D.B.Harris and H.S.Hersey, "An efficient algorithm for the design of equiripple two-dimensional FIR digital filters", *Proc IEEE Int. Symp. on Circuits and Systems*, p.405-414, April 1975.

[15] H.J.Orchard, R.S.Elliott and G.J.Stern, "Optimising the synthesis of shaped beam antenna patterns", *IEE Proc.*, Pt.H, Vol.132, No.1, pp.63-68, Feb.1985.

[16] Y.U.Kim and R.S.Elliott, "Shaped-pattern synthesis using pure real distributions", *IEEE Trans. Antennas and Propagat.*, Vol.36, No.11, pp.1645-1649, Nov.1988.

© University of Pretoria Digitised by the Department of Library Services in support of open access to information, University of Pretoria, 2019

UNIVERSITEIT VAN PRETORIA
UNIVERSITY OF PRETORIA
YUNIBESITHI YA PRETORIA

CHAPTER 5

CONCLUSIONS

Two inadequacies in the planar array synthesis field have been identified and addressed: a direct synthesis technique for high directivity discrete planar arrays that has not been studied in any detail in the literature, and a direct method to synthesise an array factor with an arbitrarily contoured main beam.

There has until the present time been no planar array equivalent of the generalized Villeneuve (linear) distribution. The generalised Villeneuve linear distribution array synthesis method has been extended to the planar array case by means the Baklanov transformation. The Baklanov transformation ensures that the resulting planar array factor is "near" ψ-symmetric. Aside from the sidelobe level, two additional parameters have been introduced; they are the transition index $\bar{n}$ that determines the starting point of the sidelobe decay and the taper rate υ that determines the decay rate of the far-out sidelobes. The generalised Villeneuve distribution for planar arrays enables the direct synthesis of discrete array distributions for high efficiency patterns of arbitrary sidelobe levels and envelope taper. The synthesis method is extremely rapid; consequently, design trade-off studies are feasible. For a set number of elements and sidelobe ratio, the values of the transition index and the taper rate for a specific application will depend on the relative importance of farther-out sidelobe levels and the excitation efficiency (or directivity) desired. Parametric studies of the distribution's performance have been conducted; such curves of directivity versus element number for planar arrays do not appear to be available elsewhere in the literature. Curves of the influence of the additional parameters ($\bar{n}$ and υ) on the array factor is also provided. It has also been shown how the generalised planar Villeneuve distribution can be used for the synthesis of planar arrays with a circular boundaries, without the directivity

© University of Pretoria Digitised by the Department of Library Services in support of open access to information, University of Pretoria, 2019

UNIVERSITEIT VAN PRETORIA
UNIVERSITY OF PRETORIA
YUNIBESITHI YA PRETORIA

performance being disadvantaged.

No direct synthesis technique existed to produce discrete planar arrays with contoured beams. The new direct synthesis technique developed in this thesis utilises a transformation that divides the problem into two decoupled sub-problems. In the antenna array context, one sub-problem consists of a linear array synthesis, for which there exist various powerful methods for determining appropriate element excitations. The other involves the determination of certain coefficients of the transform in order to achieve the required footprint contours. The number of coefficients needed depends on the complexity of the desired contour, but is very small in comparison to the number of planar array elements. The size required for this prototype linear array depends on the number of transformation coefficients used and the planar array size. Alternatively, it could be stated that the final array size depends on the number of transformation coefficients (a function of the contour complexity) and the prototype linear array size (which is dependent on the amount of ripple allowable in the coverage area, the sidelobe levels as well as the beamwidth). Simple formulas then determine the final planar array excitations from the information forthcoming from the above two sub-problem solutions. Thus the method is computational efficient and the time required to perform such a synthesis is relatively short; thus trade-of studies are feasible even for very large arrays. Simple formulas for the calculation of the transform coefficients for circular and elliptical contours have been derived, but the more general contour problem has also been discussed. Application of the newly developed transformation technique has been examined through number of specific examples. The method can be used to produce elliptical footprint contours of arbitrary major to minor axis ratios, as well as circular contours with a high degree of accuracy, something that has to yet been achieved by alternative direct methods for uniformly spaced planar arrays.

In all the work described complete details have been given of the recursive and other computational algorithms required to determine the final array excitations.

© University of Pretoria Digitised by the Department of Library Services in support of open access to information, University of Pretoria, 2019

UNIVERSITEIT VAN PRETORIA
UNIVERSITY OF PRETORIA
YUNIBESITHI YA PRETORIA

APPENDIX A

COEFFICIENTS OF A POWER SERIES FROM THE ROOTS OF A PRODUCT SERIES

A.1 INTRODUCTORY REMARKS

In this appendix a recursive relation is derived for the calculation of the coefficients of a power series from the zeros (or roots) of a product series. A computer algorithm, referred to in Chapter 3, for the computation of these coefficients will be also given.

A.2 DERIVATION OF THE RECURSIVE RELATION

A Nth order polynomial can be expressed as ether a product series,

$$P_N(x) = \prod_{k=1}^{N} (x + z_k) \tag{A.1}$$

with z_i the roots of the polynomial, or as a power series,

$$P_N(x) = \sum_{i=1}^{N+1} C_i^N x^{N+1-i} \tag{A.2}$$

with C_i the coefficient of x^{N+1-i} in the power series. The term by term multiplication of

© University of Pretoria Digitised by the Department of Library Services in support of open access to information, University of Pretoria, 2019

the first *k-1* terms product series will result in a *k-1*th order power series. Multiplication of the power series $P_{k-1}(x)$ with the next term in the product series $(x+z_k)$ gives

$$[P_{k-1}(x)][x+z_k] = \sum_{i=1}^{k} C_i^{k-1} x^{k+1-i} + \sum_{i=1}^{k} z_k C_i^{k-1} x^{k-i}$$
$$= z_k C_k^{k-1} + \sum_{i=2}^{k} \left(C_i^{k-1} + z_k C_{i-1}^{k-1}\right) x^{k+1-i} + C_1^{k-1} x^k \qquad \text{(A.3)}$$

This is a *k*th order power series. Examination of (A.3) reveals the recursive relation for the calculation of the power series coefficient as,

$$C_i^k = C_i^{k-1} + z_k C_i^{k-1} \qquad \text{(A.4)}$$
$$\text{where} \quad k = 2,3,.....N \quad \text{and} \quad i = 1,2,.....k+1$$

A.3 ALGORITHM

Step #1:

Initiate:

$C_0^k = 0$
$C_1^k = 1$ $\quad$ *for* $k = 1,2,.....,N$

$C_i^k = 0$ $\quad$ *for* $k = 2,3,.....,N$ $\quad i = k+1,k+2,.....,N$

Step #2:

$k=1$

$C_2^1 = z_1$

© University of Pretoria Digitised by the Department of Library Services in support of open access to information, University of Pretoria, 2019

Step #3:

$$k \leftarrow k + 1$$

$$C_i^k = C_i^{k-1} + z_k C_{i-1}^{k-1} \qquad for\ i = 1,2,.....,k+1$$

Repeat Step #3 up to, and including, the case $k=N$. Note that the coefficients are stored in two $N+1$ vectors. The first vector contains the coefficients of the previous iteration, and the second the values of the updated coefficients.

A.4 REFERENCE

[1] B.M.Lacquet ,P.L.Swart ,M.A. van Wyk, "Coefficients of a power series from the roots of a product series", *Trans. SAIEE*, pp.40-42, July 1988.

© University of Pretoria Digitised by the Department of Library Services in support of open access to information, University of Pretoria, 2019

UNIVERSITEIT VAN PRETORIA
UNIVERSITY OF PRETORIA
YUNIBESITHI YA PRETORIA

APPENDIX B

RECURSIVE FORMULAS AND ALGORITHMS

B.1 INTRODUCTORY REMARKS

In this appendix the recursive formulas, as well as computer algorithms for b_q, c_{mn}, c_{mn}^c and c_{mn}^s, referred to in Chapter 4, will be given. Although it may be possible to write these in what may be considered a more mathematically elegant fashion, such recursion relations are ideally suited to computation.

B.2 COMPUTATION OF b_q

The prototype linear array factor (4.4), namely

$$F(\psi) = a_0 + 2\sum_{q=1}^{Q} a_q \cos(q\,\psi) \tag{B.1}$$

can be rewritten with the use of the recurrence relation (4.5)

$$\cos^q \psi = \sum_{i=0}^{q} g_{iq} \cos(i\,\psi) \tag{B.2}$$

with

© University of Pretoria Digitised by the Department of Library Services in support of open access to information, University of Pretoria, 2019

$$g_{iq} = \begin{cases} \dfrac{1}{2^q} & \text{if } i=0 \text{ and } q \text{ is even} \\ \dfrac{1}{2^{q-1}}\binom{q}{\frac{1}{2}(q-i)} & \text{if } i \text{ and } q \text{ both even or } i \text{ and } q \text{ both odd} \\ 0 & \text{if } i \text{ even and } q \text{ odd or } i \text{ odd and } q \text{ even} \end{cases} \tag{B.3}$$

as (4.6),

$$F(\psi) = \sum_{q=0}^{Q} b_q \cos^q \psi \tag{B.4}$$

The b_q can be computed through the recursive formula

$$b_q = \frac{1}{g_{qq}}\left[a_q - \sum_{i=q+2}^{Q\,2} b_i g_{iq}\right] \tag{B.5}$$

where Σ^2 indicates a step size of two (i.e. $i \Leftarrow i+2$), in the order $q=Q, Q-1, \ldots\ldots, 0$.

B.3 COMPUTATION OF c_{mn} : THE QUADRANTAL SYMMETRY CASE

B.3.1 Formula for c_{mn}

Here the formulas for the computation of c_{mn} of Section 4.2.2 are given. The substitution of the transformation $H(u,v)$ (4.9) into the modified prototype linear array factor (4.6) results in (4.10)

$$F(u,v) = \sum_{q=0}^{Q} b_q \left[\sum_{i=0}^{I}\sum_{j=0}^{J} t_{ij}\cos(iu)\cos(jv)\right]^q \tag{B.6}$$

After multiplication, and by using the recurrence relations, (B.6) can written as (4.11)

$$F(u,v) = \sum_{m=0}^{M}\sum_{n=0}^{N} c_{mn}\cos(mu)\cos(nv) \tag{B.7}$$

© University of Pretoria Digitised by the Department of Library Services in support of open access to information, University of Pretoria, 2019

with $M=QI$ and $N=QJ$. In order to structure the computation of the power term in (B.6), let h_{kl} denominate the coefficient of the general term $cos(ku)cos(lv)$. $H(u,v)$ to the power q can then be written as

$$[H(u,v)]^q = \sum_{k=0}^{qI} \sum_{l=0}^{qJ} h_{kl}^q \cos(ku)\cos(lv) \tag{B.8}$$

and can be obtained by

$$\begin{aligned}[H(u,v)]^q &= [H(u,v)]^{q-1} H(u,v) \\ &= \left[\sum_{k=0}^{(q-1)I} \sum_{l=0}^{(q-1)J} h_{kl}^{q-1} \cos(ku)\cos(lv)\right]\left[\sum_{i=0}^{I} \sum_{j=0}^{J} t_{ij} \cos(iu)\cos(jv)\right]\end{aligned} \tag{B.9}$$

where $h^0=1$. The multiplication of the klth and ijth terms in (B.9)

$$\begin{aligned}&[h_{kl}\cos(ku)\cos(lv)][t_{ij}\cos(iu)\cos(jv)] = \\ &\quad \tfrac{1}{4} h_{kl} t_{ij} \{\cos[(k-i)u]\cos[(l-j)v] + \cos[(k-i)u]\cos[(l+j)v] + \\ &\qquad \cos[(k+i)u]\cos[(l-j)v] + \cos[(k+i)u]\cos[(l+j)v]\}\end{aligned} \tag{B.10}$$

gives contributions to four h^q components, namely

$$\begin{aligned} h^q_{|k-i|,|l-j|} &= h^q_{|k-i|,|l-j|} + \tfrac{1}{4} t_{ij} h_{kl}^{q-1} \\ h^q_{|k-i|,l+j} &= h^q_{|k-i|,l+j} + \tfrac{1}{4} t_{ij} h_{kl}^{q-1} \\ h^q_{k+l,|l-j|} &= h^q_{j+i,|l-j|} + \tfrac{1}{4} t_{ij} h_{kl}^{q-1} \\ h^q_{k+l,l+j} &= h^q_{k+i,l+j} + \tfrac{1}{4} t_{ij} h_{kl}^{q-1} \end{aligned} \tag{B.11}$$

The recursive formula for c_{mn} is, firstly

$$c_{00} = b_0 \tag{B.12}$$

then for $q=1, 2, ..., Q$

$$\begin{aligned} c_{mn} &\Leftarrow c_{mn} + b_q h^q_{mn} \\ with \quad m &= 0,1,.....qI \quad and \quad n = 0,1,.....qJ \end{aligned} \tag{B.13}$$

© University of Pretoria Digitised by the Department of Library Services in support of open access to information, University of Pretoria, 2019

B.3.2 Algorithm for the computation of c_{mn}

Step #1:

Initiate:

$$c_{kl} = 0 \qquad for \quad \begin{matrix} k = 0,1,2,.....,QI \\ l = 0,1,2,.....,QJ \end{matrix}$$

$$h_{kl}^{q} = 0 \qquad for \quad \begin{matrix} k = 0,1,2,.....,QI \\ l = 0,1,2,.....,QJ \\ q = 1,2,3,.....,Q \end{matrix}$$

Step #2:

$$q = 0$$

$$c_{00} = b_0$$

Step #3:

$$q = 1$$

$$h_{ij}^{q} = t_{ij} \qquad for \quad \begin{matrix} i = 0,1,2,.....,I \\ j = 0,1,2,.....,J \end{matrix}$$

$$c_{kl} \Leftarrow c_{kl} + b_q h_{kl}^{q} \qquad for \quad \begin{matrix} k = 0,1,2,.....,qI \\ l = 0,1,2,.....,qJ \end{matrix}$$

Step #4:

$$q \Leftarrow q + 1$$

$$h_{|k\pm i|,|l\pm j|}^{q} \Leftarrow h_{|k\pm i|,|l\pm j|}^{q} + \frac{1}{4} t_{ij} h_{kl}^{q-1} \qquad for \quad \begin{matrix} i = 0,1,2,.....,I \\ j = 0,1,2,.....,J \\ k = 0,1,2,.....,(q-1)I \\ l = 0,1,2,.....,(q-1)J \end{matrix}$$

$$c_{kl} \Leftarrow c_{kl} + b_q h_{kl}^{q} \qquad for \quad \begin{matrix} k = 0,1,2,.....,qI \\ l = 0,1,2,.....,qJ \end{matrix}$$

© University of Pretoria Digitised by the Department of Library Services in support of open access to information, University of Pretoria, 2019

Repeat Step #4 up to, and including, the case $q=Q$. Note, for h^q only two matrices are needed, the first contains the values of the previous iteration and the second contains the updated value of the current iteration.

B.4 COMPUTATION OF c_{mn}^c and c_{mn}^s: THE CENTRO-SYMMETRIC CASE

B.4.1 Formulas for c_{mn}^c and c_{mn}^s

The formulas for the computation of c_{mn}^c and c_{mn}^s of Section 4.3 are given here. The substitution of the transformation $H(u,v)$ (4.42) into the modified prototype linear array factor (4.6) results in (4.43)

$$F(u,v) = \sum_{q=0}^{Q} b_q \left[\sum_{i=0}^{I} \sum_{j=0}^{J} t_{ij} \cos(iu)\cos(jv) + \sum_{i=0}^{I} \sum_{j=0}^{J} s_{ij} \sin(iu)\sin(jv) \right]^q \qquad \text{(B.14)}$$

with

$$s_{ij} = 0 \quad \text{if } i = 0 \text{ or } j = 0 \qquad \text{(B.15)}$$

Application of the recurrence relation (B.2) in (B.14) yields

$$F(u,v) = \sum_{m=0}^{M} \sum_{n=0}^{N} \left[c_{mn}^c \cos(mu)\cos(nv) + c_{mn}^s \sin(mu)\sin(nv) \right] \qquad \text{(B.16)}$$

with $M=QI$ and $N=QJ$. In order to structure the computation of the power term in (B.14), let h_{kl} denominate the coefficient of the general term $cos(ku)cos(lv)$ and g_{kl} denominate the coefficient of the general term $sin(ku)sin(lv)$. $H(u,v)$ to the power q can then be written as

$$[H(u,v)]^q = \sum_{k=0}^{qI} \sum_{l=0}^{qJ} h_{kl}^q \cos(ku)\cos(lv) + \sum_{k=0}^{qI} \sum_{l=0}^{qJ} g_{kl}^q \sin(ku)\sin(lv) \qquad \text{(B.17)}$$

and can be obtained by

© University of Pretoria Digitised by the Department of Library Services in support of open access to information, University of Pretoria, 2019

$$[H(u,v)]^q = [H(u,v)]^{q-1} H(u,v)$$
$$- \left[\sum_{k=0}^{(q-1)I} \sum_{l=0}^{(q-1)J} h_{kl}^{q-1} \cos(ku)\cos(lv) + \sum_{k=0}^{(q-1)I} \sum_{l=0}^{(q-1)J} g_{kl}^{q-1} \sin(ku)\sin(lv) \right] \times \quad \textbf{(B.18)}$$
$$\left[\sum_{i=0}^{I} \sum_{j=0}^{J} t_{ij} \cos(iu)\cos(jv) + \sum_{i=0}^{I} \sum_{j=0}^{J} s_{ij} \sin(iu)\sin(jv) \right]$$

Using the following substitution

$$\hat{H}^{q-1} = \sum_{k=0}^{(q-1)I} \sum_{l=0}^{(q-1)J} h_{kl}^{q-1} \cos(ku)\cos(lv)$$
$$\hat{G}^{q-1} = \sum_{k=0}^{(q-1)I} \sum_{l=0}^{(q-1)J} g_{kl}^{q-1} \sin(ku)\sin(lv)$$
$$\hat{T} = \sum_{i=0}^{I} \sum_{j=0}^{J} t_{ij} \cos(iu)\cos(jv) \quad \textbf{(B.19)}$$
and
$$\hat{S} = \sum_{i=0}^{I} \sum_{j=0}^{J} s_{ij} \sin(iu)\sin(jv)$$

equation (B.18) becomes

$$[H(u,v)]^q = \left[\hat{H}^{q-1} + \hat{G}^{q-1}\right]\left[\hat{T} + \hat{S}\right]$$
$$= \hat{H}^{q-1}\hat{T} + \hat{G}^{q-1}\hat{S} + \hat{H}^{q-1}\hat{S} + \hat{G}^{q-1}\hat{T} \quad \textbf{(B.20)}$$

The multiplication of the *kl*th and *ij*th terms of each of the first two terms in (B.20)

$$\hat{H}_{kl}^{q-1}\hat{T}_{ij} = \tfrac{1}{4} h_{kl} t_{ij} \{\cos[(k-i)u]\cos[(l-j)v] + \cos[(k-i)u]\cos[(l+j)v]$$
$$+ \cos[(k+i)u]\cos[(l-j)v] + \cos[(k+i)u]\cos[(l+j)v]\} \quad \textbf{(B.21)}$$

and

$$\hat{G}_{kl}^{q-1}\hat{S}_{ij} = \tfrac{1}{4} g_{kl} s_{ij} \{\cos[(k-i)u]\cos[(l-j)v] - \cos[(k-i)u]\cos[(l+j)v]$$
$$- \cos[(k+i)u]\cos[(l-j)v] + \cos[(k+i)u]\cos[(l+j)v]\} \quad \textbf{(B.22)}$$

each gives a contributions to four h^q components, namely

© University of Pretoria Digitised by the Department of Library Services in support of open access to information, University of Pretoria, 2019

$$
\begin{aligned}
h^q_{|k-i|,|l-j|} &= h^q_{|k-i|,|l-j|} + \tfrac{1}{4} t_{ij} h^{q-1}_{kl} + \tfrac{1}{4} s_{ij} g^{q-1}_{kl} \\
h^q_{|k-i|,l+j} &= h^q_{|k-i|,l+j} + \tfrac{1}{4} t_{ij} h^{q-1}_{kl} - \tfrac{1}{4} s_{ij} g^{q-1}_{kl} \\
h^q_{k+l,|l-j|} &= h^q_{j+i,|l-j|} + \tfrac{1}{4} t_{ij} h^{q-1}_{kl} - \tfrac{1}{4} s_{ij} g^{q-1}_{kl} \\
h^q_{k+l,l+j} &= h^q_{k+i,l+j} + \tfrac{1}{4} t_{ij} h^{q-1}_{kl} + \tfrac{1}{4} s_{ij} g^{q-1}_{kl}
\end{aligned}
\qquad \textbf{(B.23)}
$$

The multiplication of the *kl*th and *ij*th terms of each of the last two terms in (B.20)

$$
\begin{aligned}
\hat{H}^{q-1}_{kl} \hat{S}_{ij} = \tfrac{1}{4} h_{kl} s_{ij} \{ & \kappa_{k-i} \kappa_{l-j} \sin[(k-i)u] \sin[(l-j)v] + \kappa_{k-i} \sin[(k-i)u] \sin[(l+j)v] \\
& + \kappa_{l-j} \sin[(k+i)u] \sin[(l-j)v] + \sin[(k+i)u] \sin[(l+j)v] \}
\end{aligned}
\qquad \textbf{(B.24)}
$$

and

$$
\begin{aligned}
\hat{G}^{q-1}_{kl} \hat{T}_{ij} = \tfrac{1}{4} g_{kl} t_{ij} \{ & \kappa_{k-i} \kappa_{l-j} \sin[(k-i)u] \sin[(l-j)v] - \kappa_{k-i} \sin[(k-i)u] \sin[(l+j)v] \\
& - \kappa_{l-j} \sin[(k+i)u] \sin[(l-j)v] + \sin[(k+i)u] \sin[(l+j)v] \}
\end{aligned}
\qquad \textbf{(B.25)}
$$

in which

$$
\kappa_i = \frac{i}{|i|} \qquad \textbf{(B.26)}
$$

each gives a contributions to four g^q components, namely

$$
\begin{aligned}
g^q_{|k-i|,|l-j|} &= g^q_{|k-i|,|l-j|} + \tfrac{1}{4} \kappa_{k-i} \kappa_{l-j} \left[t_{ij} g^{q-1}_{kl} + s_{ij} h^{q-1}_{kl} \right] \\
g^q_{|k-i|,l+j} &= g^q_{|k-i|,l+j} + \tfrac{1}{4} \kappa_{k-i} \left[t_{ij} g^{q-1}_{kl} - s_{ij} h^{q-1}_{kl} \right] \\
g^q_{k+l,|l-j|} &= g^q_{j+i,|l-j|} + \tfrac{1}{4} \kappa_{l-j} \left[t_{ij} g^{q-1}_{kl} - s_{ij} h^{q-1}_{kl} \right] \\
g^q_{k+l,l+j} &= g^q_{k+i,l+j} + \tfrac{1}{4} \left[t_{ij} g^{q-1}_{kl} + s_{ij} h^{q-1}_{kl} \right]
\end{aligned}
\qquad \textbf{(B.27)}
$$

The recursive formulas for c^c_{mn} and c^s_{mn} is, firstly

$$
\begin{aligned}
c^c_{00} &= b_0 \\
c^s_{00} &= 0
\end{aligned}
\qquad \textbf{(B.28)}
$$

then for $q = 1, 2, \ldots\ldots Q$

© University of Pretoria Digitised by the Department of Library Services in support of open access to information, University of Pretoria, 2019

$$c_{mn}^{c} = c_{mn}^{c} + b_q h_{mn}^{q}$$
$$c_{mn}^{s} = c_{mn}^{s} + b_q g_{mn}^{q} \qquad \text{(B.29)}$$
$$\text{with} \quad m = 0,1,.....,qI \quad \text{and} \quad n = 0,1,.....,qJ$$

B.4.2 Algorithm for the computation of c_{mn}^{c} and c_{mn}^{s}

Step #1:

Initiate:

$$c_{kl}^{c} = 0 \qquad \text{for} \quad k = 0,1,2,.....,QI$$
$$c_{kl}^{s} = 0 \qquad \quad l = 0,1,2,.....,QJ$$

$$h_{kl}^{q} = 0 \qquad \quad k = 0,1,2,.....,QI$$
$$g_{kl}^{q} = 0 \qquad \text{for} \quad l = 0,1,2,.....,QJ$$
$$q = 1,2,3,.....,Q$$

Step #2:

$$q = 0$$

$$c_{00}^{c} = b_0$$

Step #3:

$$q = 1$$

$$h_{ij}^{q} \Leftarrow t_{ij} \qquad \text{for} \quad i = 0,1,2,.....,I$$
$$g_{ij}^{q} \Leftarrow s_{ij} \qquad \quad j = 0,1,2,.....,J$$

$$c_{kl}^{c} \Leftarrow c_{kl}^{c} + b_q h_{kl}^{q} \qquad \text{for} \quad k = 0,1,2,.....,qI$$
$$c_{kl}^{s} \Leftarrow c_{kl}^{s} + b_q g_{kl}^{q} \qquad \quad l = 0,1,2,.....,qJ$$

© University of Pretoria Digitised by the Department of Library Services in support of open access to information, University of Pretoria, 2019

Step #4:

$$q \Leftarrow q + 1$$

$$h^q_{|k-i|,|l-j|} \Leftarrow h^q_{|k-i|,|l-j|} + \frac{1}{4}\left[t_{ij} h^{q-1}_{kl} + s_{ij} g^{q-1}_{kl}\right]$$

$$h^q_{|k-i|,l+j} \Leftarrow h^q_{|k-i|,l+j} + \frac{1}{4}\left[t_{ij} h^{q-1}_{kl} - s_{ij} g^{q-1}_{kl}\right]$$

$$h^q_{k+l,|l-j|} \Leftarrow h^q_{j+i,|l-j|} + \frac{1}{4}\left[t_{ij} h^{q-1}_{kl} - s_{ij} g^{q-1}_{kl}\right]$$

$$h^q_{k+l,l+j} \Leftarrow h^q_{k+i,l+j} + \frac{1}{4}\left[t_{ij} h^{q-1}_{kl} + s_{ij} g^{q-1}_{kl}\right]$$

$$g^q_{|k-i|,|l-j|} \Leftarrow g^q_{|k-i|,|l-j|} + \frac{1}{4}\kappa_{k-i}\kappa_{l-j}\left[t_{ij} g^{q-1}_{kl} + s_{ij} h^{q-1}_{kl}\right]$$

$$g^q_{|k-i|,l+j} \Leftarrow g^q_{|k-i|,l+j} + \frac{1}{4}\kappa_{k-i}\left[t_{ij} g^{q-1}_{kl} - s_{ij} h^{q-1}_{kl}\right]$$

$$g^q_{k+l,|l-j|} \Leftarrow g^q_{j+i,|l-j|} + \frac{1}{4}\kappa_{l-j}\left[t_{ij} g^{q-1}_{kl} - s_{ij} h^{q-1}_{kl}\right]$$

$$g^q_{k+l,l+j} \Leftarrow g^q_{k+i,l+j} + \frac{1}{4}\left[t_{ij} g^{q-1}_{kl} + s_{ij} h^{q-1}_{kl}\right]$$

$$\text{for} \quad \begin{array}{l} i = 0,1,2,.....,I \\ j = 0,1,2,.....,J \\ k = 0,1,2,.....,(q-1)I \\ l = 0,1,2,.....,(q-1)J \end{array}$$

$$c^c_{kl} \Leftarrow c^c_{kl} + b_q h^q_{kl}$$

$$c^s_{kl} \Leftarrow c^s_{kl} + b_q h_{kl}$$

$$\text{for} \quad \begin{array}{l} k = 0,1,2,.....,qI \\ l = 0,1,2,.....,qJ \end{array}$$

Repeat Step #4 up to, and including, the case $q=Q$. Only two matrices for each of h^q g^q are needed. The first matrix of each contain the values of the previous iteration and the second matrices contain the updated value of the current iteration. Although this algorithm seems formidable, it is easy to program and execution is very rapid.

© University of Pretoria Digitised by the Department of Library Services in support of open access to information, University of Pretoria, 2019